# GABA SUPPRESSES THERMAL AND MECHANICAL SENSITIVITY OF MOUSE CUTANEOUS AFFERENT FIBERS

Alaine L. Pribisko

A dissertation submitted to the faculty of the University of North Carolina at Chapel Hill in partial fulfillment of the requirements for the degree of Doctor of Philosophy in the School of Nursing.

Chapel Hill
2009

Approved by:

Dr. Barbara Germino, PhD

Dr. Susan Brunssen, PhD

Dr. Barbara Carlson, PhD

Dr. Virginia Neelon, PhD

Dr. Edward Perl, MD

Dr. Virginia Shea, PhD

# ABSTRACT

ALAINE L. PRIBISKO: GABA Suppresses Thermal and Mechanical Sensitivity of Mouse Cutaneous Afferent Fibers
(Under the direction of Dr. Barbara Germino)

Exogenous γ-aminobutyric acid (GABA) and GABA agonists attenuate nociceptive behaviors in animals and decrease excitability and conduction in somatic and vagal nerves. The present exploratory study examines the effects of GABA on the responses of 38 single primary afferent sural and plantar fibers to electrical, mechanical, chemical, and thermal stimulation.

Numerous stimulus techniques were developed, implemented, and tested to establish the validity, reliability, and suitability for use on the mouse skin-nerve *ex vivo* preparation. A major finding was that a 980 nm infrared diode laser proved very suitable for evoking repeatable graded responses from heat-responsive C fibers and for the study of GABA effects.

None of 7 low threshold mechanoreceptors and cooling thermoreceptors had a change in response properties in the presence of GABA. All fibers sensitive to noxious heat and protons were also sensitive to strong mechanical stimuli and were presumed nociceptive. During repetitive activation by electrical stimulation of the nerve, 3 of 6 C fibers had a continued progression of conduction velocity slowing in the presence of GABA. During mechanical stimulation, GABA suppressed the responsiveness of 5 of 17 C and Aδ fibers.

During noxious heat or proton stimulation, 4 of 7 heat-sensitive and 1 of 1 proton-sensitive C fibers had suppressed responsiveness in the presence of GABA.

GABA-induced changes in the responses of nociceptors to noxious stimulation are in agreement with animal behavior studies and lend support to the further investigation of GABA and GABA agonists as peripheral analgesics.

ACKNOWLEDGEMENTS

To my committee members, I thank you for your knowledge, experience, and encouragement. To Dr. Germino and Dr. Shea, I thank you for your pragmatic approach to stylistic writing and effective editing. I am much obliged to the North Carolina Association of Nurse Anesthetists and the American Association of Nurse Anesthetists for the funds to purchase the diode laser and the University of North Carolina for a dissertation fellowship that made my last year of study productive and financially stable.

To Dr. Edward R. Perl, I am most grateful for making this project possible. He has shown me the way and instilled in me the desire to transform from a student to a shrewd researcher and systematic scientist. He has taught me to observe closely, use the senses broadly, detail carefully, immerse in the rich history behind the evidence, and write with a fresh description. He has provided me the intellectual and financial opportunity to design and implement difficult projects within the interdisciplinary study of pain. I value most his respect for the field of nursing and his desire to engage nurses in the study of pain at the cell and molecular level.

TABLE OF CONTENTS

LIST OF TABLES

LIST OF FIGURES

# LIST OF ABBREVIATIONS AND SYMBOLS

| | |
|---|---|
| Aα, | Rapidly conducting sensory (proprioceptive) and motor fibers |
| Aβ | Rapidly conducting sensory (tactile, few nociceptive) and motor fibers |
| Aδ | Tactile and nociceptive fibers, approximate CV < 10m/s and > 1m/s |
| AδM | Aδ fiber responsive to noxious mechanical stimulation |
| AδMHC | Aδ fiber responsive to noxious mechanical, heat, and cold stimulation |
| AδMH | Aδ fiber responsive to noxious mechanical and heat stimulation |
| AδLTh | Aδ low threshold tactile fiber |
| AM | Aδ fiber responsive to noxious mechanical stimuli |
| ATP | Adenosine triphosphate |
| BAC | Baclofen |
| BIC | Bicuculline |
| CACA | *cis*-4-amino crotonic acid |
| CAP | Compound action potential |
| CGRP | Calcitonin gene-related peptide |
| CLTh | C low threshold tactile fiber |
| CM | C fiber responsive to noxious mechanical stimuli |
| CMHA | C fiber responsive to noxious mechanical and heat stimuli and protons |
| CMHAC | C fiber responsive to noxious mechanical, heat, cold, acidic stimuli |
| CMH | C fiber responsive to noxious mechanical and heat stimuli |
| CNS | Central nervous system |
| $CO_2$ | Carbon dioxide |
| CSF | Cerebral spinal fluid |

| | |
|---|---|
| CV | Conduction velocity |
| DNFB | 2,4-dinitrofluorobenzene |
| DRG | Dorsal root ganglia |
| EMI | Electromagnetic interference |
| g | Glabrous |
| GABA | γ-aminobutyric acid |
| GAD | Glutamate decarboxylase |
| GAT-1 | GABA transporter-1 |
| h | Hairy |
| HCl | Hydrochloric acid |
| Hz | Hertz |
| kPa | Kilopascals |
| J | Joules |
| LMEE | Linear motion end-effector |
| LTh | Low mechanical threshold fiber |
| m | Meters |
| min | Minute |
| MIA | Mechanically insensitive afferent |
| mA | Milliamperes |
| mg | Milligrams |
| mm | Millimeters |
| mN | Millinewtons |
| ms | Milliseconds |

| | |
|---|---|
| mV | Millivolts |
| MUS | Muscimol |
| NDG | Nodose ganglia or inferior ganglia of afferent visceral vagus |
| NF200 | Neurofilament protein 200 |
| NKCCl | Sodium-potassium-chloride co-transporter |
| nm | Nanometer |
| PAN | Primary afferent neuron, a first order somatic sensory neuron |
| PAF | Primary afferent fiber |
| $PGE_2$ | Prostaglandin $E_2$ receptor ligand |
| PITX | Picrotoxin |
| PMN | Polymodal nociceptor |
| PMP22 | Peripheral myelin protein 22 |
| PNS | Peripheral nervous system |
| R | Ring reservoir |
| RA | Rapid adapting |
| RF | Receptive field |
| S | Superfusate |
| s | Seconds |
| SA | Slow adapting |
| SIF | Synthetic interstitial fluid |
| TGG | Trigeminal ganglion |
| TPMPA | (1,2,5,6-tetrahydropyridin-4-yl) methylphosphinic acid |
| TRPV1 | Transient receptor potential, subfamily vanilloid, member 1 |

| | |
|---|---|
| V | Volts |
| VF | Von Frey filament |
| W | Watts |

# CHAPTER 1

# INTRODUCTION

One of many postulates of Charles Sherrington was the existence of sensory cells specific to the detection of noxious events (Sherrington, 1906). Nociceptors identify noxious stimuli, translate the signals into action potentials, and conduct the signals to the spinal cord and brain in a process call nociception. Sixty years later, Perl and colleagues successfully recorded responses of these cells and delineated their functional characteristics as: 1) silent except to noxious thermal, mechanical and/or chemical stimulation that threatens tissue integrity; 2) maximal responsiveness requires substantial increases in stimulus intensity compared to warm and fine touch receptors; and 3) increased responsiveness (sensitization) with repeated activation (Bessou & Perl, 1969; Burgess & Perl, 1967).

Today, research on nociception diverges along seemingly limitless paths. Two areas of interest are the search for endogenous molecular constituents strongly or exclusively associated with the transduction and propagation of signals by nociceptors, and the greater understanding of the change in density, localization, and availability of molecular constituents with repeated activation. My interest in peripheral pain mechanisms is founded in the convictions that most pain starts with and is often maintained by nociceptors, the reversible interruption of signals prior to central integration is the single most important mechanism of peripheral analgesia, and one characteristic of an ideal analgesic is targeting pain at its source in the periphery.

Anesthesia clinicians are challenged daily to provide acute pain management by convenient, effective, and safe techniques for complex ambulatory procedures. Peripherally acting analgesics offer distinct advantages to this subset of patients. Peripheral nerve blocks, incisional infiltration, and intra-cavity and intra-articular instillation with local anesthetics are frequent choices of anesthesia providers and patients (White, 2002). However, local anesthetic activity is not restricted to nociceptors. Sodium channels of all excitable cells are blocked by local anesthetics (Ragsdale, McPhee, Scheuer, & Catterall, 1994). Residual side effects occur from distribution of local anesthetic to non-targeted motor, proprioceptive and autonomic nerve fibers and diffusion away from the administration site to distant cardiac and central nervous system (CNS) excitable cells. Common side effects include motor weakness, hypotension, seizures, and cardiac arrhythmias (de Jong, 1994; Tetzlaff, 2000). New approaches to selectively block the generation and conduction of impulses by nociceptors with low risk of side effects are attractive. In this basic science project, I proposed to study the effects of γ-aminobutyric acid (GABA) on individual peripheral nerve fibers as a foundation for future evaluation of experimental compounds as peripheral analgesics.

The inspiration for this project comes from observations from the 1970s and 1980s that GABA alters the amplitude and conduction velocity (CV) of components of the compound action potential (CAP) of mammalian peripheral nerves. Figure 1 (Appendix A) summarizes the components of the CAP. Application of GABA to *ex vivo* sciatic nerves resulted in a 10% decrease in amplitude of the A component (collective responses of the heavily myelinated and rapidly conducting neurons) of the CAP to electrical stimulation (Bhisitkul, Villa, & Kocsis, 1987). Also, GABA application to *ex vivo* vagal nerves reduced the amplitude of the C component (collective response of slowest conducting, unmyelinated

fibers) of the CAP by up to 50%, and decreased the C component CV (Brown & Marsh, 1978). Reduction in the amplitude of the C component of the CAP infers that fewer neurons generate and propagate impulses and decrease the contribution to the sum of C-fiber action potentials. Slowing of CV infers fewer impulses over time will reach second order spinal neurons. Since the majority of cutaneous C fibers are nociceptive (Bessou & Perl, 1969), the expectation is the change in functions would result in a decrease in nociception. While Bhisitkul, et al. (1987) studied somatic nerves, the Brown and Marsh study was of vagal nerves. Differences in peripheral nerve composition may have contributed to observed differences between these studies. The vagus is a mixed visceral, somatic, and special sensory, and visceral and somatic motor nerve, while the sciatic nerve is a mixed somatic sensory and motor, and sympathetic postganglionic motor nerve.

Other early electrophysiological observations challenged the supposition of an antinociceptive function of GABA in the peripheral nervous system (PNS). GABA depolarized primary afferent nerve (PAN) cell bodies in dorsal root ganglia (DRG) (de Groat, Lalley, & Saum, 1972; Desarmenien, Feltz, Occhipinti, Santangelo, & Schlichter, 1984; Desarmenien, Santangelo, Loeffler, & Feltz, 1984; Gallagher, Higashi, & Nishi, 1978; Nishi, Minota, & Karczmar, 1974); dorsal roots (Bhisitkul et al., 1987) and whole nerves (Bhisitkul et al., 1987; Brown & Marsh, 1978; Morris, Di Dostanzo, Fox, & Werman, 1983). GABA-induced depolarization, the shift toward zero in the voltage difference relative to the inner and outer surface of a biological membrane or structure, is primarily mediated by outward ionic movement of chloride through ligand-gated anion channels (Gallagher et al., 1978). In addition, the GABA application increased the excitability in peripheral nerves and cell bodies (Aptel et al., 2007; Bhisitkul et al., 1987; Morris et al., 1983).

While electrophysiology is a very important method to better understand the structural relationships and functions of cells and molecules, changes in animal behavior often support quick advancement of endogenous and pharmacological agents to human applications. The most important evidence for GABA-induced antinociception or analgesia comes from the more recent observations of effects of peripherally applied GABA and GABA receptor subtype agonists on animal nociceptive behavior. Healing was accelerated, inflammation decreased, and pain behaviors attenuated in animals experiencing noxious events with the administration of GABA agonists (Carlton, Zhou, & Coggeshall, 1999; Denda, Fuziwara, & Inoue, 2003; Denda, Inoue, Inomata, & Denda, 2002; Han, Kim, Lee, Shim, & Hahm, 2007; Reis & Duarte, 2006; Reis & Duarte, 2007; Reis et al., 2007), although paradoxical pro-nociception has occurred at increased GABA concentrations in the rat (Carlton et al., 1999; Ocvirk, Murphy, Franklin, & Abbott, 2008).

Not all evidence supports a decisive role for GABA in the periphery. As few as 11% of cutaneous nerve endings have been observed to contain GABA receptors (Carlton et al., 1999; Charles et al., 2001; Stoyanova, 2004), and only 20% of sensory nerve cell bodies have been noted to synthesize GABA (Nakagawa, Hiura, & Kubo, 2003; Stoyanova, 2004).

Possibly because the evidence is equivocal, no systematic survey has been published of the effects of GABA on individual somatosensory primary afferent nerve fibers (PAF). The specific aims of this project were: 1) to classify GABA-responsive PAFs by excitability and conductivity, and by sensory modality and stimulus intensity; 2) to establish the anatomic loci for this response (the peripheral process versus peripheral terminal and cutaneous receptive field (RF); and 3) to determine the optimal GABA concentration to suppress or enhance the activity of nociceptors. Cutaneous RF refers to a region of skin

where energy is transduced from a specific stimulus mode (thermal, mechanical, chemical, or electrical) of sufficient strength to generate action potentials. Table 1 (Appendix B) summarizes the relationship of specific aims and research methodology of studies designed for the project proposal.

The model for these experiments was the *ex vivo* mouse skin-nerve preparation (Reeh, 1986). Figures 2 and 3 (Appendix C) are a schematic representation and a photograph of the skin-nerve preparation. Electrical, thermal, mechanical, and chemical measures were tailored to challenge or support the above mentioned electrophysiological and animal findings. The biochemical, biophysical, pharmacological and physiological properties of GABA and GABA receptors were examined to maximize the chance of finding GABA effects. The specific aims of the project were to study the effects of GABA exposure on PAF, but a major goal was to develop *ex vivo* mouse skin-nerve preparation techniques and adequate measurement instrumentation to test anti-nociceptive and analgesic endogenous and pharmacological compounds.

# CHAPTER 2

# PROPERTIES OF GABA AND GABA RECEPTORS – A LITERATURE REVIEW

## GABA as a Neurotransmitter, Signaling and Trophic Molecule

GABA is a four carbon, non-proteinogenic amino acid. GABA synthesis and activity are remarkably conserved as signaling and trophic agents among animal, plant, and other living kingdoms. GABA is the principle inhibitory neurotransmitter in vertebrate and non-vertebrate CNS, but is also synthesized in a minority of cells of sensory ganglia, glia, and cutaneous non-neuronal tissues.

### *Conservation of GABA synthesis and activity among species*

In plants, fungi, and bacteria, GABA functions as a regulator of nitrogen balance and is rapidly synthesized and secreted in response to plant stress. GABA metabolites and transporters are utilized for seed production and ripening, transport of nutrients, defense against insects, and osmotic and hydrogen ion regulation. GABA agonists and antagonists induce opposite actions on plant growth (Ben-Ari, 2002; Bouche & Fromm, 2004). In invertebrates, GABA is an inhibitory neurotransmitter at the neuromuscular junction and counterbalances the excitatory actions of acetylcholine, its close structural and phylogenetic relative (Korpi, Grunder, & Luddens, 2002; Richmond & Jorgensen, 1999). GABA is highly, but unevenly distributed in the immature and adult vertebrate CNS. In Xenopus tadpoles, Zebra fish, drosophila, chick embryos, and turtles, GABA depolarizes central immature neurons and hyperpolarizes mature neurons (Ben-Ari, 2002). GABA receptors are

functional days before the formation of central spinal and supra-spinal synapses in mammalian embryonic central neurons, and GABA modulates neuronal differentiation, proliferation, migration, and survival in cultured cells (Represa & Ben-Ari, 2005).

*Mammalian peripheral GABA distribution*

Twenty percent of cat nodose ganglia, trigeminal ganglia (TGG) and DRG neurons and PAFs contain GABA. The most intense GABA distribution is in small and medium sized cell bodies and apposed processes in the cat (Stoyanova, 2004). These data suggest a nociceptive role for GABA because small to medium DRG cell size is associated with nociception. The cell bodies of neurons with C fibers generally are small in diameter, A$\delta$ fibers are small to medium, A$\alpha\beta$ fibers are medium to large, and many neurons with C and A$\delta$ fibers are nociceptors (S. N. Lawson, 2005). As reviewed by Torebjork and colleagues, A$\delta$ nociceptor activation leads to the human sensation of sharp pricking, stinging pain, and C nociceptor activation leads to dull, aching, boring, burning pain (Torebjork, Schady, & Ochoa, 1984). Several excellent reviews of the characteristics of C and A$\delta$ cutaneous sensory nociceptors are available for reference (Birder & Perl, 1994; Lewin & Moshourab, 2004). Consistent with findings in the cat, 18% of rat small to large size TGG cells contain GABA (Nakagawa et al., 2003). GABA synthesis in DRG cells does not infer uniform transport to and storage in processes and terminals. Direct evidence of transport of GABA from DRG cells to peripheral terminals has only been observed in the chick (Roy, Philippe, Gaulin, & Guay, 1991). Peripheral glial Schwann cells (peripheral myelin-forming glia) also synthesize, redistribute, and metabolize GABA, and express functionally active $GABA_A$ and $GABA_B$ receptors. Glial cells also have been observed to synthesize neuroactive steroids that

bind at $GABA_A$ receptor modulation sites (Magnaghi, 2007). GABA receptor types are described in a later section.

GABA is distributed in and may act as a signal transduction molecule in non-neuronal tissues. Keratinocytes, the vast majority of epithelial cells, also synthesize GABA (Canellakis, Milstone, LL, Young PR, & Bondy, 1983), and closely approximate the free-nerve endings of nociceptive PAFs (Kruger, Perl, & Sedivec, 1981) that localized $GABA_A$ receptors (Carlton et al., 1999). Other non-neuronal sources of GABA may include cutaneous fibroblasts (Ito, Tanaka, Nishibe, Hasegawa, & Ueno, 2007).

GABA is found in the adrenal gland, red blood cells and platelets, gastrointestinal tract, kidney, hepatocytes, epiphyseal growth chondrocytes, and pancreas (Magnaghi, 2007; Tamayama, Kanbara, Maemura, Kuno, & Watanabe, 2001). Direct physiological responses to GABA on the smooth muscle of the myenteric plexus are contraction from $GABA_A$ agonists and relaxation with $GABA_B$ agonists. In addition, $GABA_A$ agonists inhibit urinary bladder motility. In other viscera, GABA plays an indirect role by evoking the release of hormones, neuromodulators, and neurotransmitters from the gall bladder, respiratory vasculature, stomach, and pancreas. Most of these responses are blocked by $GABA_A$ and $GABA_B$ antagonists (Erdo, 1985).

*Biochemical properties of GABA*

The primary pathway of GABA biosynthesis is a single step γ-decarboxylation of glutamate. As a product of γ-decarboxylation, GABA is excluded from protein synthesis functions. A precursor of GABA is glutamate and synthesis is governed by one of two isoforms of the ubiquitous enzyme, glutamate decarboxylase (GAD), $GAD_{65}$ and $GAD_{67}$. Glutamate is localized in most of the same peripheral tissues as GABA, including platelets,

keratinocytes, and DRG neurons. Peripheral glutamate concentration is not static. Tissue content and percentage of glutamate-positive DRG neurons increase with inflammation (Battaglia & Rustioni, 1988; Carlton, 2005; Skerry & Genever, 2001). Inflammation-induced upregulation of GABA has not been reported. $GAD_{65}$ most likely is responsible for the synthesis of GABA stored in synaptic and nerve ending vesicles, and $GAD_{67}$ for diffusible cytosolic GABA of non-neuronal tissues (Soghomonian & Martin, 1998). Hence, synaptic and extrasynaptic GABA is made available by two distinct pathways.

While the GABA synthesis pathway limits GABA from peptide formation, the functional characteristics of GABA are expanded by its interaction with distinct physiologically and phylogenetically unrelated receptor types. The phylogenetically more ancient GABA receptor types, $GABA_A$ and $GABA_C$, form ligand-gated chloride channels and are of prokaryote origins. The more modern receptor type, $GABA_B$, couples to G proteins and is of eukaryote origins (Ben-Shlomo & Hsueh, 2005). Accordingly, the expression of multiple receptors allows the economic use of a single endogenous agent to activate seemingly unrelated physiological mechanisms in a variety of organ systems and under different environmental and developmental conditions.

Availability of an endogenous agent by local synthesis and storage in or transport to a tissue is an essential characteristic of neurotransmitter activity. However, an agent must not be so ubiquitous that its constant presence is ineffective to initiate a biological change. Thus, transport, deactivation, metabolism, and re-uptake all balance GABA availability. In the CNS, where GABA kinetics are best understood, GABA is synthesized and packaged into presynaptic vesicles, through the action of $Mg^{2+}$-activated ATP-ase, for release in response to sensory stimulation. An increase in intracellular calcium drives the release of stored GABA

and leads to diffusion into the synaptic cleft. A transient rise in GABA concentration leads to activation of GABA receptors on pre- and post-synaptic membranes. Termination of action is primarily due to rapid uptake and removal by GABA transporters into the pre-synaptic neuron and surrounding glia. Once returned to the neuron or glia, GABA is rapidly recycled into glutamate by GABA transaminase and once again available for synthesis (Perves et al., 2004).

*Biophysical properties of GABA*

The GABA molecule is a simple and flexible molecule that rotates freely around all its bonds. The ability to adopt different energetically favorable conformations accommodates binding to various receptor types and subtypes. Figure 4 (Appendix D) summarizes the chemical structures of GABA and common GABA analogs. GABA analogs (agonists and antagonists that mimic the active moiety of GABA) have more rigid, high energy structures and are more confined at a specific receptor subtype binding site, with $GABA_B$ receptors more so than $GABA_A$ (Chebib & Johnston, 1999; Krogsgaard-Larsen, Scheel-Kruger, & Koford, 1979).

*Pharmacological properties of GABA*

GABA possesses pharmacological properties both favorable and unfavorable as an analgesic or adjuvant to general and regional anesthesia. GABA is hydrophilic and poorly penetrates the lipophilic membranes of neural structures (Kerr & Ong, 1992). However, the hydrophilic state affords a safety advantage. Peripherally administered GABA does not penetrate the blood brain barrier and CNS side-effects are minimized. In addition, GABA possesses minimal cardiovascular and motor effects (Bhisitkul et al., 1987; de Groat et al., 1972), a definite advantage over amide and ester local anesthetics.

## $GABA_{A-C}$ Receptors

GABA activates three distinct receptor types: $GABA_A$ and $GABA_C$ are ligand-gated ion channels and $GABA_B$, is a complex of second messenger signal transduction molecules. GABA receptor classification is based on molecular subunit structure and pharmacological sensitivity to agonistic and antagonistic GABA analogs. Similar to GABA expression, $GABA_A$ and $GABA_B$ receptors also are believed to have limited localization on PAN structures.

*GABA receptor biophysical properties*

The $GABA_A$ and $GABA_C$ receptor types are transmembrane anion channels that rapidly open in response to GABA binding and lead to an enhanced conductance of $Cl^-$, and to a lesser extent bicarbonate ($HCO_3^-$) (Farrant & Nusser, 2005). Figure 5 (Appendix D) is a schematic representation of $GABA_{A-C}$ receptor structures.

The primary differences between $GABA_A$ and $GABA_C$ receptors are: 1) a ten to forty-fold greater sensitivity of $GABA_C$ receptors to GABA; 2) $GABA_C$ pore opens slower and remains open longer; 3) lack of desensitization by $GABA_C$ receptors; and 4) the majority of $GABA_C$ receptors are localized to the visual system (Cherubini & Strata, 1997; Johnston, 1996b). The subject of desensitization will be discussed in a later section.

The ionotropic $GABA_A$ and $GABA_C$ receptors are pentameric (five $\alpha_{1\text{-}6}$, $\beta_{1\text{-}4}$, $\gamma_{1\text{-}4}$, $\delta$, or $\rho_{1\text{-}3}$ subunits) molecules that form a GABA binding site coupled with a $Cl^-$ channel. $GABA_A$ receptors are heteromeric and frequently form a ring of $\alpha$, $\beta$, $\alpha$, $\beta$, and $\gamma$ or $\delta$ subunits, in a combination of 1 to 2 pair(s) of $\alpha$ and $\beta$ subunits with at least one other subunit type. $GABA_C$ receptors are often homomeric $\rho_{1\text{-}3}$ subunits. The $GABA_A$ and $GABA_C$ receptors consist of four transmembrane domains with a long N-terminal extracellular

domain and an intracellular loop between the 3rd and 4th transmembrane domain. The binding site for GABA and analogs to the $GABA_A$ and $GABA_C$ receptor is either on the N-terminal domain or in the transmembrane region of the $Cl^-/HCO_3^-$ pore (Bowery & Smart, 2006; Enna, 2007; Enz & Cuttin, 1998; Farrant & Nusser, 2005; Zhang, Pan, Awobuluyi, & Lipton, 2001).

The binding of GABA with the $GABA_B$ metabotropic receptor initiates a multi-step, slow and prolonged change in trans-membrane $K^+$ and $Ca^{2+}$ ion permeability to decrease membrane excitability (Bowery, 1993; Chebib & Johnston, 1999). $GABA_B$ receptors are heterodimeric G protein-coupled (2 dissimilar, 7-transmembrane) sub-units with an extracellular surface binding site for GABA and $K^+$ and $Ca^{2+}$ channel-apposed cytosolic site (Bormann, 2000; Chebib & Johnston, 1999). Functional activity is conferred by the $B_2$ subunit and receptor binding is at the $B_1$ subunit (Bowery & Smart, 2006).

Although sub-unit specific biophysical and pharmacological properties are voluminous, a few observations are relevant. Various domains on the β subunits are required for barbiturate activity and on the γ subunits for general anesthetic and benzodiazepine activity (Johnston, 1996a). The $\delta$ unit is extrasynaptic in the brain and the absence of a γ unit prevents synaptic localization of the $GABA_A$ receptor (Farrant & Nusser, 2005). Similar subunit requirements in the periphery have not been reported.

*$GABA_{A\text{-}C}$ receptor pharmacology*

Most GABA receptor pharmacology is derived from study in the CNS. $GABA_A$ receptor is agonized by muscimol (MUS), antagonized by bicuculline (BIC) and picrotoxin (PITX), and modulated by barbiturates, benzodiazepines, and neurosteroids. $GABA_B$ receptor is agonized by baclofen (BAC) and antagonized by saclofen and phaclofen. $GABA_C$

receptor is agonized by *cis*-4-amino crotonic acid (CACA), partially agonized by MUS, antagonized by (1,2,5,6-tetrahydropyridin-4-yl)methylphosphinic acid (TPMPA), inconsistently antagonized by PITX, and generally unresponsive to all other $GABA_A$ and $GABA_B$ antagonists and allosteric modulators (Bormann, 2000; Bowery, 1993; Johnston, 1996a, 1996b; Murata, Woodward, Miledi, & Overman, 1996; Reis & Duarte, 2007; Wang, Hackam, Guggino, & Cutting, 1995; Wegelius et al., 1996). Table 2 (Appendix E) provides a detailed description of receptor types, agonist, antagonists and modulators.

In addition to GABA and GABA agonistic binding sites, $GABA_A$, $GABA_B$ and $GABA_C$ receptors also have recognized allosteric binding sites (Bormann, 2000; Bowery & Smart, 2006; Johnston, 1996b). Allosteric modulation is the remodeling of a receptor protein shape and subsequent activity, through the formation of a bond at an alternative location other than the agonist recognition binding site. BAC and many allosteric modulators have analgesic and anesthetic uses, but the remaining compounds are in general only useful for laboratory study.

$GABA_A$ has distinct allosteric sites for volatile anesthetics, alcohols, barbiturates, benzodiazepines, calcium, etomidate, furosemide, loreclezole, magnesium, mefenamic acid, PITX, propofol, protons, and steroids, to increase or decrease the affinity of the receptor for GABA and competitive agonists, and increase or decrease the duration or frequency of channel openings (Enna, 2007). The $GABA_B$ receptor has a single proposed allosteric site for an unknown endogenous ligand (Bowery & Smart, 2006). $GABA_C$ has allosteric sites for PITX, protons, and zinc (Bormann, 2000; Enz & Cuttin, 1998; Johnston, 1996b). If allosteric modulation sites are found on GABA receptors in the periphery, their presence may increase the chance for pharmacological interventions.

Most data on GABA and analogs have been generated from sub-mammalian and mammalian vertebrates, but fascinating observations arose from a study of rapidly extracted human DRG cells. Inward currents were induced by GABA and MUS and enhanced by benzodiazepines and barbiturates (as would be expected), but, the currents were not antagonized by BIC and PITC in opposition to effects found in sub-human DRG cells. BAC had no effect on inward currents, in opposition to effects found in sub-human DRG cells (Valeyev, Hackman, Wood, & Davidoff, 1996). If human peripheral GABA receptors hold unique properties, the question arises as to the suitability of the mouse model in the assay of GABA-based drugs for human use.

*GABA receptor localization on PAF and cell bodies*

In the cat, $GABA_A$ β2/β3 and α1 subunits are localized on 10 to 14% of PAF peripheral processes that terminate at the dermal-epidermal border, while almost 100% of cell bodies express β2/β3 subunits (Carlton et al., 1999). $GABA_B$ receptors have been localized to DRG cell bodies, but have not been located on PAF peripheral processes. $GABA_B$ subunits are differentially expressed by large and small diameter cell bodies; the $GABA_{B1b}$ subunit is restricted to larger diameter, and $GABA_{B1a}$ and $GABA_{B2}$ subunits are expressed by both large and small diameter neurons (Charles et al., 2001). In DRG, $GABA_A$ and $GABA_B$ receptors may coexist on Aδ and C cells, but not all Aδ and C cells respond to $GABA_B$ agonist exposure (Desarmenien, Feltz et al., 1984). DRG neuronal sensitivity to $GABA_C$ agonists has not been reported. Inferences are often made from intracellular DRG recordings, but a direct relationship between cell body activities and the functional properties of the neuron as a whole has not been established.

## GABA Physiology

Commonly recognized central GABA effects may serve as a model for study of the actions of GABA on PAFs and adjacent cutaneous tissues. In the CNS, GABA activated $GABA_{A-B}$ receptors exert tonic and phasic inhibition, but much less is known of its actions in the periphery. GABA depolarizes and excites DRG cell membranes and peripheral processes, but may have reduced effectiveness with repeated exposure.

*Central tonic and phasic GABA effects*

Some central neuronal networks are characterized by synchronized oscillatory patterns and GABA receptor activation is the primary counter balance to neuronal excitability. GABA is the main CNS rapid and slow inhibitory synaptic neurotransmitter, by way of $GABA_A$ and $GABA_B$ receptor activation, respectively (Farrant, 2007). $GABA_C$ receptors are primarily localized to the visual system and will be excluded from the review. In the CNS, activation of neuronal $GABA_A$ receptors leads to hyperpolarization of plasma membranes (Enna, 2007). With $GABA_A$ activation, $Cl^-$ pores open to allow $Cl^-$ flux into CNS cells. In general, this drives the membrane potential in a more negative direction and further from the electrical threshold for impulse generation.

Not all CNS GABA activity is synaptic; $GABA_A$ receptors have also been localized on dendritic membranes (Nusser, Roberts, Baude, Richards, & Somogyi, 1995). Extrasynaptic receptors often are comprised of different subunits than the classical synaptic type, hold different sensitivities to allosteric modulators, and have variable receptor affinity to GABA. These properties may favor tonic inhibition rather than rapid synaptic inhibition. Tonic inhibition is the persistent increase in a cell's input conductance to change the magnitude and duration of voltage response, and make it less likely to generate or propagate

an action potential. Tonic inhibition is proposed to alter the gain of the synchronized oscillating patterns, a second major process for regulating excitability. Tonic GABA sources are extracellular spillover from synapses and glia, and use-dependent intracellular GABA synthesis by and transport from neuronal cell bodies (Hamann, Rossi, & Attwell, 2002).

*GABA at the junction of CNS with PNS*

In the spinal cord, $GABA_A$ expressing dorsal horn neurons form axon to axon contacts with PAF central terminals (Bowery, 1993). CNS dorsal horn neurons are hyperpolarized upon exposure to GABA, while the nearby PAF central terminals are depolarized. $Cl^-$ pores open in both types of neurons, but the net flux of ions is generally reversed in PANs. The direction of $Cl^-$ current is dependent on the relationship between the membrane potential and the resting-state intracellular and extracellular $Cl^-$ concentrations and is tightly correlated with the cation-chloride cotransporters, specific to neuronal type. $Cl^-$ content of cerebral spinal fluid (CSF) is greater than that of interstitial fluid. NKCC1, a $Na^+$ -$K^+$ -2$Cl^-$ cotransporter, significantly raises internal $Cl^-$ against the predicted electrochemical gradient in peripheral neurons, while KCC2, a $K^+$-$Cl^-$ cotransporter, generally lowers internal $Cl^-$ in mature central neurons (Delpire, 2000).

$GABA_B$ receptors demonstrate activity at axo-axon spinal contacts in the spinal cord. The activation of PAF central terminal $GABA_B$ receptors mediates a slow hyperpolarization due to an increase in $K^+$ conductance. $GABA_B$ activation also decreases $Ca^{2+}$ conductance, predominantly through voltage-dependent N class $Ca^{2+}$ channels to decrease excitatory neurotransmitter release (Bowery & Smart, 2006).

*Desensitization*

Desensitization is the observation of a peak and ebb response in the continuous presence or repeated exposure to an agonist. Desensitization is a feature of many central and peripheral ligand-gated ion channels, is often voltage-dependent, and may be attributed to a use-dependent conformational change in a receptor and/or channel (Hablitz, 1992). Desensitization complicates experimental study and the avoidance of desensitization requires brief applications. In DRG cells, application of GABA for as short of a duration as one second leads to depolarization, mostly as a result of an increase in $Cl^-$ conductance, while GABA applications for more than one second lead to a sustained fade in ion flux (Desarmenien, Feltz, & Headley, 1980). The coactivation of allosteric binding sites slows GABA-induced desensitization of central $GABA_A$ receptors (Bai, Pennefather, MacDonald, & Orser, 1999).

*Depolarization in the periphery*

Depolarization of PAFs is the rule, but contradictions are found. The cell bodies of A$\alpha\beta$, A$\delta$, and C fibers are all depolarized by GABA and $GABA_A$ agonists, but depolarization is greater in the cell bodies of A$\alpha\beta$ and A$\delta$ than in C fibers of the intact nerve DRG preparation (Desarmenien, Santangelo et al., 1984). In contrast, cells with T-type $Ca^{2+}$ currents (most often A$\delta$ and C neurons), the depolarization is triple that of similarly sized cells (Aptel et al., 2007).

How can GABA be both depolarizing and be inhibitory? Carlton, et al. (1999) has proposed that because the chloride equilibrium potential in peripheral afferent nerves is near -30mV, the transmembrane chloride flux from GABA is in the extracellular direction and the cell is depolarized. Conducted action potentials are smaller in amplitude; hence less

algogenic neurotransmitters are released. With increased concentrations of GABA, the extracellular chloride flux is increased to the point of nociceptor activation (Carlton et al., 1999).

Moreover, in a few locations in the CNS, GABA-induced depolarization is inhibitory. In the continued presence of GABA, accommodation of the threshold for impulse generation occurs from putative inactivation of $Na^+$ and $Ca^{2+}$ voltage-dependent inward currents (Monsivais & Rubel, 2001). Since the cell is unable to repolarize, the voltage gated cation channels can not reprime and remain in the inactivated phase. A similar arrangement may apply to PAFs.

Also, an observation made in cortical neurons is that a cell is not restricted to only depolarization or hyperpolarization from GABA exposure, but differential polarities and amplitudes of polarity occur along the axon, cell body and dendrite (Khirug et al., 2008). A similar effect is possible in the periphery and may help to explain cell body and central terminal depolarization, but inhibition of signals in the distal peripheral process.

*GABA-induced excitation*

GABA is also known to possess excitatory actions in mature PNS structures. Bhisitkul, Villa, and Kocsis (1987) observed an increase in electrical excitability of dorsal root cells and whole nerves of the rat. Changes in excitability were measured as a decrease in stimulus intensity to achieve the same CAP amplitude after GABA, compared to before GABA exposure. Morris, et al. (1983) observed a similar effect in the cat.

*Relationship of GABA, calcium, and nociception*

Though activation of $GABA_A$ receptors leads to the direct action of $Cl^-$ flux, in a subset of PAN an indirect link to calcium ion movement may influence excitation and

nociception. Aptel et al., (2007) found GABA to have excitatory actions on a subset of thinly myelinated and unmyelinated cultured DRG cells, putatively from A$\delta$D-hair, A$\delta$ nociceptors, and C nociceptors. GABA and MUS-induced activation of $GABA_A$ receptors depolarizes cell membranes sufficiently to generate action potentials and evoke a net increase in intracellular $Ca^{2+}$ in neurons expressing T-type $Ca^{2+}$ currents. Due to their activation at near resting membrane potentials, T-channels are thought to modulate cellular excitability, rather than hold a role in synaptic transmission (Aptel et al., 2007). Pathiranthna et al. (2005) found positive GABA allosteric neurosteroids simultaneously blocked T-type $Ca^{2+}$ and $Cl^-$ currents in acutely dissociated DRG cells. In animal behavior studies, intradermally administered neurosteroids possessed pronounced anti-nociceptive properties that were only partially blocked by BIC. These authors suggest the presence of intracellular $Ca^{2+}$ tonically inhibits $GABA_A$ $Cl^-$ channel activity and the blockade of $Ca^{2+}$ currents disinhibits $GABA_A$ $Cl^-$ channel activity (Pathirathna et al., 2005).

Two mechanisms come to mind to explain this apparent dichotomy: 1) GABA binding at $GABA_A$ receptor induces inward $Ca^{2+}$ current and subsequent action potentials in a subset of thinly and unmyelinated neurons; and 2) GABA allosteric neurosteroids co-bind at $Ca^{2+}$ and $Cl^-$ channels for potent peripheral analgesic effects in this same neuronal subset. The common message from these two studies is that a subset of DRG cells (most likely nociceptors) require $Ca^{2+}$ current blockade for GABA to inhibit neuronal excitability.

## Pro- and Anti-nociceptive GABA Effects in Animal Models

So far it has been established that GABA and functional GABA receptors are expressed in skin and PAFs, and that peripheral GABA and $GABA_{A,B}$ receptors share some pharmacological and physiological properties with their counterparts in the CNS. These

observations alone do not rationalize the study of GABA as anti-nociceptive, but a number of animal behavior studies are very supportive.

*Pro- and anti-nociceptive effects of $GABA_{A-C}$*

Carlton, Zhou, & Coggershall (1999) demonstrated a reduction in formalin-induced nociceptive behaviors of paw licking and lifting and paw withdrawal from radiant heat after intraplantar injection of low concentration MUS, but a pro-nociceptive effect from a higher concentration in the rat. Reis et al. (2007) demonstrated intraplantar injection of MUS reduced rat nociceptive behavior from a prostaglandin $E_2$ ($PGE_2$) stimulus. MUS was antagonized by BIC and PITX, but not by saclofen, TPMPA, or $K^+$ channel blockers. Reis and colleagues did not observe a pro-nociceptive effect with increased concentrations.

Reis & Duarte (2006, 2007), in a similarly designed study, applied a $PGE_2$ stimulus to examine $GABA_B$ and $GABA_C$ receptor activation. They demonstrated a concentration-dependent anti-nociceptive effect from BAC, an effect antagonized by saclofen and $K^+$ channel blockers, but not BIC or TPMPA. They also demonstrated a concentration-dependent anti-nociceptive effect in PGE-induced behaviors from intraplantar injection of CACA, an effect antagonized by TPMPA and PITX. Because $GABA_C$ receptors are primarily restricted to the visual system, it was possible CACA was administered at a concentration that activated neuronal and glial $GABA_A$ receptors, induced local release of GABA, or upregulated glial GABA transporters (Johnston, 1996b).

*Pro- and anti-nociceptive effects of neuroactive allosteric steroids*

Ocvirk and co-workers demonstrated that allopregnanolone and other positive GABA receptor allosteric steroids are anti-nociceptive in the second phase of formalin-induced pain, an effect completely blocked by BIC. These authors co-administered the steroid and BIC

subcutaneously and admitted to not being able to draw conclusions of the origins of the effect as peripheral, supraspinal, or spinal (Ocvirk et al., 2008). Similar to the finding of Carlton, et al. (1999), an inverse or negative modulatory effect was observed; at higher concentrations, neurosteroids were pro-nociceptive.

## Pathophysiology and Therapeutics of GABA

Both GABA synthesis disruption and $GABA_B$ receptor mediated inhibition of myelination are associated with human heritable painful disorders. Recognition of GABA related disorders responsive to GABA interventions lends a modicum of support to the notion of GABA-induced analgesia. However, the activity of GABA most likely is as trophic agent rather than as a signaling molecule. Supporting evidence of GABA-based therapeutics is meager at best.

### *Pathophysiology of GABA synthesis and $GABA_B$ receptor function*

No deficiencies or structural polymorphisms leading to lack or gain in function of human GABA receptors or of agents of GABA synthesis, storage, transport, and metabolism have been reported. A few reports relate increased human $GAD_{65}$ antibody production and peripheral myelination protein dysregulation in $GABA_{B1}$ -/- mice to the painful neurological disorder of polyneuropathy.

An abnormal increase in $GAD_{65}$ antibodies is associated with type-1 (insulin dependent) diabetes and stiff-man syndrome, a rare disease of severe, progressive axial and lower extremity muscle stiffness and spasm. Autoantibody binding to GAD inhibits local synthesis of GABA and availability to activate $GABA_A$ and $GABA_B$ receptors. Peripheral blood T-cell antibody influence on $GAD_{65}$ is thought to contribute to the destruction of islet-cells of type 1 diabetes and the impaired neurotransmission of stiff-man syndrome (Lohmann

et al., 2000). An association of $GAD_{65}$ antibodies with diabetic neuropathy has not been made. In individuals with type-1 diabetes and stiff-man syndrome, the $GAD_{65}$ autoantibodies are strongly associated with the HLA DQB1*0201 allele (Pugliese et al., 1993). BAC, a $GABA_B$ agonist, and benzodiazepines, allosteric $GABA_A$ modulators, are effective interventions to alleviate the symptoms of rigidity, pain, and myoclonus for the individual with stiff-man syndrome (Meinek et al., 1994). The response to GABA agonists cannot be assumed to be mediated only in the sensory PNS.

An association between $GABA_B$ receptor-mediated inhibition of peripheral myelin protein 22 (PMP22) expression and human diseases of dysmyelination has been suggested (Magnaghi et al., 2008). PMP22 is a minor but essential constituent of Schwann cell proliferation, differentiation, and maintenance of stable compact myelin. A marked over- or under-expression of the PMP22 protein leads to a reduced population of myelinated fibers (Magnaghi et al., 2008). BAC-induced activation of cultured Schwann cell $GABA_B$ receptors reduces cell proliferation and decreases over-expression of PMP22. Neuronal injury is often associated with Schwann cell proliferation. For Schwann cells to exert neuroprotective and antineurogenic actions on ensheathed PAFs, they must cease proliferation and progress to a cellular differentiation phase of development (Magnaghi et al., 2004).

$GABA_{B1}$ -/- mice upregulate and accumulate PMP22 and are hyperalgesic. These mice have smaller diameter PAFs with thinner myelin sheathing, an increase in calcitonin gene-related peptide (CGRP), but a decrease in neurofilament protein 200 (NF200)-positive fibers, and smaller DRG cell bodies. CGRP expression is associated with a subset of heat responsive nociceptors (Mendell, Albers, & Davis, 1999), and NF200 is a marker of

myelination. In the skin, no increase in C-fiber peripheral terminals was observed. An assumption was made that the increase in thinly myelinated and small caliber fibers was from A$\delta$ nociceptors with an associated reduction in large myelinated fibers (Magnaghi et al., 2008).

Duplication and point mutations of the PMP22 gene are associated with congenital Charcot-Marie-Tooth, hypomyelinating, and Dejerine-Sottas polyneuropathies (Magnaghi et al., 2008). BAC is one effective treatment for the neuropathic pain of peripheral dysmyelination (Hoffman, Jensen, Abresch, & Carter, 2005), although the possibility exists that BAC is acting on spinal and/or supraspinal $GABA_B$ receptors or has an action unrelated to $GABA_B$ receptor activation.

*Therapeutic significance of GABA*

Meager evidence exists for a modern Western therapeutic use for peripheral GABA. No reports are found of GABA application to the human blister base. The blister base method for experimental testing of anti-inflammatory and analgesic agents is the creation of a dermal blister from exposure to a chemical irritant and deliberate debridement of the separated epidermis. A similar technique to the blister base method has been developed in the hairless mouse. Denda et al. (2002, 2003) found $GABA_A$ agonists accelerate epidermal barrier recovery and prevent epidermal hyperplasia following tape stripping and acetone treatment of skin. These effects were blocked by BIC, but not by saclofen. GABA has also been found to enhance surgical wound healing by inflammation reduction, fibroblast proliferation, and stimulation of growth factor expression (Han et al., 2007) .

Duthey and coworkers reported that BAC attenuates the inflammatory effects induced by the contact allergen 2,4-dinitrofluorobenzene (DNFB). They observed a significant

decrease in observed tissue edema, histological evidence of significantly lower tissue infiltration by leukocytes, and a decrease in tumor necrosis factor expression in mice and humans (Duthey, Diehl, Hubner, Pfeffer, & Boehncke, 2008).

## Summary

GABA and GABA receptors are expressed by a small percentage of PAFs, and by keratinocytes and glia. GABA depolarizes peripheral neuronal processes and cell bodies via $GABA_A$ receptor activation, and animal nociceptive behaviors are generally suppressed by $GABA_{A\text{-}C}$ agonists. Conversely, GABA induces pro-nociceptive animal behaviors at higher concentrations, excitatory effects in cells with T-type $Ca^{2+}$ channels, and desensitizes cells expressing $GABA_A$ receptors with prolonged exposure. Lack of $GABA_B$ receptors in knock-out mice may preferentially promote the development of C and Aδ neurons over heavily myelinated fibers. Minimal human clinical evidence supports the effectiveness of GABA in pain reduction, but pharmaceutical GABA receptor agonists and modulators are effective in treating symptoms of neuropathies. The aggregate of evidence supports the further study of peripherally administered GABA as a neurotransmitter, signaling and trophic molecule to interrupt and prevent nociception in animals, pain in humans, and to enhance the healing of surgical wounds

# CHAPTER 3

# MATERIALS AND METHODS

## Materials

The model for the electrophysiological experiments described below was the *ex vivo* mouse skin-nerve preparation. Electrical, thermal, mechanical, and chemical stimulus instruments were designed and used to measure GABA effects on cutaneous PAFs. Experiments were tailored to maximize the chance to observe GABA effects and to challenge or support electrophysiological and animal behavioral findings presented in the literature review.

For clarity, the following conventions are followed. The full extent of the PAN is from the peripheral terminal(s) in cutaneous or other tissue structures to the central terminal(s) in the CNS (Burgess & Perl, 1973). The term 'fiber' refers to a PAF unit that is comprised of a peripheral process, peripheral terminals and/or sensory organ bodies, and the receptive field, but not the cell body in the DRG, central process in the dorsal root, or the central terminal in the spinal cord. In this project, the responses of a fiber are recorded from a single peripheral process contained within a bundle of PAFs in contact with the recording electrode. Accordingly, a 'bundle of fibers' refers to the collection of peripheral processes in contact with the recording electrode.

*Animals*

All experimental and animal care procedures conformed to the Department of Laboratory Animal Management guidelines and were approved by University of North Carolina Institutional Animal Care and Use Committee Application 05-342.0C. Efforts were made to minimize the number of animals used and duration of the non-survival surgery in these experiments. The juvenile and adult, male and female C57Bl6J mice used in this study were obtained from Charles River Laboratory, Raleigh, NC.

The C57Bl6J strain was selected because mechanical and heat sensitive C fibers display a greater number of action potentials in response to noxious heat and lower noxious heat thresholds than similar fibers of other mouse strains. The rationale for the decision was that a less damaging thermal energy from a novel heat flux instrument developed for this exploratory study would be required to excite these fibers. No significant differences in sensitivity to noxious mechanical stimuli have been recognized among strains (Mogil et al., 2005).

*Solutions and agents*

Dissection and superfusion of the skin-nerve preparation was carried out in a modified synthetic interstitial fluid (SIF) solution (Bretag, 1969). SIF was prepared from: 123 NaCl, 3.5 KCl, 0.70 $MgSO_4$, 2.0 $CaCl_2$, 9.50 sodium gluconate, 1.70 $NaH_2PO_4$, 5.50 glucose, 7.50 sucrose, and 10.0 HEPES in mM, pH adjusted to 7.40 with NaOH, osmolarity adjusted to 290 osmoles/liter with sucrose, oxygenated, and superfused at a rate of 10 ml per min. The SIF temperature for dissection (17 $^0$C) and superfusion (32 $^0$C) was maintained by a Peltier device (CH module, Cell MicroControls, Norfolk, VA). GABA was prepared fresh in SIF for every experiment. Chemicals were obtained from commercial suppliers and prepared

in SIF. Table 3 (Appendix F) summarizes agents and concentrations used for electrophysiological recordings.

## Model Preparation

*Skin-Nerve preparation*

The model for this project was an *ex vivo* skin-nerve preparation as developed and described in detail by Reeh (1986). The *ex vivo* preparation controls variables that interfere with the study of the physiology of receptors (examples: circulating neuroactive agents, reflex movement). The critical success of this preparation rests with the facts that receptor behavior remains unchanged in electrophysiological experiments lasting up to 12 hours, and after 24 hours of storage at 4$^{o}$C in pre-gassed solution a preparation demonstrates no obvious receptor behavior changes (Reeh, 1986).

Animals were anesthetized with an intraperitoneal injection of ketamine (100 mg/kg) and xylazine (10 mg/kg). Surgical excision with the aid of a dissection microscope commenced when animals were obtunded to sensory stimuli. Skin in continuity with at least a 10 mm length of nerve was dissected free from the right (sural) or left (plantar) hind paw. Perineurium, tendons, muscles, and vascular structures were debrided from the skin and nerve trunk, in a bath of circulated, chilled, oxygenated SIF. The dissociated preparation was allowed to rest for several hours prior to electrophysiological examination in order to recover from the trauma of dissection (Maurer, Bostock, & Koltzenburg, 2007).

The skin-nerve preparation was placed corium side up in a dual compartment recording chamber. Advantages and disadvantages of this arrangement are discussed below. The dermis was exposed to laminar SIF flow and the epidermis was pinned without tension against the Sylgard (Dow Corning) basement of the organ compartment. The organ

compartment was superfused by gravity-fed inflow of SIF and waste solution outflow was removed by negative pressure suction. The nerve portion of the preparation was passed through a channel into a second compartment filled with a bilayer of SIF and mineral oil. The bilayer serves to isolate a single gold, hook-shaped, extracellular recording electrode suspended in mineral oil from a SIF-submerged gold reference electrode. The proximal end of the nerve was elevated onto a small mirrored palette within the oil bath, and dissected free of epineurium and perineurium. Sections of nerve were progressively divided from the main nerve trunk using sharpened forceps (0.05 x 0.02 mm mirrored Dumont #5 forceps, Fine Science Tools), and the finest bundle of fibers was placed on the recording electrode.

*Advantages and disadvantages of skin orientation in organ bath*

The corium-up orientation of the skin was chosen to facilitate hydrophilic drug absorption and proton sensitivity assessment. Other advantages of a corium-up arrangement are better coverage of the irregular skin patch contours by SIF and a better surface to anchor the skin and to press against with mechanical stimulation instruments. In the corium-down orientation, oxygen and SIF are delivered only to the dermal surface of the skin patch suspended on a semi-rigid, perforated, plastic grid. Disadvantages of corium-up orientation are the inability to see identifying epidermal features (example: guard hairs, Merkel discs), and the unnatural application of a mechanical or thermal stimulus to an internal tissue and not the epidermal surface of the RF.

As a part of evaluation and refinement of the methods for this project, the latter disadvantage was briefly examined. A comparison was made of corium and epidermal mechanical thresholds of four high mechanical threshold fibers. Von Frey (VF) mechanical threshold and CV from search electrode stimulation were first measured from the corium

surface. Mechanical threshold measurement with VF filaments and the method for CV calculation are discussed in later sections. The entire skin preparation was inverted in the organ bath to expose the epidermal surface. VF threshold and CV were again measured. Three of the four fibers had no difference between corium and epidermal mechanical thresholds. The remaining fiber had a difference of only one ordinal filament in the VF sequence between corium and epidermal surface. Equal epidermal and corium CVs and identical action potential shapes indicated that the epidermal and corium RF of the same fiber was examined.

*Cutaneous nerve selection process and RF identification*

Plantar and sural nerves were used in this project. The cutaneous distribution of the plantar nerve offers the advantage of a relatively flat skin surface which easily accommodates mechanical instrumentation unlike the sural distribution with its extensive ankle contours. However, the dissection and debridement of the plantar skin-nerve preparation requires approximately 2.5 hours compared to 1.5 hours for the sural nerve.

Unlike the plantar nerve, the sural nerve provides the opportunity to study glabrous and hairy skin receptors. The cutaneous distribution of the sural nerve follows the glabrous and hairy border of the lateral aspect of the fifth toe, and foot, and the hairy skin of the lateral ankle and lower hind limb. The plantar nerve distribution is primarily of glabrous skin of the hind paw plantar surface. To confirm the skin type at the end of the experiment, a pin was used to penetrate the center of the fiber's RF. The skin was inverted in the recording chamber and the skin type determined. Figures 6, 7, and 8 (Appendix G) summarize mouse plantar and sural nerve RF distribution of single fibers from the GABA studies and control studies.

## Single Fiber Activity Isolation and Characterization

*Isolation of single fiber activity*

Two strategies were employed for the isolation of single fiber activity captured by extracellular recording techniques. The success of the first method was dependent on culling extraneous fibers from the recording electrode, and the second method by restriction of the number of mechanical RFs within a selected area of skin to that of a solitary responsive fiber.

In the first strategy, a laboratory-constructed suction electrode (silver/silver chloride electrode isolated from a reference electrode by a glass capillary tube), was secured by gentle suction to the nerve at least 10 mm distal to the recording electrode. Nerves were excited by a square wave generator (Grass S88) with a pulse duration (0.01 to 0.5 milliseconds (ms)) and voltage (1.5 to 10 V) to test for single fiber activity and to measure the electrical threshold and conduction latency. The measurement of electrical threshold and conduction latency is discussed in a later section. Interstimulus intervals exceeded 10 seconds (s). In a few cases, a distinctive impulse shape served to differentiate the activity of several single fibers. Signals were amplified (1000x) and filtered (> 2000 hertz (Hz); < 50 Hz), viewed on an oscilloscope, transmitted over an audio headphone, and digitized and stored using pClamp 10.2 software (Molecular Devices, Union City, CA).

The skin was mechanically stimulated with a glass probe or VF to determine the approximate mechanical RF size, or was thermally stimulated with heated or cooled SIF or a diode laser to locate a thermal RF. Heated or cooled irrigation of a RF within the low volume organ bath frequently led to unstable recording conditions and was seldom used after laser acquisition. VFs and laser techniques are described in later sections. Fibers that were

unresponsive to both mechanical and noxious heat stimuli were not selected for study of GABA-induced changes in activity.

The alternative isolation strategy made use of a laboratory-constructed search electrode to locate an electrical RF. The search electrode was constructed from an epoxy insulated tungsten electrode (A-M Systems, Inc. 0.010 inch, 5 megaohms) encased in a stainless steel reference electrode. An observation made in the development of the methods of this project was the difficulty of locating the electrical RF of mechano-sensitive fibers with very large RFs in comparison to the relative ease of locating the electrical RF of mechano-sensitive fibers with small RFs. This observation is in agreement with Lawson et al. (2008) where a similar search electrode technique excited no fiber with a very large RF. After an electrical RF was identified, the mechanical and/or thermal RF was located and marked.

To exclude extraneous signals and confirm complete correspondence between impulses generated by electrical stimulation of the fiber and mechanical or thermal stimulation of the RF, the action potential shape, amplitude, and duration were analyzed on-line prior to further characterization of single fiber receptive properties.

*Characterization of single fibers*

Full characterization of single fibers was completed in stages. CV, mechanical sensitivity, and in a few cases, thermal sensitivities were examined prior to agent testing. In most cases sensitivity to thermal and chemical stimulation was examined after the GABA treatment condition in order to minimize fiber sensitization.

Single fibers were classified by CV, glabrous or hairy skin type, and responses to sensory stimuli as collectively described in small mammals (Bessou & Perl, 1969; Burgess &

Perl, 1967; Horch, Tuckett, & Burgess, 1977; S. M. Lawson, Crepps, & Perl, 1997; Leem, Willis, & Chung, 1993; Lynn & Carpenter, 1982; Shea & Perl, 1985; Spray, 1986), and specific to the mouse (Blunk, Seifert, Schmelz, Reeh, & Koppert, 2003; Cain, Khasabov, & Simone, 2001; Koltzenburg, Stucky, & Lewin, 1997; J. J. Lawson, McIlwrath, Woodbury, Davis, & Koerber, 2008).

*Characterization by conduction velocity*

First, single fibers were classified by CV. CV was calculated as the nerve length in meters, from the stimulating or search electrode to recording electrode, divided by the conduction latency, in seconds. Conduction latency was measured as the time in ms from the start of the stimulus artifact to the start of the first upward deflection of the evoked impulse. For rapidly conducting fibers, the duration of the stimulus was varied to differentiate the stimulus artifact from the first upsweep of the action potential. Conduction latencies were averaged from three consecutive trials. During the experiment, the nerve length between electrodes was estimated from millimeter (mm) markings in the recording chamber. At the end of the experiment, the portion of nerve length between the stimulating, or search electrode and recording electrodes was measured *in situ*.

Fibers with CVs greater than 10 m/s were classed as A$\beta$, 1.01-10 m/s were classed as A$\delta$, and less than 1.01 m/s as C. A$\beta$ includes fibers associated with Ruffini endings and Merkel cells and signal stimulus velocity and position, fibers associated with hair follicles and signal velocity distortion; and fibers associated Meissner's corpuscles and signal velocity. A$\delta$ includes fibers associated with down hairs and signal slow moving distortion and nociceptors and signal potential and actual tissue damage. C includes fibers that signal warming, cooling, very slow tissue deformation, and potential and actual damage (Birder &

Perl, 1994). While fibers with CV in the A$\beta$ and A$\delta$ ranges most often fitted into distinct categories based on responses to innocuous and noxious natural sensory stimuli, fibers with CV in the A$\delta$ and C ranges were not as easy to differentiate. Wenk, Brederson and Honda (2005) reported a fourth category (C/A$\delta$) of rat *ex vivo* fibers with CVs of 1 to 3 m/s. CAP of whole nerves demonstrated no overlap of A$\delta$ and C components in agreement with the CAP presented in Figure 1 (Appendix A), but 13 of 107 not inflamed fibers had CV between 1 and 3 m/s. In the mouse, the categorical divide between A$\delta$ and C fibers is 1 m/s (Price et al., 2001) or 1.2 m/s (Koltzenburg et al., 1997). With this in mind, a fourth category of C/A$\delta$ was created for fibers with CVs between 1.01 and 1.2 m/s.

*Characterization by responsiveness to mechanical stimuli*

After characterization by CV, single fibers were characterized by the sensory stimuli they responded to best. Mechanical thresholds were estimated by use of ordinal-scaled, calibrated VF (Semmes Weinstein Von Frey Aesthesiometer, Stoelting, Wood Dale, IL). Mechanical threshold was measured in kilopascals (kPa) and defined as the least applied filament pressure capable of evoking more than two impulses. Applied pressure was calculated in kPa (pascal: Pa = Newtons/meter$^2$ = kilograms/meter·second$^2$). Average actual measurements for force and cross-sectional area were obtained from Stoelting catalog 58011. Table 4 (Appendix H) summarizes VF conversion factors and units of measure. The entire range of VF filaments was not used. Repetitive RF stimulation with a VF stimulus ≥ 786 kPa almost always resulted in a visibly traumatized area of corium, and VF < 33 kPa could not reliably penetrate the surface tension of the organ bath without buckling.

Fibers were classified as having a high or low mechanical threshold similar to the classification used in the rat skin-nerve preparation (Steen & Reeh, 1993). Kolzenburg et al.

(1997) measured an average force of 5.6 millinewton (mN) for high mechanical threshold A$\delta$ fibers (AM) and similar results for presumed C polymodal nociceptors. A force of 5.6 mN roughly equaled the pressure generated between the 160 and 209 kPa VF filaments used in this project. A threshold of VF < 160 kPa was deemed low threshold in this study. The results of a survey conducted to establish the suitability of the diode laser technique also suggested the boundary for high and low mechanical threshold pressure as 160 kPa. Two C fibers sensitive to noxious heat, protons, and laser irradiation had VF thresholds as low as 160 kPa. The results of the survey of laser properties and laser-sensitive fibers are reported in Chapter 4.

An examination was made to determine responsiveness to: 1) stretch, indentation, retraction, slow or rapid vertical motion from a hand-held glass probe or fine brush; 2) adaptation; 3) ongoing activity; and 4) after-discharges. In combination with CV, hairy/glabrous skin type and responsiveness to various high or low intensity mechanical stimuli, single fibers were categorized as rapid adapting (RA) or slow adapting (SA) to mechanical stimuli. SA-mechanoreceptors respond continuously and best to a constant stimulus (examples: indentation, distortion, stretch) and RA-mechanoreceptors respond briefly and best to a change in stimulus (examples: vibration, velocity and displacement, accelerated movement) (Birder & Perl, 1994; Horch et al., 1977). No low threshold rapid adapting mechano-sensitive fibers were examined in this study due to the difficulty of statistical analysis of their limited responses of only one or two action potentials.

Fibers classified by CV and responsiveness to natural stimuli were categorized into the following groups: A$\beta$-low mechanical threshold SA (A$\beta$ SA), A$\delta$-low mechanical threshold (A$\delta$ LTh); A$\delta$-high mechanical threshold (A$\delta$ M); C-high mechanical threshold

(CM); C-high mechanical threshold and noxious heat (CMH); C-high mechanical, noxious heat, and protons (CMHA); and C-high mechanical threshold, noxious heat and cold, and protons (CMHAC). Methodology for testing chemical and thermal sensitivity follows.

*Fibers sensitive to noxious heat and mechanical stimuli*

Frequently, fibers requiring ≥786 kPa of pressure had inconsistent responses after several trials of mechanical stimulation. Consequently, very high mechanical threshold fibers were examined for noxious heat sensitivity and reserved for Study IV or excluded from further study. A limited number of cutaneous nociceptors are insensitive to mechanical stimuli, and are better stimulated by noxious thermal and chemical stimulation (J. J. Lawson et al., 2008; Meyer, Davis, Cohen, Treede, & Campbell, 1991). This may not be the case with all mechanically insensitive afferent fibers. Some very high threshold mechanoreceptors may initially fail to respond to heat, but develop ongoing activity with repeated very high temperature stimulation (Shea & Perl, 1985).

C fibers that briskly responded to heat and to mechanical stimuli were selected for either mechanical or laser study dependent on available instrumentation. As described in Chapter IV, A$\delta$ nociceptors were not subject to laser instrumentation for GABA testing because of low discharge frequencies.

*Mapping of receptive field*

The mechanical RF was located and mapped with a brush, VF, or glass probe. In cases where the electrical RF was mapped, most mechanical RF and electrical RF overlapped. The mechanical RF was tested for the presence of 'hot-spots' of increased activity. A 'hot-spot' does not respond to innocuous pressure or skin movement, does

demonstrate graded responses to shearing forces and punctate pressure, and is unresponsive in the areas between 'hot spots' to suprathreshold mechanical stimuli (Birder & Perl, 1994).

Prior to GABA testing, the most responsive spot(s) of the electrical, thermal and/or mechanical RF was marked by an off-side placement of colored glass bead fragment(s) (0.25 mm diameter). The C57Bl6J mouse glabrous (pink) and hairy (black) epidermal border is visible through the corium surface with the aid of light microscopy, and the location of the RF was estimated as hairy or glabrous. Glabrous and hairy skin differences in sensitization and heat sensitivity are well recognized (Campbell & Meyer, 1983; Treede, Meyer, Raja, & Campbell, 1995).

*Characterization by responsiveness to chemical and thermal stimuli*

After GABA testing, fibers selected for electrical, mechanical, or thermal instrumentation were examined for thermal and chemical sensitivity by one of two similar methods, a ring reservoir and an inflow/outflow reservoir. In the first, a laboratory constructed small plastic ring (2mm diameter) with an inverted external diameter Sylgard lip was secured over the RF and sealed with Baysilone high viscosity paste (Dow Corning). The SIF within the ring reservoir was replenished with gassed SIF every minute. Thermal and chemical stimuli of iced SIF (2 $^{o}$C), heated SIF (53 $^{o}$C), and HCl-acidified SIF (pH $\leq$ 4.0) were sequentially hand-instilled and fiber responses were recorded. Figure 9 (Appendix I) illustrates the ring reservoir.

The second method made use of a laboratory constructed reservoir with a Sylgard lip and gravity inflow and suction outflow ports. Similar to the ring reservoir, it was placed over the RF and the same thermal and chemical stimuli were remotely instilled by syringe. A disadvantage of the inflow/outflow reservoir was its awkward shape. An advantage of the

reservoir was the remote application of the stimulus solutions avoided electromagnetic interference (EMI) from the researcher's movements within the Faraday cage. Figure 10 (Appendix I) illustrates the inflow/outflow reservoir for thermal and chemical stimulation *in situ*.

*Experimental design, variables, and statistical analyses*

The repeated measures design of the study was consistent throughout the study phases and was represented as: $\boldsymbol{O_1\ X\ O_2}$ for most studies and $\boldsymbol{O_1\ X_1\ O_2\ X_2\ O_3}$ for the wash-out and increased concentration conditions. The observation (***O***) represents the neural response and the treatment (***X***) was GABA exposure or wash-out of GABA. This extracellular study limited the variables to a change in the frequency of action potentials, the timing of action potentials, and the amplitude of the stimulus necessary to induce action potentials. The project was exploratory in nature with the goal to determine the best way to study GABA in the PNS. Mouse single fibers were electrically and mechanically, thermally, or chemically stimulated and differences in their responses during treatment with GABA were observed. Descriptive data were presented as means ± standard error.

## Measurement Instrumentation: Specific Aim 1

In the course of this project, fibers were often selected for a measurement technique based on the availability of measurement instrumentation. Over several years, instruments were purchased or developed and 'scaled down' to an appropriate size to investigate mouse response properties. Adequate electrical instrumentation was the first to be implemented and presumed noxious heat from a diode laser was the last. A total of 11 measurement methods were implemented over the course of this project in the comprehensive search for peripheral effects of GABA exposure on PAFs.

*Study I: Non-activity dependent electrical stimulation*

Electrical threshold and CV were measured before and after GABA testing when feasible. Many fibers, included in Study I, were also subjected to mechanical stimulation. As previously described, electrical stimuli of an adequate duration and amplitude to generate a discrete action potential were delivered by either a suction electrode lightly attached to a nerve fascicle or the search electrode applied over the RF. Study I was designed to examine non-activity dependent changes in CV and electrical threshold. Electrical interstimulus intervals exceeded 10 s.

*Study II: Activity dependent electrical stimulation*

Repetitive cutaneous electrical stimulation is not naturally encountered by most mammals, but activity dependent changes in CV and electrical threshold may model discharge frequency code changes found in chronic injury and neuropathic patients (De Col, Messlinger, & Carr, 2008). In the comprehensive search for peripheral GABA effects, several measurement methods not included in the project proposal were designed and implemented. One method in the broader search for GABA effects was an experiment designed to measure activity dependent changes in C-fiber CVs.

A full discussion of activity dependent changes in CV is beyond the scope of this discussion, but a few points are important. The CV of a resting fiber (one not having undergone recent stimulation), is stable and is directly related to axonal diameter and degree of myelination at physiological temperature (Light & Perl, 1993). In addition, neurons with unmyelinated fibers demonstrate unique activity dependent changes by group classification. Sustained electrical activation of nociceptors leads to a progressive slowing of CV, decrease in excitability, and eventual conduction block, while innocuous thermoreceptors show only

an initial mild slowing of CV (Raymond, Thalhammer, Popitz-Bergez, & Strichartz, 1990; Thalhammer, Raymond, Popitz-Bergez, & Strichartz, 1994). Nociceptors demonstrate a decrease in CV of 29%, innocuous cooling receptors of 11%, and mechanoreceptors and sympathetic efferents of 14% (Gee, Lynn, & Cotsell, 1996). The fundamental mechanisms driving this variability are unclear. Postganglionic sympathetic efferent fibers demonstrate latency shifts of initial CV slowing, but rapid recovery with prolonged pulsed stimulation (De Col et al., 2008).

To test for activity dependent shifts in conductivity, a protocol as described by de Col et al. (2008) was used. Single fibers were stimulated with 2 Hz frequency for 180 s and 0.5 Hz for 600 s by a suction stimulating electrode gently applied to the RF of the fiber. The time features of the protocol allowed for observable slowing of CV and an adequate duration for conduction block development and controlled recovery. The RF of the fiber was not electrically stimulated for a minimum of 5 minutes (min) before initiation of frequency stimulation. The CV of the fiber was allowed to recover to the pre-test condition before superfused application of GABA and initiation of post-test stimulation. Superfusion of GABA for 2 min began before and continued throughout the high frequency stimulation. Variables examined were percentage change in CV (relative change $1^{st}$ action potential to $360^{th}$) of baseline and during GABA exposure, change in electrical threshold, and time of conduction block onset. After examination for conduction shifts, the fiber was characterized for mechanical, thermal, and chemical sensitivity, as previously described. Of note, the chamber used in this study is not optimal for examination of agent effects on graded potentials. The recording electrode and most proximal fiber end are isolated from agent contact by the oil layer. A sucrose gap chamber is more suitable for this purpose (Stampfli,

1954). However, in this project, three-fourths of the nerve fiber length was exposed to GABA and only one fourth had no exposure to GABA.

*Study IIIa, IIIb, and IIIc: Mechanical stimulation*

Several instruments were utilized to test for either GABA-induced changes in mechanical threshold or discharge frequency from a constant mechanical stimulus. Recording chamber and skin-nerve preparation size, and cost constraints added to the level of complexity in the development of appropriate measurement instrumentation. Proprietary constant force and pressure instruments, with the exception of VF filaments, proved to be too bulky for the 'scaled down' organ bath. Consequently, laboratory-constructed instruments were developed and implemented to provide a suprathreshold pressure stimulus.

To simply measure a comparative GABA-induced change in mechanical threshold (Koltzenburg et al., 1997), or change in discharge frequency in response to a suprathreshold force (Kwan et al., 2006; Potenzieri, Brink, Pacharinsak, & Simone, 2008), hand-held VF filaments were used (Study IIIb and IIIa respectively). Multiple attempts were made to mobilize VF filaments with an XYZ micromanipulator, but the standard length of the filament (8 cm) plus the micromanipulator anchor exceeded the available space between the microscope and the organ bath.

In a first series of experiments, a VF was used as a supra-threshold (Study IIIa), constant pressure mechanical stimulus. The filament capable of evoking an observable discharge rate was applied twice for 1.5 s, with an interstimulus interval of 15 s, and the sum of the action potentials of the two trials was averaged. In the event the mechanical threshold increased to such a degree that $\leq 2$ impulses were evoked, a higher pressure filament was used for the remainder of testing. Because nociception is the primary focus of this project, a

simple modification to the regimen was developed to refine the examination of high mechanical threshold fibers. Four interval-scaled hand-held VF with approximate constant pressures of 168, 333, 509, and 684 kPa were used. The fiber was deemed to have enhanced, suppressed, or no change in mechanical sensitivity after GABA application. Fibers were classified as GABA-sensitive when the change in the posttest response compared to the pretest baseline exceeded 44%, which would represent a greater than two standard deviation change had sufficient, normally distributed data from an independent random sample been collected (Potenzieri et al., 2008; Wenk, Brederson, & Honda, 2006). Recovery from a GABA-induced response was recognized as a 50% return to baseline (personal communication, Christopher Honda, 2007).

In Study IIIb, VF thresholds were determined prior to and at intervals of 3 and/or 5 min of GABA exposure. In some cases of prolonged stable recording conditions, VF threshold was measured following a SIF wash-out period. A mild threshold change was defined as a progression or regression of one ordinal filament in the sequence of VF filaments to elicit a response of $\geq 2$ action potentials. A substantive change was defined as progression or regression in the VF series of $\geq 2$ filaments. All fibers included in Study IIIa were also studied in Study IIIb.

Handheld VFs were fraught with inherent error (example: vibration from operator hand). As the project evolved several remotely operated mechanical stimulators were constructed and implemented (Study IIIc). Attempts at remote RF mechanical stimulation were complicated by the inability to obtain a force generator that could displace a probe tip > 1 mm and not damage the RF during placement. Early in the project, a constant force device was constructed from a VF attached to a miniature mobile phone loudspeaker and driven by a

waveform generator (Wavetek 112). Advancement and retraction of the filament, in the form of a square-shaped pulse, was applied to the most responsive spot in the RF. Maximal probe displacement with this device was only 1mm. The loudspeaker device proved to generate insufficient pressure to activate any fibers except those with the lowest of mechanical thresholds, and was abandoned.

Late in the project, the second mechanical stimulation measurement method was developed, standardized, and utilized (Study IIIc). No fiber from Study IIIa or IIIb was included in Study IIIc. A permanent magnet-series electrodynamic vibration actuator (LDS Test and Measurement LLC) coupled to a flexible linear motion end-effector (LMEE) device (open system Kimberly-Clark polypectomy snare terminally encased in a tuberculin syringe) was driven by the same waveform generator. Figure 11 (Appendix J) is a schematic representation of the LMEE device. The LMEE device was capable of generating a reproducible pressure up to 760 kPa just below the pressure recognized as visibly destructive to skin. Vertical displacement and mass generated on a standard laboratory scale was dependent on the voltage delivered to the waveform generator; the maximal voltage of 4.5 V generated 2 mm displacement of a filament tip (surface area of 0.25 $mm^2$), and 19.5 g on a laboratory scale. The device was not capable of interval-scaled changes in stimulus intensity.

The probe tip was positioned by a hand-controlled XYZ micromanipulator and applied to the most sensitive area of the RF. It was retracted until ongoing activity was equal to ongoing activity observed prior to probe application and the tip was visible above the skin surface with light microscopy. To insure that the stimulus delivered was sufficient to measure a change and avoid a floor effect, the tip was placed as close as possible to the skin so as to

generate at least half the discharge frequency of vigorous glass probing or application of a suprathreshold VF to the RF.

A trial consisted of 2 to 5 pulses, 1.25 to 2.5 s duration, and separated by 10 s remotely signaled by the waveform generator. Duration was varied in an attempt to obtain more than 5 action potentials per trial, but not distort or destroy the RF. As the project progressed, the number of pulses was decreased to two and the duration increased to 2.5 s. A delay of 2 min between trials was observed to minimize sensitization (a more vigorous response from repeated applications of the same stimulus) (Slugg, Meyer, & Campbell, 2000). Figure 12 (Appendix J) is a representation of two stimulus pulses and responses. The variable measured was the change in averaged number of spikes pre-test compared to post-test. Fibers were classified as GABA-sensitive when the change in the posttest response exceeded 44% of the pretest baseline.

*Study IVa, IVb, and IVc: Noxious heat stimulation*

For this project, a 980 nanometer (nm) near infrared, 7.5 watt (W), class IV diode laser (LASMED, Lass/DLD-7-NM3, Mountain View, CA) was specifically developed for a noxious heat stimulus. Chapter IV provides a full description of the suitability and the properties of the diode laser. A 2.5 mm diameter spot from a visible light locator beam was first focused on the electrical and often mechanical RF. The optical cable filament was held near perpendicular and approximately 1.5 mm above the organ chamber fluid surface by a hand-controlled XYZ micromanipulator. Time for each trial was 7 s and corresponds to a duration that successfully stimulated *in vivo* rat and human cutaneous C fibers (unpublished communication M. Nemenov, the developer and manufacturer of the diode laser used in this project, 2008). Threshold was defined as the current to the driver, in milliamperes (mA),

necessary to generate ≥ 5 action potentials. To determine an optimal range of current to the driver to excite noxious heat-receptive fibers, a survey of laser susceptible and resistant fibers was conducted. Optimal current to the driver for C fibers ranged from 600 to 2000 mA, for C/A$\delta$ from 1300 to 1400 mA, and for A$\delta$ fiber from 2000 to 3000 mA. A minimum of 10 action potentials per trial was selected as optimal for agent testing and was generally within 200 mAs of the threshold current. As recommended by the manufacturer, the interstimuli interval exceeded 10 s to allow dissipation of accumulated heat within the optical cable filament.

During an initial investigation of the laser's properties by the manufacturer in the Perl Lab, a dramatic increase in ongoing activity occurred after multiple trials. To minimize this sensitization, only one trial was conducted for each treatment condition with a 2 min interval between treatment conditions. No fiber was studied that previously had laser irradiation of its RF. Three methods were derived for estimating possible sensitization: 1) observe for new-onset ongoing activity; 2) observe for decrease in mechanical threshold after laser stimulation; 3) observe for increase in number of action potentials generated from a constant mechanical stimulus after laser stimulation. In cases where sensitization was suspected, the question arose as to whether the observed changes during GABA exposure were from the treatment, or from a testing effect from repeated laser stimulation and the data from the fiber was eliminated from the analysis.

In Study IVa, laser irradiation of the RF for 7 s was accomplished before and every 2 min during GABA application for up to 6 min. In a few cases, a change in noxious heat sensitivity occurred under extremely stable recording conditions, and the opportunity was taken to observe for a return to baseline after 20 or more minutes of wash-out with SIF.

Fibers were deemed to have enhanced, suppressed, or no change in noxious heat sensitivity during GABA exposure, and recovery or no recovery to baseline after a wash-out period. Similar to mechanical stimulation, fibers were classified as GABA-sensitive when the posttest response change exceeded 44% of the pretest baseline. Recovery from a GABA-induced response was recognized as a 50% return to baseline.

In an attempt to garner data in a more time efficient manner, the laser was used as a search stimulus to locate a distinct cutaneous area innervated by multiple laser responsive fibers. Study IVb included the responses from non-characterized fibers to a threshold laser driver current delivered for 7 s. This technique had several limitations. The optimal driver current had not been determined for each of the multiple fibers and it was unlikely to be the same for all. In addition, changes in leading recording conditions altered action potential shapes and hindered the sorting of action potentials by size into a reasonable schema as the experiment progressed through treatment and wash-out. Changes in leading recording conditions resulted from fluid evaporation and drainage from or accumulation on the segment of fiber in contact with the recording electrode. Consequently, small action potentials disappeared into the baseline EMI and larger action potentials dominated the tracing. With this in mind, the decision was made to count only the largest of the action potentials from every trial of the three experiments. Again, a 44% change in the discharge frequency of large action potentials between the pre- and posttest condition and a 50% return to the pretest condition with wash-out were considered significant.

Finally, in the interim period before laser acquisition, a very simple noxious heat experiment (Study IVc) was designed to test for change in responsiveness to noxious heat

from superfusion of GABA. Heated SIF, at known temperatures (42 and 48 $^{o}$C), was applied in a ring reservoir and pre- and post-test discharge frequencies were compared.

*Study V: Noxious chemical stimulation*

Early in the project when neither thermal nor mechanical instrumentation were available, the inflow/outflow reservoir was used to apply protons as a chemical stimulus (Steen, Steen, & Reeh, 1995). The inflow/outflow reservoir is discussed previously. The protocol for instillation of solutions, agents, and protons was as follows: SIF for 1 min; SIF acidified with HCl to pH 4.0 for 1 min; GABA 100 $\mu$M for 1 min; acidified SIF + GABA 100 $\mu$M for 1 min; and 3 min wash-out period. Advantages of the technique were the device restricts exposure of agents to the remainder of the cutaneous surface and reduces electrical interference. Disadvantages were the dependence on isolation of a proton-sensitive fiber with a brisk discharge frequency, in an area of the preparation accommodative to the bulk of the device. Thus, it was a very inefficient method for the rapid collection of data.

*Study VI: Innocuous cooling stimulation*

For fibers most active at temperatures below 32 $^{o}$C, ongoing activity was measured before and during GABA superfusion in the absence of intentional mechanical, thermal, and electrical stimulation.

*Measurement of Loci of Activity: Specific Aim 2*

In the event significant GABA-induced responses were found, three methods of administration were devised to estimate the location of GABA receptors. The first method would have been to apply GABA to the entire organ bath and is analogous to a systemic route of administration with RF, peripheral terminals and process exposure. The second method would have been to apply GABA only within the ring reservoir and is analogous to

topical or local route of administration with exposure confined to RFs and peripheral terminals. The last method would have been to apply GABA to only the organ bath and not the skin within the ring reservoir. This method would be analogous to a perineural injection with only peripheral process exposed to GABA. A ring reservoir and mechanical stimulus interaction was observed during the project (see results) and this method had to be abandoned.

### Measurement of Concentration Response Relationship: Specific Aim 3

In cases of prolonged stable recording conditions, attempts were made to investigate concentration and response relationships from increasing concentrations of GABA and constant mechanical or noxious heat stimuli. The selection of GABA concentrations of 10 $\mu$M, 100 $\mu$M, and 1000 $\mu$M was based from a review of organ bath studies of whole nerve, cell bodies, DRG, nerve roots, cutaneous tissues, and single visceral fibers (Agrawal & Evans, 1986; Ault & Hildebrand, 1994; Bhisitkul et al., 1987; Brown & Marsh, 1978; Denda et al., 2003; Denda et al., 2002; Desarmenien, Feltz et al., 1984; Desarmenien, Santangelo et al., 1984; Morris et al., 1983; Page & Blackshaw, 1999; Valeyev et al., 1996).

# CHAPTER 4

# ANCILLARY EXPERIMENTS: SUITABILITY OF THE DIODE LASER AS A NOXIOUS HEAT STIMULUS

## Laser Specifications and Advantages

The diode laser has been proposed by the Perl Laboratory to be a powerful, functional, and precise instrument, for heat stimulation of mouse PAFs, in a 'scaled down' organ bath. The diode laser offers several advantages over the older carbon dioxide ($CO_2$) laser. The $CO_2$ laser is frequently used in a dry environment to evoke human somatosensory potentials, animal withdrawal behavior, and single fiber responses in animals, but rarely in a liquid environment (MacIver & Tanelian, 1993). The diode laser has greater cutaneous penetration due to lesser light energy absorption by water and requires a smaller power supply and cooling system due to better electrical efficiency (Plaghki & Mouraux, 2003; Walsh, 1997). The diode laser light energy is easily handled by flexible optical cable, unlike some $CO_2$ lasers which require hollow tubes and mirrors (Razum, 2001).

Laser is an acronym for light amplification by stimulated emission of radiation. Lasers emit radiative energy in focused beams of parallel monochromatic electromagnetic waves. The LASMED Lass/DLD-7-NM3 7.5W infrared laser is the first model released and tested on the *ex vivo* skin-nerve preparation. It consists of a driver, footswitch, trigger input/output, and silica optical cable, and is capable of delivering a driver current of 4200 mA for up to 20 s, at intervals of 1 to 60,000 ms, and up to 200 pulses. Instantaneous tissue

heating from laser irradiation is not a natural stimulus, but the Lass/DLD was chosen to serve as a proxy for natural conductive, convective, and radiant heat stimuli. The diode laser possesses several advantages over other laboratory methods for thermal stimulation. The integrated thin, flexible optical cable conducts the stimulus pulse at the speed of light with minimal signal decay, and introduces little EMI into the miniature recording chamber. More importantly, the laser is capable of generating an easily controlled and reproducible stimulus amplitude and beam area of irradiation. A simple laser detector card (THORLABS, VC-VIS/IR 800-1700nm) serves to roughly estimate the stimulus amplitude and beam area.

Digital photography readily captures infrared light to confirm that visible and infrared beam areas are approximately the same size and in the same location. The photographs in Figure 13 (Appendix K) were captured with minimal visible light and no camera flash, and the beam focus was set for a 5 $mm^2$ area. The upper photograph is an infrared (white spot) image and lower photograph is of the visible light locator beam (pink spot). Correspondence of images supports the use of visible light locator beam as an effective method to identify and limit the irradiated area of the corium. Since diode laser irradiation minimally raises the organ bath temperature, the non-irradiated portion of the skin preparation is preserved from potential heat-induced injury.

### Laser-Induced Bath Temperature Changes

The temperature increase of solution-submerged non-homogeneous tissues from infrared radiation has not been determined by the manufacturer, but is not believed to be the result of heating of the organ bath solution. In a series of experiments on superfused human embryonic kidney and DRG cells, the manufacturer used infrared temperature scans and

observed no change in average bath temperature with the laser pulses (personal communication, Michael Nemenov, 2008).

To determine if the same is true with the skin-nerve preparation, a thermistor was placed tangential to the laser beam on either the corium surface or concealed beneath the epidermal surface, but not within the area directly illuminated by the visible light locator beam. This was accomplished in the superfused organ chamber (24 $^{o}$C), and in the ring reservoir. In all four conditions (superfusion – epidermal contact; superfusion – corium contact; ring – epidermal contact, ring - corium contact) the maximum increase in organ bath fluid temperature after 7 s of cutaneous irradiation was $\leq 0.5$ $^{o}$C. In contrast, when the thermistor was directly exposed to laser irradiation, measured temperature increased to 51 $^{o}$C at 1000 mA, and exceeded 80 $^{o}$C at 2000 mA (data not shown). Unlike radiant light from a halogen bulb, the diode laser does not appear to act as a noxious thermal stimulus by heating the solution in the organ bath.

## Laser Irradiation as a Noxious Heat Stimulus

A series of experiments were performed to determine the suitability of the diode laser as an instrument to predict noxious heat sensitivity, estimate noxious heat threshold, judge endogenous and pharmacological agent effectiveness, and search for fibers responsive to noxious heat. Results have previously been presented in abstract form at the University of North Carolina at Chapel Hill 5$^{th}$ Annual University Research Day.

The Lass/DLD diode laser has been tested on *in vivo* rat DRG neurons, *in vivo* rat ear/rostral auricular nerves, and human skin for selective activation of C and A fibers (Greffrath et al., 2002; Tzabazis et al., 2005; Veldhuijzen et al., 2009), but untested in the submerged *ex vivo* mouse skin-nerve preparation. A detailed description of the process of

photon penetration of submerged, cutaneous tissues is beyond the scope of this project, but key phenomena include absorption of light energy by the tissue and solution, reflection and scatter of light by the fluid and cutaneous surfaces, and transmission of light energy through the tissue plane of interest. To hold these phenomena constant between pre- and post-test trials and among experiments, the duration of the square-wave laser pulse, area of the beam focus, angle of approach, and stand-off distance between the optical cable tip and the preparation were held constant. Only the laser driver current (mA) was varied. The laser driver current set point estimates the energy density or radiant flux in Joules (J) per unit of surface area. The laser driver current set point range was 700 to 3000 mA and the energy density range was 120 $mJ/mm^2$ to 1.1 $J/mm^2$. Values were derived from the proprietary diode laser specifications and from U.S. Patent No. 7402167 (Nemenov, 2008).

Figure 14 (Appendix K) is a photograph of laser irradiation of a mouse cutaneous RF submerged in organ bath. In this photograph, the visible locator beam appears pink and beam area is enlarged for improved visibility in the photograph.

Fiber response properties from laser irradiation were compared to three published reports of mouse noxious heat response properties. Cain, et al. (2001) tested Peltier contact on the *in vivo* glabrous skin-nerve preparation; Koltzenburg, et al. (1997) tested radiant heat from a halogen bulb on the *ex vivo* hairy skin-nerve preparation; and Lawson, et al. (2008) tested Peltier contact on the *ex vivo* hairy skin-DRG-spinal cord preparation. All three studies reported tissue temperatures.

In this study, 41 high and low mechanical threshold fibers, from 10 C57Bl6J mice, were examined for susceptibility to laser stimulation. Figures 15 and 16 (Appendix L) are frequency histograms for conduction velocities and pressure thresholds of the 41 fibers.

Thirteen of 21 high mechanical threshold C fibers (CV ≤ 1 m/s), 2 of 3 A$\delta$/C (1.01-1.2 m/s), and 4 of 13 A$\delta$ (> 1.2, ≤ 9 m/s) fibers responded to laser radiation. None of 4 low mechanical threshold fibers responded: 1 Aδ mechanoreceptor, 2 A$\alpha\beta$ mechanoreceptors, and 1 C mechanoreceptor. This survey is in agreement with published observations of mouse cutaneous afferent fiber responses to noxious heat delivered by conventional means. Of high threshold mechanoreceptors, Koltzenburg, et al. (1997) found 26% of A$\delta$ fibers (CV > 1.2 m/s) and 41% of C fibers (CV ≤ 1.2 m/s) responded to noxious radiant heat and Lawson, et al. (2008) found 30% of Aδ neurons and 75% of C neurons responded to noxious heat from contact with the Peltier device. Cain, et al. (2001) found 12% of all glabrous A$\delta$ fibers and 82% of all C fibers responded to noxious heat.

A subset of C fibers was observed for sensitivity to a comparative heat source applied to the RF. Heated saline (53 $^{o}$C) was gently instilled into a ring reservoir applied to the fiber's RF. Two laser-insensitive fibers (one low and one high mechanical threshold) failed to respond. Five laser-sensitive fibers did respond; 4 were also responsive to protons (pH ≤ 4.0) and 2 to noxious cold (2 $^{o}$C).

Fibers were observed for graded responses to increased laser emissions. Figure 17 (Appendix L) illustrates the responses of a single high mechanical threshold C fiber (CV = 0.49 m/s) to four graded laser emissions of 7 s duration. A series of square wave pulses were delivered in ascending order of magnitude of driver current, beginning at the fiber's threshold for laser responsiveness. The interstimulus interval was ≥ 2 min to minimize sensitization, and all fibers had minimal (< 6 impulses per min) spontaneous discharge activity prior to each laser emission.

C fibers demonstrated consistent stimulus response curves and had reproducible responses at identical suprathreshold driver currents, a favorable property for agent testing. Figure 18 (Appendix L) illustrates stimulus response relationships from laser stimulation of a high mechanical threshold C fiber (CV = 0.25 m/s). A graded increase in driver current of 400 mA led to an increased discharge frequency up until 1500 mA and 6 pulses at 1700 mA resulted in a consistent discharge frequency. C fiber stimulus-response curves were in agreement with published reports (Cain, et al., 2001; Koltzenburg, et al., 1997, Lawson, et al., 2008). In contrast, 4 Aδ fibers did not respond with linear stimulus-response curves, had lower discharge frequencies (< 1/s), and required higher laser driver currents. Three fibers weakly and inconsistently responded with 3-6 impulses at the end point of the final laser emission (3000 mA). One A$\delta$ fiber (CV = 2.3 m/s) demonstrated an erratic accelerated and decelerated discharge pattern of the stimulus-response curve, a maximal response rate of 13 impulses per trial, and demonstrated a delay of more than 5 s from the onset of the laser emission represented by Figure 19 (Appendix L). The fiber had a maximal discharge frequency from a glass probe stimulus of 9 impulses/s. Published reports of A$\delta$ stimulus response curves are discussed below.

C and C/A$\delta$ fibers were observed to respond more vigorously at lower laser energies (700-2000 mA) than A$\delta$ fibers (2000-3000 mA), and their responses grossly paralleled published mouse C and A$\delta$ noxious heat threshold ranges. Figure 20 (Appendix L) represents the relationship of CV to laser threshold in 19 high mechanical threshold fibers. In the sample of fibers examined, A$\delta$ fibers required a greater laser driver current than C and C/A$\delta$ fibers. For C fibers, the average discharge frequency at laser threshold (8.4 impulses/7 s) exceeded the average A$\delta$ maximal discharge frequency at any driver current (6.5

impulses/7 s). Koltzenburg, et al. reported a maximal number of impulses for A$\delta$ fibers of 15.8±9.7 and for C fibers of 22.0±6.0 over a 15 s trial, and average heat thresholds for C fibers = 37.6 ± 1.4 $^{o}$C and A$\delta$ = 42.5 ± 1.9 $^{o}$C. Cain, et al. (2001) reported mean heat thresholds C = 40.3±0.4 $^{o}$C, A$\delta$ = 42±3.0 $^{o}$C; A$\delta$ fibers responded weakly to heat stimuli, and were of two types: Type I responded at the end point of the stimulus range of 53 $^{o}$C, and Type II between 39 to 51 $^{o}$C.

## Other Response Changes from Laser Irradiation

Several additional laser-induced changes in the response properties were observed. As many as 50% of fibers became unresponsive to mechanical or electrical stimulation after exposure to 2000 mA for C fibers, and 3000 mA for A$\delta$ fibers. These fibers had remained responsive to mechanical stimulation after a lesser laser driver current of 1500 mA or 2500 mA respectively. The question arises as to whether these changes are the consequence of accommodation, sensitization, fiber attrition, or laser ablation. In any case, 3000 mA was selected as the upper limit of exposure for A$\delta$ fibers, and 2000 mA for C fibers.

A second observation was that cutaneous RFs frequently were found at the junction of the whole nerve and/or fascicle with the corium and all structures were irradiated. To test the hypothesis that laser radiation of nerve fascicles and/or whole nerves could elicit impulses, an experiment was conducted. Two dissociated sural nerve fascicles from two nerves were examined for changes in excitability and conductivity before and after laser irradiation. A 2.5 mm section of each nerve was irradiated with graded square waves of driver current for 7 s up to 4000 mA and CAPs were recorded between trials. No change in amplitude or conduction latency of the components of the CAP was observed and no spontaneous neural activity was observed (data not shown).

## Laser Use for Measurement of Drug Effects

In a separate study designed to grossly examine the suitability of the laser as an instrument to measure drug effects, 2 high mechanical threshold (1 C and 1 C/A$\delta$) fibers were exposed to suprathreshold laser emissions before and during the application of either a recognized 'gold standard' algesic or a local anesthetic. Adenosine triphosphate (ATP) (100 $\mu$M) and capsaicin (10 $\mu$M) increased discharge frequency to 62 impulses/7 s at 2 min of exposure, from a pretest discharge frequency of 20 impulses/7s (CV=0.24 m/s, laser driver current of 1700 mA). Lidocaine (1mM) decreased the discharge frequency to 6 impulses after 30 s of exposure from a pretest discharge frequency of 12 impulses/7 s (CV=1.23, driver current = 1400 mA). These alterations in discharge frequencies parallel alterations observed in published reports for heat sensitive fibers ((Guenther, Reeh, & Kress, 1999; Wagers & Smith, 1960).

## Laser as a Search Stimulus

On three occasions, the laser activated fibers without obvious mechanical or electrical RFs. Multiple attempts were made to locate the electrical RF with an electrical search electrode and mechanical RF with a glass probe without success. These observations discouraged use of the laser to locate heat-sensitive but mechanically insensitive afferent fibers.

In a separate series of experiments, the laser was tested as a search stimulus for C fibers in advance of mapping the mechanical RF and measuring the mechanical threshold. Since the laser stimulus threshold for impulse generation was unknown (only a range, 700-2000 mA), as little as two suprathreshold laser emissions led to fiber sensitization. In one case, the extremely low starting driver current of 800 mA led to a striking increase in

discharge frequency upon a second stimulus 5 min later and the fiber had to be excluded from further study. Figure 21 (Appendix L) represents an electrophysiological recording from a C fiber (CV = 0.33 m/s) demonstrating possible sensitization in response to use of the laser as a search stimulus. In one example of laser-induced sensitization, the second pulse at suprathreshold driver current (800mA for 7 s), C fiber demonstrated an increase in discharge frequency, despite a tonic discharge delay compared to the first pulse. The upper trace is from the first pulse (15 impulses) and middle trace is from a second pulse delivered 5 min later (32 impulses). The frequent necessity to exclude fibers due to possible sensitization suggests that the diode laser may be inefficient as a search stimulus.

In a final experiment, an absence of C fibers sought by the electrical search technique was compared to an absence of heat sensitive C fibers that comprised a small teased strand of sural nerve. The electrical RFs of many A$\alpha\beta$ and A$\delta$ fibers were located, but no fiber with a CV in the C fiber range was identified. In 5 $mm^2$ sections, the entire corium surface was laser irradiated at a driver current of 2000 mA, but no response from the fibers was recorded. To insure no failure of recording equipment had occurred, a subsequent teased strand of fibers possessed multiple laser-sensitive C fibers as identified by electrical search and laser techniques. This experiment suggests a useful application of the diode laser is for the examination of an absence of noxious heat sensitive C fibers, possibly in a transgenic mouse pain model.

## Incidental Observation

An incidental observation was the strong association of CV to laser susceptibility in high mechanical threshold C and A$\delta$ fibers: the CV of laser-insensitive C fibers (0.56 ± 0.07 m/s) exceeded those of laser-sensitive (0.38 ± 0.03 m/s) and the CV of laser-insensitive A$\delta$

fibers (4.16 ± 0.49 m/s) exceeded those of laser-sensitive (2.56 ± 0.42 m/s). The CV of 2 C/A$\delta$ fibers were essentially the same (laser insensitive CV= 1.0 and laser sensitive = 1.13 m/s). Koltzenburg, et al. (1997) found similar results in the Aδ fibers (heat-sensitive = 2.3 ± 0.2 m/s; all A$\delta$ = 5.7 – 7.0 m/s), but not in C fibers. Lawson, et al. (2008) found that C heat-sensitive mechanically insensitive afferent fibers had the slowest CV (0.38 m/s) of all C fibers (0.55 m/s), but noted no difference between CMH and CM groups.

## Summary of Findings

Several conclusions can be made from these experiments. Responses from diode laser stimulation mirror those from conventional noxious heat sources. The laser is an adequate instrument to predict noxious heat sensitivity of mechanically sensitive fibers. The technique grades heat thresholds in C fibers and possibly in A$\delta$ fibers and shows promise to gauge endogenous and pharmacological agent effectiveness in C fibers responsible for pain. Because the mouse and other rodents have a paucity of innocuous warming receptors, laser-sensitive fibers in these experiments were presumed nociceptive (Cain et al., 2001; Leem et al., 1993).

A final conclusion is that the CVs of laser-sensitive C and A$\delta$ fibers are slower than laser-insensitive fibers. This may be the first report of slower CVs in both mouse C and A$\delta$ noxious heat-sensitive, high mechanical threshold fibers. The ability to predict the characteristics of PAF input by CV is advantageous in the investigation of first and second order neuronal pain signal transmission and cellular spinal cord organization.

# CHAPTER 5

# RESULTS OF GABA EXPERIMENTS

## Specific Aim 1: Classification of Fibers in Studies I-VI

A total of 45 single fibers from 40 male and female C57Bl6J mice were studied for sensitivity to GABA in response to mechanical, noxious heat, chemical, electrical, or innocuous cooling stimuli. The disparity between number of animals and fibers is explained by the performance of multiple experiments per animal. This occurred when GABA was isolated in the ring reservoir in a first experiment and superfused in a subsequent experiment. On occasion, two fibers with distinct action potentials responded to the same stimulus and were examined simultaneously. Studies I and III had equal representation of the sexes, but the vast majority of animals in Studies II and IV were female. The decision to include females was based on easier upkeep and a moral imperative to not ignore the contribution of sex differences in the study of pain (Mogil & Chanda, 2005).

Fibers were isolated from plantar ($n$=8) and sural nerves ($n$=37). Fibers were eligible for inclusion in one or more study phases (examples: I, IIIa and IIIb). The duration of experiments ranged from 9 to 15 hours per animal and included the procedures of preparation dissociation, excision of extraneous tissues, isolation of single fibers, examination for response property changes, and fiber characterization. In three additional experiments, sections of skin innervated by multiple uncharacterized fibers from the sural nerve were

studied in an attempt to expedite data collection by shortening the duration of the experiments.

The focus of the study was nociception; thus, the majority of fibers selected had conduction velocities consistent with the C and A$\delta$ components of the CAP. The mean CVs (m/s) were: 4 A$\beta$ fibers = 22.0 ± 4.94; 8A$\delta$ = 4.97 ± 0.79; 3 C/A$\delta$ = 1.08 ± 0.06; and 30 C = 0.46 ± 0.03. The fibers in the C/A$\delta$ category shared response properties of C and A$\delta$ fibers (examples: 'hot-spots', laser driver threshold currents in the C-fiber range, vastly expanded RFs after mechanical stimulation and GABA treatment). CVs for 45 fibers are summarized in Figure 22 (Appendix M).

Mechanical RFs of sural nerve fibers were tightly distributed within 0.5 centimeter of the course of the sural nerve and were divided between glabrous ($n$=12) and hairy ($n$= 25) skin. RFs from plantar nerves were distributed across the entire plantar surface and none was encountered on hairy skin. RF size was noted in most cases before and after GABA administration. Many cutaneous mechanical RFs were single spots and the electrical and mechanical RF overlapped. Thermal RF areas were not mapped for size, but often were in close proximity of the mechanical and/or electrical RF. The rare laser-responsive, but mechanically insensitive fiber without an identifiable electrical RF was excluded from further examination because of the inability to classify the fiber by CV.

Single fibers were categorically sorted by RF response properties of minimally responsive to mechanical stimuli, mechanical threshold, thermal sensitivity, proton sensitivity, and sensitivity to additional mechanical stimuli of brushing, stretching, and puncture. The addition of the diode laser technique for identification of single units demonstrated that C fibers with VF thresholds of 160 kPa were sensitive to noxious heat

stimuli; accordingly, the high mechanical threshold group range was expanded to include 160kPa.

In the series of experiments designed for the project proposal, all fibers except for one C cooling receptor were mechanically sensitive. One additional fiber was mechanically sensitive only to fine brush strokes, but not pressure. Mechanical thresholds are summarized in Figure 23 (Appendix M). In general, the boundary between low and high mechanical threshold fibers was < 160 kPa, but other characteristics were taken into account (examples: after-discharges, discharge frequency, adaptation, responsiveness to noxious protons and noxious heat). The distribution of high mechanical threshold fibers in this project was not spread as broad, and the median VF threshold was higher than the findings of Koltzenburg, et al. (1997). The median VF threshold of all C fibers (357 kPa or 39 mN) exceeded the median threshold (25 mN) found by Cain, et al. (2001).

Early in the project, characterization methods were not fully developed. For example, over the course of the experiment the ring reservoir was created and the optimal ring-instilled SIF temperature to test for noxious heat sensitivity was determined to be 53 $^{o}$C. Application of this temperature led to clearly visible and sustained discharges, but seldom damaged the RF or terminated impulse generation. Thermal (53 $^{o}$C) and proton (pH $\leq$ 4.0) stimuli generally were not graded; consequently, characterization of sensitivity was nominal scale data. Ten of 34 high and 10 of 10 low mechanical threshold fibers were partially characterized due to unstable recording conditions or unavailability of characterization methods. The 25 fully characterized fibers (22 C and 3 A$\delta$ fibers) from Studies 1-6 are summarized in Figure 24 (Appendix M). Lawson et al. (2008) found polymodal (mechanical, heat, and sometimes cold/cooling) nociceptors comprised 72%, mechano-

sensitive 11%, CH (noxious heat only) 9%, mechano- and cold/cooling-sensitive 7%, and cooling thermoreceptor 1%. The subset of fully characterized C fibers of this project shares a similar distribution.

Study I: Non-Activity Dependent Changes in Excitability and Conduction

Six fibers from 6 animals were examined for a change in electrical threshold from superfused 100 $\mu$M GABA for > 6 min. Three high mechanical threshold C fibers, one low mechanical threshold C fiber, one Aδ high mechanical threshold fiber, and one A$\alpha\beta$ low mechanical threshold fiber had no change in the threshold voltage to consistently elicit an action potential during 100 $\mu$M GABA superfusion (data not shown). Three fibers exposed to 1000 $\mu$M GABA (1 high mechanical threshold C and A$\delta$, and 1 low threshold A$\alpha\beta$ fiber) had no change in electrical threshold. Three fibers were exposed to GABA exclusively within the ring reservoir and all demonstrated no change in electrical threshold. In all experiments, a suction electrode served as the stimulating electrode. Due to the fact that the length of nerve between the stimulating and recording electrodes had no contact with ring reservoir instilled GABA, these experiments served as controls for the superfused experiments.

Fourteen high mechanical threshold fibers and 5 low mechanical threshold fibers, from 17 animals, were examined for changes in CV following the superfusion of 100 $\mu$M GABA for 6 min. All of these fibers were included in other study phases. No fiber had greater than a 1% change from GABA 100 $\mu$M (data not shown). The mean CV before GABA 100 $\mu$M exposure was 3.01 ± 1.57 m/s and 2.99 ± 1.57 m/s after 6 or more minutes of GABA exposure. A total of 13 C, 4 A$\delta$, 1 C/A$\delta$ and 1 A$\beta$ fibers were examined.

A subset of two high mechanical threshold C fibers (1 CM and 1 CMHA) had no change in CV from 10 $\mu$M GABA superfusion. Another subset of three fibers (one high threshold A$\delta$ mechanoreceptor, one low threshold A$\delta$ mechanoreceptor, and 1 C high threshold mechanoreceptor) were exposed to GABA 1000 $\mu$M and none had a change in CV greater than 2% over the pre-test condition.

Eight fibers from 8 mice were studied with GABA instilled exclusively within the ring reservoir for > 6 min and none demonstrated any alteration in CV. Similar to Study Ia, the ring reservoir cases were intended as control experiments.

After implementation of the search electrode approximately midway through the project, very few fibers were studied for GABA-induced changes in electrical threshold and CV, and Study I was terminated. The search electrode placed over the RF interfered with the delivery of mechanical, thermal, and chemical stimulation; whereas the suction electrode attached to the main nerve trunk produced no RF obstruction, was capable of reproducible electrical stimulation for many hours, and allowed the fiber to be included in several study phases.

### Study II: Activity dependent Shifts in Conduction Velocity

Six high mechanical threshold C fibers (mean CV 0.46 ± 0.02 m/s) from four animals were examined for activity dependent latency shifts from high frequency electrical stimulation during superfused 100 $\mu$M GABA (data not shown). The size of the suction electrode and its angle of approach for attachment to the RF precluded use in the ring reservoir. To observe for concentration response variability, two fibers were also studied for latency shift from 10 $\mu$M GABA. No fiber tested for activity dependent changes was included in mechanical or thermal studies due to RF visible distortion or displacement upon

removal of the suction electrode. All fibers were allowed to return to the baseline CV before institution of GABA superfusion, and no fiber had a change from the original baseline latency (1st stimulus of the high frequency series) from superfusion of GABA. Figure 26 (Appendix N) represents electrophysiological recordings of activity dependent conduction delay shift before and during GABA treatment from a CMA fiber (CV = 0.45 m/s).

Three CMHA fibers (CV = 0.45, 0.56, 0.44 m/s) demonstrated > 11 percentage point enhancement of the latency shift (19, 11, 11 respectively) during treatment with 100 $\mu$M GABA. One fiber was washed for 25 min, underwent a third episode of high frequency stimulation, and demonstrated a partial return to the baseline frequency latency shift.

One CMHA fiber (CV = 0.38 m/s) had a converse 8 percentage point shortening in the latency shift during 100 $\mu$M GABA exposure. See Chapter VI for analysis and interpretation of activity dependent results. One CMHA (CV =0.38 m/s) and one CM fiber (CV= 0.43 m/s) had less than a three percentage point enhancement of the latency shift during 100 $\mu$M GABA exposure. 10 $\mu$M GABA effected minimal alteration in the latency shift on two of the less reactive fibers. One presumed post-ganglionic sympathetic efferent (CV = 0.49 m/s), insensitive to mechanical, chemical and thermal stimulation, was inadvertently studied with the 6 mechanically sensitive C fibers. The presumed efferent fiber demonstrated a minimal response to high frequency stimulation before and during treatment with 100 $\mu$M GABA. No fiber was tested with 1000 $\mu$M GABA.

To check the reliability of this activity dependent method, two high mechanical threshold C fibers (CV= 0.45, 0.47 m/s) were studied under the same protocol, but only exposed to SIF during the two high frequency stimulus periods. The two fibers had no difference in conduction latency after the first high frequency stimulation (14%, 19%) period

compared to the second (14%, 18%). One additional high mechanical threshold C-fiber was exposed to four periods of high frequency stimulation with only SIF. The latency change remained consistent for the first three periods, but with the onset of the fourth period the action potential shape promptly widened, conduction blocked, and the fiber failed to respond to any increase in stimulus amplitude. The decision was made to restrict the number of high frequency stimulus periods to two for most experiments.

## Study III: Mechanical Stimulation

Over the course of this project, three methods were implemented to study single fibers that responded to mechanical stimulation. In Study IIIa, VF filaments were used as a supra-threshold constant pressure stimulus. In Study IIIb, VF filaments were used to measure a change in mechanical threshold. In Study IIIc, a LMEE was used as a supra-threshold constant pressure stimulus to measure a change in discharge frequency.

### *Study IIIa.*

Eight fibers from 7 animals were examined. GABA 100 $\mu$M was superfused for 4 and/or 6 min in 4 of 8 cases; the remainder had GABA 100 $\mu$M instilled in the ring reservoir. Supra-maximal was defined as a stimulus capable of reproducibly generating more than 4 action potentials over 1 s. For most fibers, a VF filament within the nociceptive range was selected.

No superfused fiber had a significant change in discharge frequency during GABA treatment, but most ring reservoir fibers had a discharge frequency change during GABA treatment. Table 5 (Appendix O) summarizes fiber responses from suprathreshold VF stimulation. Of 4 fibers in the superfusion group, 3 had no change in discharge frequency. One CMA (not characterized for heat, CV= 0.73 m/s), had a less than 44% increase in

discharge frequency (before GABA = 8 impulses/s, during GABA = 13 impulses/s). The latter fiber was included in Study IIIb and also had a mild decrease in VF threshold during GABA exposure. In contrast, 3 of 4 fibers (2 Aδ, 1 C/Aδ) treated with GABA by ring reservoir had bidirectional and greater than 44% changes in discharge frequency. In view of the erratic results associated with ring reservoir use, the merit of the ring reservoir technique to limit GABA exposure was questioned. Two C/A$\delta$ fibers (low mechanical threshold fiber, CV = 1.04 m/s; high mechanical threshold fiber, CV = 1.00 m/s) had large increases in RF size after GABA exposure, in comparison to the pre-treatment condition (see below).

*Study IIIb.*

Seventeen fibers (3 A$\alpha\beta$, 7 A$\delta$, 2 C/A$\delta$, 5 C) from 16 animals were examined during exposure to 100 $\mu$M GABA at 3, 5 and/or 10 min. A subset of fibers was exposed either to 1000 $\mu$M GABA or to 10 or more minutes of wash-out. All eight fibers from Study IIIa were included in Study IIIb. Hence, a minimum of 5 observations (1 min apart) were made of pre-test and post-test conditions on these eight fibers. Mild threshold change was defined as a progression in either direction of one ordinal filament in the sequence of VF filaments. A substantial change was defined as a progression in either direction of more than one filament of the VF sequence. Table 6 (Appendix P) summarizes mechanical threshold changes from VF stimulation.

Two of 3 superfused high mechanical threshold A$\delta$ fibers met the criterion of a significant increase in VF threshold. One fiber (CV = 2.95 m/s) had one measurement point at 5 min of 100 $\mu$M GABA exposure, but the other fiber (CV = 6.36 m/s) had an incremental increase of VF threshold during 100 $\mu$M and 1000 $\mu$M GABA exposure. The increase in mechanical threshold did not reach significance until the 1000 $\mu$M measurement point. One

superfused high mechanical threshold A$\delta$ fiber, not included in Study IIIa, had an expansion of the RF and an increase in VF threshold during GABA exposure (see below).

One of 3 superfused high mechanical threshold C fibers met the criterion of a significant increase in VF threshold. The heat-sensitive fiber (CV = 0.31 m/s) had a substantial increase in VF threshold at 3 min of 100 $\mu$M GABA, but the effect was not sustained until the 5 min observation point.

Again, an obvious bidirectional ring effect was observed. Two of 3 high threshold fibers had substantial and striking decreases in VF threshold (A$\delta$, CV = 8.8 m/s; C/A$\delta$, CV = 1.00 m/s) and 1 of 4 low mechanical threshold A$\delta$ (CV= 5.16) fibers had a substantial increase in VF threshold during ring reservoir applied 1000 $\mu$M GABA. No fiber in the ring reservoir group had an increase in ongoing activity after placement of the ring.

*Study IIIc.*

Thirteen single fibers from 11 animals were examined for changes in responsiveness during exposure to 100 $\mu$M GABA for 3 or more minutes. Twelve fibers were superfused and only the first fiber in the series was LMEE stimulated within the ring reservoir. Six fibers were exposed for up to 5 min and 4 fibers for up to 7.5 min. One fiber was exposed to 1000 $\mu$M GABA for 3 min and 7 fibers were washed for 10 or more minutes after exposure. Six of the 13 fibers developed ongoing activity during LMEE stimulation. As in Studies IIIa and IIIb, 1 of the 6 had an increase in RF area and is described below. Table 7 (Appendix Q) summarizes single fiber response from constant pressure LMEE stimulation.

Standardization of the treatment condition sounds ideal, but the stability of recording conditions was influenced by alterations in fluid levels, inability to attenuate EMI (signal to EMI ratio < 3), and the threat of time-dependent cellular and membrane changes over

duration of experiment in hours. Often a change in leading conditions was sufficient to warrant termination of the post-test condition and institute final 'just in time' characterization of the fiber for sensitivity to protons and noxious heat and cold. Keep in mind that the duration and concentration of GABA exposure necessary for effect was not known from the start of the project. Also, GABA had been anticipated to have a greater effect than had been demonstrated up to this point. As the project was exploratory in nature, a standardized protocol developed over time.

Since the focus of the project was nociception, fibers with a CV in the C and A$\delta$ fiber range were selected over other fibers. Intraneural microstimulation of human C fibers produces the sensation of a dull aching, boring or burning pain and of A$\delta$ fibers yields the sensation of sharp, pricking or stinging pain (Torebjork et al., 1984). C fibers were also selected so as to test the LMEE device on the most difficult fibers to stimulate, but not damage. Two low mechanical threshold fibers (1 C and 1 A$\alpha\beta$) and 11 high mechanical threshold fibers (10 C and 1 A$\delta$) were studied. Two of 13 fibers met the criterion of a sensitivity to GABA by a change in posttest response exceeding the pretest baseline by greater than 44%.

The first fiber (CMHAC, CV=0.34 m/s) had no ongoing activity during testing, had an adequate LMEE to maximal mechanical discharge frequency ratio, and a suppressed discharge frequency from GABA 100 $\mu$M (pre-test: 8.2 impulses/s; post-test 4.6 impulses/s). The fiber demonstrated no recovery from the GABA effects after a 10 min wash-out period. The second fiber (CMHA, CV=0.29) had sustained spontaneous ongoing activity the duration of the experiment, an adequate LMEE to maximal discharge frequency ratio, and a suppressed discharge frequency during exposure to GABA 100 $\mu$M (pre-test: 3.7 impulses/s;

post-test: 2.0 impulses/s). The fiber was also tested with 1000 $\mu$M, but had no further significant decrease in discharge frequency.

As in Studies IIIa and IIIb, one high mechanical threshold A$\delta$ fiber (CV = 2.4 m/s) experienced an increased RF area. The fiber was exposed to 100 $\mu$M GABA for 5 min and had been washed for greater than 10 min before the final RF examination was made.

Of the four expanded RFs in Studies IIIa, IIIb, and IIIc all had distinct, apposed, small hot spots surrounded by unresponsive areas prior to GABA exposure. All RFs were subjected to repeated mechanical stimulation in the attempt to locate the most sensitive area of the RF. After GABA exposure, all RFs had an increase in area up to 10 $mm^2$, and the newly responsive area included and extended well beyond the hot spots. The sensitivity of the expanded RFs was best summarized as a mosaic of high and low thresholds with no unresponsive areas. The magnitude of the increase in the RF area in these fibers was so dramatic that it would have been impossible not to take notice. One fiber had regression of RF area to baseline after more than twenty min wash-out period. Two fibers exhibited suppressed responses during GABA exposure, one had enhanced responsiveness, and one had no change. Three of 4 fibers were high mechanical threshold. Three fibers were exposed to GABA by superfusion. Three fibers innervated hairy skin. Two fibers had associated ongoing activity. Less striking expansion was not observed in other fibers of this study.

## Study IV: Noxious Heat Stimulation

Three methods of thermal stimulation were implemented over the course of the project. Study IVa employed laser irradiation of the RF of single fibers, Study IVb employed

laser irradiation of the RFs of multiple noxious heat sensitive fibers, and Study IVc employed noxious heated SIF stimulation of a single fiber RF.

*Study IVa.*

Six high mechanical threshold and laser sensitive fibers from 6 animals were exposed to laser irradiation and examined for a change in discharge frequency after 4 to 6 min of superfused 100 $\mu$M GABA. Three (1 uncharacterized, CV = 0.37 m/s; 1 CMH, CV = 0.35 m/s; and 1 CMHA, CV = 0.49 m/s) of 5 C fibers demonstrated > 44% decrease in discharge frequency during 100 $\mu$M GABA. One C fiber was washed for 25 min and had a greater than 50% return to pre-test discharge frequency. The other 2 fibers were not washed. One C/A$\delta$H (CV= 1.21 m/s) fiber exceeded a 44% decrease in discharge frequency at 4 min from 100 $\mu$M GABA and had a return to pre-test discharge frequency with a 25 min wash-out period.

In this sample, no single characteristic was unique to the fibers with discharge frequency suppression. No laser sensitive, but mechanically insensitive C fibers were studied during availability of the laser, but Lawson, et al. (2008) estimates up to 9% of the C-fiber population are CH fibers and 81% of all C fibers are heat sensitive. Table 8 (Appendix R) summarizes single fiber responses to laser stimulation in Study IVa.

*Study IVb.*

Three receptive fields with multiple heat sensitive fibers from 3 animals were stimulated with laser irradiation and examined for changes in generated discharge frequency during 10 min superfusion of 100 $\mu$M GABA. One section was also exposed to 4 min of 1000 $\mu$M GABA and the other 2 sections were washed for 25 min. The first section had several action potential shapes that contributed to the large sized action potential count. In

the latter 2 experiments, a singular pre- and post-test action potential shape suggested a single fiber source.

In the first experiment, a significant decrease in discharge frequency was observed during 6 min of superfused 100 $\mu$M GABA, from laser stimulation of the RF, with a return to the pre-treatment discharge frequency upon treatment with 1000 $\mu$M GABA. No wash-out condition was administered. The latter two experiments did not test for a concentration response relationship, but for a return to the pretest condition after a wash-out period. In the second experiment, all large action potential activity was blocked the duration of 100 $\mu$M GABA exposure with a return to 50% of the pretest condition after 10 min of wash-out. In the third experiment, pre-treatment activity decreased by 50% during 4 min of 100 $\mu$M GABA and returned to pretest condition after 25 min wash-out period. The action potential discharge pattern of the latter two innervated sections bore a strong resemblance to the discharge pattern of laser-sensitive A$\delta$ fibers. Figure 27 (Appendix S) summarizes the discharge frequency generated by heat sensitive fibers from laser irradiation of 3 receptive fields exposed to either 100 $\mu$M GABA for 10 min and 1000 $\mu$M GABA for 4 min in experiment 1 or 100 $\mu$M GABA for 10 min and washed for 25-30 min in experiment 2 and 3 from laser stimulation. The lines above and below the graph represents the time sequence for the application of GABA and wash.

*Study IVc.*

In a preliminary experiment, heated SIF was instilled into a ring reservoir as a simple method of thermal stimulation (Study IVc). Insertion of the researcher's hand into the Faraday cage decreased the signal to EMI ratio of electrophysiological recordings and limited the number of experiments analyzed. Nevertheless, the one experiment served to test if the

ring reservoir effect (see mechanical stimulation results section) carried over to thermal testing. One CMHA fiber (CV=0.57 m/s) had no significant change in discharge frequency from 48$^{o}$C SIF (pre-treatment = 17 impulses/s, at 3 min of 100 $\mu$M GABA = 13.5 impulses/s, and after wash = 17 impulses/s).

### Study V: Noxious Chemical Stimulation

A solitary CMHA fiber (CV = 0.66 m/s) was stimulated with protons (pH SIF = 4.0) and examined for a change in discharge frequency during superfusion of 100 $\mu$M GABA within the confines of the inflow/outflow device. Although this is only one case, the fiber demonstrated a significant decrease in discharge frequency during GABA 100 $\mu$M exposure (pretest SIF = 0 impulses per minute; protons = 31 impulses per minute; GABA = 0 impulses per minute; GABA + protons = 13 impulses per minute; SIF wash = 4 impulses per minute).

### Study VI: Ongoing Activity from an Innocuous Cooling Stimulus

Two fibers exposed to GABA had consistent tonic regular on-going activity (6 or more action potentials per minute for greater than 10 min) in the absence of induced mechanical or chemical stimulation. Both fibers were sensitive to cooling and were recorded at a stable temperature. One mechanically insensitive cooling C fiber (CV = 0.54 m/s, recorded at 27 $^{o}$C) had no change in ongoing activity during 100 or 1000 $\mu$M GABA exposure and one low mechanical threshold A$\beta$ fiber (CV =10 m/s, recorded at 30 $^{o}$C, and included in Study IIIC) had no change in ongoing activity during 100 $\mu$M GABA exposure.

## Specific Aim 2: Loci of Activity

Early in the project a potential interaction between mechanical stimulation and the ring reservoir was noted (see above). In view of the scant number of GABA sensitive fibers

from any delivery method, the decision was made to terminate further investigation of the locus of GABA receptor activation.

### Specific Aim 3: Concentration - Response Relationship

Across all the study phases, too few fibers were examined to estimate significant concentration effects. Two fibers were exposed to 10 $\mu$M GABA and had a minimal alteration of activity dependent latency shifts (Study II). At the time Study II was conducted, high frequency stimulation delivered by a suction electrode was thought to be the most precise of the available methods. Nine single fibers and 1 innervated cutaneous section were exposed to 1000 $\mu$M GABA over Study I, II, III, and IV. Exposure of fibers to 1000 $\mu$M GABA yielded minimal changes compared to either the pre-test condition or 100$\mu$M GABA, except in 3 cases. One CMHA fiber had a decrease in discharge frequency from LMEE stimulation during 100 $\mu$M GABA for 5 min, a partial return to baseline at 7.5 min and a further decrease in discharge frequency with 3 min exposure to 1000 $\mu$M. One high mechanical threshold A$\delta$ fiber had a graded increase in VF threshold during 100 $\mu$M and 1000 $\mu$M GABA exposure. Finally, one group of fibers exposed to laser irradiation of their collective RF had a return to the pretest condition during 1000 $\mu$M GABA exposure. This followed a sustained decrease in discharge frequency during 100 $\mu$M GABA exposure.

### Summary of Results

Thirteen of 31 high mechanical threshold fibers and 0 of 7 low mechanical threshold fibers demonstrated a suppression of responsiveness from mechanical, noxious heat, innocuous cooling, laser, or chemical stimulation during GABA exposure and results are summarized in Table 9 (Appendix T). Three of 3 RFs innervated by multiple heat-sensitive

fibers had a suppression of large action potentials from laser irradiation during GABA exposure. No fiber had a change in non-activity dependent CV or electrical threshold. A concentration effect was not demonstrated in the 6 fibers exposed to 100 $\mu$M, and then 1000 $\mu$M GABA. Too few fibers were exposed to 10 $\mu$M GABA for results to be meaningful.

Several problems were identified. A potential ring reservoir interaction with the mechanical probe tip led to the exclusion of 7 fibers from the project. The ratio of LMEE generated impulses to suprathreshold hand-held probe generated impulses continued to be inadequate to assume that C fibers were sufficiently stimulated without damage to the RF.

# CHAPTER 6

# DISCUSSION

The chief objective of this project was to determine if peripherally applied GABA changed PAF response properties. Despite early setbacks from imprecise equipment and techniques, this project provided the most extraordinary opportunity to investigate the suitability and properties of electrical, mechanical, thermal and chemical testing methods. There is no better way to personally judge or professionally referee publications than to employ the methods and techniques of colleagues. It is safe to say that the knowledge gained about the design and implementation of measurement instruments far exceeded that of GABA effects.

## Study I: Non-Activity Dependent Changes in Excitability and Conduction

No fiber had a change in electrical threshold from GABA at any concentration as measured by the simple technique employed in Study I. Bhitsitkul et al. (1987) and Brown and Marsh (1978) observed a decrease in the size of components of the CAP in peripheral nerves. A reasonable explanation for their results is that conduction and/or excitability was altered by GABA. In order to refute or confirm these authors' work, a more exact technique to measure electrical threshold was needed.

The chronaxie unit of time is a much more precise test of excitability. Chronaxie is an index of the time factor of excitation and the least duration of current exposure to an excitable tissue that will excite at stimulus amplitude double the rheobase. The rheobase is

the minimum stimulus amplitude required to induce a response to infinitely long stimulus duration (Davis & Forbes, 1936). Chronaxie allows direct comparisons among fibers with different stimulus duration and amplitude requirements. In future study, the chronaxie should be considered as a superior method to measure agent-induced changes in excitability.

Seventeen single fibers had no change in CV from exposure to any concentration of GABA, and further study was abandoned. This finding contradicts the Brown and Marsh observation of a 25% decrease in CV. The Brown and Marsh recording chamber exposed the portion of the nerve on the recording electrode to GABA, but the skin-nerve recording chamber was constructed so GABA was isolated with oil from the small portion of the nerve on the recording electrode. Due to the lack of evidence of a GABA-induced change in electrical threshold and CV and inability to change the orientation of the recording chamber, an activity dependent test was added to the experiment.

## Study II: Activity Dependent Changes in Conduction

Activity dependent increases in conduction latency > 10% after high frequency stimulation were observed in 3 of 6 high mechanical threshold C fibers exposed to GABA. This finding may possibly lend support to the notion that GABA interferes with the conduction of high frequency nociceptive signals analogous to the barrage of action potentials generated from inflammation and injury. In agreement with the results of Study Ia, no CV change occurred between the pre-treatment first stimulus of the series of high frequency stimuli and the first in the series during 2 min of GABA exposure. The significance of these results to the study of GABA is unknown and difficult to interpret. Conduction block of several fibers was encountered in this series of experiments, but the significance was unknown and a relationship to GABA was not established. The tracking of

conduction block and recovery from conduction latency shifts require the use of more sophisticated software (example: LabVIEW) than was available in this study phase.

The high frequency stimulation protocol of De Col and colleagues has been limited to the investigation of sodium channel inactivation. De Col et al. (2008) have proposed that in contrast to sympathetic efferent and innocuous thermo- and mechano-sensitive C fibers, nociceptors possess intrinsic mechanisms of self-inhibition. This local inhibition is in part dependent on the balance of $Na^+$-$K^+$-ATPase-driven hyperpolarization and cumulative $Na^+$ channel inactivation. Nociceptors selectively express tetrodotoxin resistant slow-inactivating sodium channels (Akopian, Sivilotti, & Wood, 1996; Djouhri et al., 2003) and DRG cell bodies differentially express ATP-ase functional isoforms by cell body size (Dobretsov, Hastings, & Stimers, 1999). Fewer sodium channels available for activation lead to slower conduction velocity and fewer action potentials reach second order neurons in the spinal cord. Could GABA also play a role in nociceptive self-inhibition?

Cutaneous nociceptors are devoid of more specialized structures to moderate the force of stimuli to the RF over time (Belmonte, 1996) and an endogenous physiologic extrasynaptic inhibitory or lateral inhibition system has been proposed as anti-nociceptive. The endogenous activation of functional M2 acetylcholine receptors by muscarine (Bernardini, Reeh, & Sauer, 2001; Bernardini et al., 2002; Bernardini, Sauer, Haberberger, Fischer, & Reeh, 2001) and somatostatin receptors by somatostatin (Carlton, Du, Davidson, Zhou, & Coggeshall, 2001; Carlton, Du, Zhou, & Coggeshall, 2001) serve as possible candidates for tonic control of nociception in the periphery. Carlton and colleagues propose the mechanism for inhibition arises from decreased $Ca^{2+}$ channel conductance and resultant attenuation of endogenous algogenic substance release. The structures involved are

inhibitory receptors coupled to calcium channels by pertussis toxin sensitive G-proteins (Gammon, Lyons, & Morell, 1990).

An advantage of the activity dependent technique lies with the ease of heat- or mechano-sensitive C-fiber identification with conventional VF, laser, and search electrode stimulation and the very simple maneuver of attachment of the suction electrode to the RF. This technique is by far the most efficient of all devised for the project and no experiment was prematurely terminated due to technical problems. All six fibers were fully characterized after testing. A disadvantage of the technique is fiber characterization is completed after high frequency stimulation and agent treatment. The RF was easily identifiable, but appeared distorted by the suction electrode. Experience gained from the implementation of the test and analysis of results may be valuable in future pharmacological studies.

## Study III: Mechanical Stimulation

### *Correlation of Findings to Animal Studies and GABA and GABA Receptor Content*

Five of 17 high mechanical threshold fibers from Study IIIb and IIIc had suppression of responsiveness from superfused GABA exposure. The proportion of fibers with suppressed responsiveness exceeds that of the 20% of DRG cells and surrounding peripheral processes that contain GABA (Stoyanova, 2004) and the 10-14% of epidermal/dermal terminal PAF peripheral processes with localized $GABA_A$ receptors (Carlton et al., 1999), but is low in comparison to proportions found in the other study phases (see II, IVa, IVb, IVc).

Several explanations are offered. First, the contribution from $GABA_B$ receptor activation is not appreciated. At present, $GABA_B$ receptors have only been localized on DRG cells (Charles 2001) and have not been reported on peripheral terminals. A second

explanation is rooted in the fallibility of hand-held VF filaments (examples: hand vibration, inability to deliver an identical force) and inconsistency of the LMEE (see below). Three (2 A$\delta$ and 1 C) of 6 high mechanical threshold fibers (IIIa and IIIb) had suppressed responsiveness while only two of 10 high mechanical threshold C and 1 C/A$\delta$ fibers (IIIc) had a decrease in discharge frequency from LMEE stimulation. The observation of group differences may be attributable to systematic error in one or both measurement methods. An alternative hypothesis is A$\delta$ fibers demonstrate a greater change in responsiveness to mechanical stimulation from GABA exposure than C fibers. The results from this subset of fibers provide a starting point for further study with a standardized protocol and refined instrumentation.

The findings of GABA-induced suppression of mechanical sensitivity in some high mechanical threshold fibers lend indirect support to the hypothesis that GABA and GABA agonists induce anti-nociceptive effects on animal behavior (Carlton et al., 1999; Reis & Duarte, 2006; Reis & Duarte, 2007; Reis et al., 2007). As reviewed by Slugg and colleagues, maximum discharge frequencies from C nociceptors to mechanical stimuli are frequently below pain threshold in human microneurography studies and differ from the responses of heat sensitive nociceptors which mirror the activity from electrical stimulation that does reach the pain threshold (Slugg et al., 2000). Thus, the direct relationship between agent-induced response property changes from mechanical stimulation in the *ex vivo* mouse skin-nerve preparation and agent-induced changes in nociceptive animal behavior is an inferred, but not a causal, relationship.

*LMEE Evaluation*

Several comments are relevant to the use of the LMEE technique. From the onset, the use of the LMEE technique on C fibers was fraught with problems. Despite multiple adjustments in the device's pulse configurations, cable length, and probe tip shape, many experiments failed. Fiber unresponsiveness after several LMEE pulses, excessive ongoing activity, and an inadequate ratio of LMEE to maximal discharge frequency were common causes and fatigue, tension, and probe tip placement may be contributing factors. In the absence of intentional stimulation, most C fibers have no ongoing or spontaneous activity at physiological temperatures. For example, only 10.5% of mechano-sensitive nociceptors in the *in vivo* rat and 6.5% of all C fibers in the *ex vivo* mouse demonstrate regular ongoing activity (Chen, Tanner, & Levine, 1999; Stucky et al., 1999).

Nociceptor fatigue (response decrease from previous stimulus pulse) is more common in C fibers than Aδ fibers and recovery is longer, 5 min compared to 1 min (Slugg et al., 2000). Lengthening of interstimulus intervals may help solve the fiber unresponsiveness problem. Directional tension created by the corium attachment to the organ bath basement may contribute to C-fiber unresponsiveness. C nociceptor average discharge frequency is less in low-compliant tissue than in high-compliant tissue. The opposite is the case with Aδ fibers (Slugg et al., 2000). This suggests prior to placement of the LMEE, the corium should be examined for obvious tension in the measurement of C nociceptor responses. Prevention of ongoing activity and an inadequate ratio of LMEE generated discharges to maximal discharge frequency generated by glass probe or supramaximal VF require careful vertical placement of the probe tip and tuning of the stimulus amplitude.

The use of the LMEE in the *ex vivo* mouse skin-nerve preparation will become a reliable and efficient mechanical measurement instrument, but much more time is required to refine and standardize the technique.

*Expansion of RF*

Two A$\delta$ (CV = 2.4, 3.7 m/s) and two C/A$\delta$ (CV = 1.04, 1.0 m/s) sural nerve fibers from Studies IIIa, IIIb, and IIIc, had dramatic increases in RF area after GABA exposure. No observed characteristics were shared by the fibers except all had multiple hot-spots.

Both mechano-sensitive Aδ- and C-fiber RFs possess 'hot-spots' (Slugg et al., 2000). Of two obvious explanations, induction of an inflammatory condition from repeated stimulation rather than a GABA related action is the more likely in these four cases. Heat injury adjacent to a RF expands the RF area of *in vivo* monkey glabrous skin (Raja, Campbell, & Meyer, 1984). RF area of A and C nociceptors is greater in the *in vivo* inflamed paw of complete Freunds adjuvant (CFA) treated rats than control rats (Andrew & Greenspan, 1999). Inflammation may initiate an acute diffusion of sensitizing factors, and tissue edema may alter the coupling of peripheral terminal arborizations with functional membrane receptors. The one fiber with a retraction of RF area after the wash condition indicates RF expansion may be transient and acute rather than an injury or inflammatory process and lend support to a GABA-induced effect.

This incidental finding of expanded RFs in fibers with CVs as low as 1 m/s may be helpful in the establishment of the CV boundary between Aδ and C fibers in the mouse. High mechanical threshold A$\delta$, but not C fibers exhibit an increase in RF area after a conditioning protocol of mechanical stimulation in the *in vivo* rat tail (Reeh, Bayer, Kocher, & Handwerker, 1987). The two 'conditioned' C/A$\delta$ fibers in Study III may very well have

been A$\delta$ fibers and the empiric boundary of 1-1.2 m/s (Koltzenburg et al., 1997; J. J. Lawson et al., 2008; Price et al., 2001) may need to be lowered in the mouse.

*Erratic Ring Reservoir and Probe Tip Interaction*

A methodological concern emerged early in the project from the use of the ring reservoir. Five of 7 fibers exposed to GABA by ring reservoir in Study IIIa and IIIb had dramatic bidirectional changes in discharge frequency and/or VF threshold and include one C/Aδ fiber with a substantial increase in RF area (see above). These findings were not in agreement with those of the superfused fibers. The question arose as to whether a mechanical interaction was present between the ring reservoir and the VF filament on the RF. The observation that ring reservoir effects were primarily associated with the slower conducting, higher mechanical threshold fibers may be due to their lack of peripheral terminal myelination and other protective peripheral terminal structures and corpuscles. Incidental tension on the corium or the corium held in a non-compliant position from ring reservoir pressure may have disrupted the normal coupling of functional membrane receptors on terminal arborizations to explain the variable response to mechanical stimulation.

Alternative explanations are: 1) application of VF filaments over the most responsive area of larger RFs comprised of multiple hot spots was more difficult in the ring reservoir than in the open organ bath; 2) inadequate oxygen was available to the corium within the confines of the ring; and 3) one subset of GABA receptors was located on the RF within the ring and a different subset on the peripheral process outside the ring. In support of GABA effect from a subset of receptors, two fibers with enhanced responsiveness returned to the pre-test measure after a wash-out period.

The ring reservoir has been used on the rat skin-nerve preparation for more than 23 years and more recently in the mouse (Blunk et al., 2003; Reeh, 1986), but the most commonly used skin patch is derived from the saphenous nerve which is flat and square. Most ring reservoir experiments of this project were conducted on the irregularly shaped and unevenly contoured skin innervated by the sural nerve.

A final disadvantage to the ring reservoir and mechanical stimulation comes from LMEE usage within the confines of the ring reservoir. The reservoir volume was sufficient to allow free movement of the tip of the LMEE, but insufficient to allow instillation of a reasonable volume of agent to insure an adequate dose of GABA was delivered.

On the basis of these observations, the ring method was abandoned from any further mechanical stimulation use for the investigation of the loci of GABA activity. In defense of the ring reservoir, it remained a very effective tool for characterization of the responses of fibers to chemicals and hot and cold SIF at the end of each experiment.

One control VF threshold and LMEE constant pressure experiment (A$\delta$M, CV = 4.06 m/s, glabrous skin) was conducted early in the project to test the newly created ring reservoir. The control fiber had no change in VF threshold after repeated SIF treatment to the reservoir, but had a decrease in discharge frequency (pre-treatment = 26 impulses/s, post-treatment = 22 impulses/s). At the time the control experiment was conducted, a 15% decrease in discharge frequency was considered meaningless. Change in ring size, ring application technique, or selection of skin without contours may resolve the ring reservoir – mechanical probe tip interaction question.

## Study IV: Noxious Heat Stimulation

Four of six high mechanical threshold C and C/A$\delta$ fibers exceeded a 44% reduction in discharge frequency from laser stimulation during GABA exposure. Prior to laser acquisition, high mechanical threshold fibers during GABA exposure had a decreased responsiveness of 28% and 50% to mechanical and high frequency electrical stimulation, respectively. Some possible explanations for the disagreement in percentage of response fibers across the stimulus modalities are: 1) laser irradiation ablated cellular membrane functions separate and distinct from the effect of GABA; 2) noxious heat-sensitive fibers were better stimulated with the laser than mechanical stimulation; 3) selection of laser-sensitive fibers was biased towards an optimal GABA response. A difference exists between the latter two explanations. The second explanation refers to transformation of the project from 'underpowered' in Studies I, II and III, to adequately 'powered' in Study IV due to the precision of the laser technique. Since 72% of mouse C fibers respond to noxious heat and mechanical stimuli (J. J. Lawson et al., 2008), the laser may possibly be the best instrument to test the vast majority of nociceptive C fibers. Volumetric laser penetration of corium rather than the limited mechanical probe tip contact with the corium surface may be more likely to stimulate the most sensitive portion of RF to initiate many more peripheral terminal local receptor potentials. The third explanation refers to an obvious selection bias. Fibers selected for laser stimulation were chosen for robust, metered responses over the duration of a stimulus pulse. These fibers may inadvertently have been the most likely to respond to GABA. The first explanation was examined in control experiments where the treatment condition was SIF instead of GABA and is not likely to be the case. The second explanation may have to wait until the LMEE technique is mastered and the results can be compared to

laser results. The third explanation will have to be tested in future experiments by the use of the laser on fibers with lesser discharge frequencies, smaller action potential amplitudes, and more complex discharge patterns.

Laser stimulation of three RFs, innervated by multiple heat-sensitive fibers, yielded significant decreases in discharge frequency during 100 $\mu$M GABA and was reversed to baseline by either 1000 $\mu$M GABA or a wash-out period. The largest action potentials were selected for ease of analysis. In the latter two corium sections, the action potential discharge pattern bore a strong resemblance to the discharge pattern of laser-sensitive A$\delta$ fibers. The action potential amplitude, discharge pattern, and discharge latency of an uncharacterized fiber from Study IVb in Figure 25 (Appendix M) closely resembles the same properties of a characterized A$\delta$ fiber in Figure 19 (Appendix L). Again, a potential selection bias (see above) was present. An alternative analysis method is to compare the sum of all action potentials in the tracing before and during GABA treatment.

A very desirable laser technique is to irradiate the surface area of a RF within the confines of the ring reservoir for agent testing. The use of the ring reservoir allows sectional testing of the corium surface area for agent effects, whereas superfusion allows only one period of agent exposure per animal. Minimization of the number of animals used governs the design and execution of every project. However, the consequences of an analogous laser/ring reservoir interaction to the mechanical probe tip/ring reservoir interaction were a concern. Only one experiment was conducted that used noxious, heated SIF as the stimulus and no change in discharge frequency during GABA exposure was observed. The results indicate that the mechanical probe tip/ring reservoir effect does not necessarily cross sensory

modalities. In the future, a series of control experiments will be conducted to test for the presence of a laser/ring reservoir interaction prior to agent testing experiments.

The diode laser technique is a suitable instrument to deliver a noxious heat stimulus to heat-sensitive PAFs in the organ bath. It is adequate for the prediction of noxious heat sensitivity in C/Aδ fibers and capable of gauging drug effectiveness in C fibers. Future laser study will determine: 1) sensitivity of warming thermoreceptors by a lower driver current than of presumed nociceptors; 2) efficacy of laser stimulation to RF within a ring reservoir; 3) the optimal stimulus amplitude and duration to stimulate, but not sensitize A$\delta$ fibers; and 4) driver current required to adequately stimulate RFs on the broadened dermal and epidermal depth of the CFA mouse model.

## Study V: Noxious Chemical Stimulation

Only one fiber was examined for GABA sensitivity with the inflow/outflow reservoir technique. The CMHA fiber had a striking decrease in discharge frequency during GABA instillation and a return to baseline with wash-out. The data from one fiber is a case study, but this difficult experiment provides a cross-modality technique to measure GABA effects.

Key to the success with this technique is identification of a fiber with pronounced sensitivity to protons, and a RF located on a central portion of the corium, amenable to placement of the inflow/outflow reservoir. Both circumstances are seldom met. Several modifications are possible to increase the chance of success in an experiment where the difficult process of placement of the inflow/outflow reservoir is required before proton sensitivity is determined.

The first modification is to select fibers most likely to respond to protons prior to placement of the reservoir, and the second is to deliver a broader stimulus than just protons.

In this project, thirty-eight C and C/A$\delta$ fibers were examined for sensitivity to protons. Sixteen fibers with no response to protons (mean CV = 0.55 ± 0.06 m/s) were evenly distributed throughout the C and C/A$\delta$ range. Twenty-two fibers demonstrated a minimum of 2 action potentials upon exposure to protons (mean CV = 0.43 ± 0.03 m/s) and were evenly distributed throughout the C and C/A$\delta$ range. However, five fibers (mean CV = 0. 52 ± 0.09 m/s) had a vigorous metered discharge frequency from the proton stimulus and their CVs clustered (0.69, 0.66, 0.67 and 0.29, 0.29 m/s) at the higher and lower ends of C-fiber CVs. These CVs suggest the efficiency of Study 5 could be increased by a selection of fibers by a known measure (CV) prior to reservoir placement.

The second modification is to select a noxious chemical stimulus more likely to result in a robust metered response than protons alone. The addition of ATP and/or capsaicin to the proton stimulus solution increases the chance of selecting a cutaneous peptidergic (capsaicin sensitive and deeper epidermal/dermal layer) or non-peptidergic (ATP sensitive and superficial epidermal layer) fiber (Zylka, Rice, & Anderson, 2005) to induce a more robust response (Petruska, Napaporn, Johnson, Gu, & Cooper, 2000).

### Fibers with No Change in Responsiveness

No subset of characterized high mechanical threshold A$\delta$ or C fibers had changes in responsiveness more than any other subset from GABA exposure. So the question becomes: was there any fiber group that did not have a change in responsiveness from GABA exposure? All three CM fibers identified in this project (one each in Study II, IIIb, and IIIc) failed to have a change in responsiveness during GABA exposure. Three fibers studied by three different techniques can only provide a starting point for the formation of hypotheses and further GABA investigation.

## Conclusions and Perspectives

The specific aims of this project were to study the effects of GABA on afferent fibers, and the major goal was to develop the *ex vivo* mouse skin-nerve preparation and measurement instrumentation to adequately test anti-nociceptive and analgesic endogenous and pharmacological compounds.

First, let me express my thoughts about development of the mouse skin-nerve preparation and a functional electrophysiological rig. Although I had many challenges, I also had several accomplishments. Perhaps my greatest advancement was the design of a dual compartment recording chamber that maintained receptor behavior for greater than 10 hours. Inspiration came from Peter Reeh and Stephen Schneider (former postdoctoral student of Dr. Perl), but 'trial and error' led to the design and construction of a very functional, durable, and reproducible chamber, scaled to mouse proportions. Figures 28 and 29 (Appendix U) represent my design plans for the mouse skin-nerve recording chamber. Other advances were: 1) economical 'top to bottom' construction of an electrophysiological rig (inclusive of hardware, pClamp and Spike2 software, and diode laser) for under $23,000; 2) creative laboratory construction of a constant pressure mechanical stimulator from disposable surgical supplies for high mechanical threshold fibers and from a miniature mobile phone loudspeaker for low mechanical threshold fibers; 3) pharmacological examination of responses of somatosensory C fibers to high frequency stimulation; 4) development of a technique to compare corium- and epidermal-derived responses from electrical and mechanical stimulation of a single fiber; and 5) the implementation of a diode laser as a noxious heat stimulus. These accomplishments were directly applied to the achievement of the Specific Aims.

Specific Aim 1 was to classify GABA-responsive PAFs by excitability and conductivity and by sensory modality and stimulus intensity. No change in non-activity dependent excitability or conductivity was observed in any classification of fibers during GABA exposure. These results challenge the findings of Bhistkul, et al. (1987) and Brown and Marsh (1978) of slowing of conduction and decreased amplitude of CAP components. On the other hand, an increase in activity dependent conduction latency was observed in half (all CMHA) of high mechanical threshold C fibers during GABA exposure and may lend support to the notion that GABA interferes with the conduction of high frequency impulses.

In support of the animal behavioral work of Carlton, et al. (1999), Denda, et al. (2002, 2003), and Reis, et al. (2006, 2007a, b), a portion of high mechanical threshold single fibers had suppressed responsiveness to mechanical stimuli during GABA exposure. In the subset of fully characterized fibers, no group of high mechanical threshold fibers was identified as the most likely to have a change in responsiveness during GABA exposure. However, CM fibers were observed to be the least likely to have a change in responsiveness during GABA exposure.

A majority of noxious heat sensitive fibers had suppressed responsiveness during GABA exposure and one CMHA fiber had suppressed responsiveness to a noxious proton stimulus during GABA exposure. Results from noxious heat and proton study phases support the notion that GABA may not only influence noxious mechano-sensitive mechanisms as reported in the animal behavior literature, but also noxious thermo-sensitive and chemo-sensitive mechanisms. The aggregate of the observations from Studies II-V supports the view that the action of GABA in the periphery is inhibitory.

The probable confounding mechanical force interaction between the ring reservoir and the tip of mechanical probes limited the search for the anatomic loci of GABA activity (Specific Aim 2) and it remains unknown if GABA agonists are better suited for topical, perineural, or systemic applications. A reasonable approach for drug delivery is to apply the GABA agonist to the anatomical structures that localize functional GABA receptors. Future work will emphasize the validity and reliability of laser stimulation within the ring reservoir for identification of anatomic loci of GABA activity. A limited number of experiments were conducted to determine optimal GABA concentrations to suppress activity of high mechanical and heat threshold fibers. A subset of GABA responsive fibers was exposed to a 10 fold increase or decrease in concentration and a paucity of evidence supported a difference from responses to 100 $\mu$M GABA (Specific Aim 3).

Why do PAFs and peripheral terminals localize GABA and GABA receptors? Nociception and pain are subject to the competitive influence of excitatory and inhibitory endogenous mechanisms, a balance infrequently studied more peripheral than the first synapse in the spinal cord. Critical to correlating afferent activity to pain are clear signals from sensory structures in response to both brief and persistent noxious stimulation. Peripheral endogenous inhibition by GABA and exogenous inhibition by GABA-derived analgesics may serve to maintain high fidelity signals from sensory cells specific to the detection of noxious events.

While this research was not designed to reach the point of application of GABA as an adjuvant analgesic, the methodology required for peripheral pharmacological testing has been advanced by this basic work. New approaches to the selective inhibition of nociceptive

impulse generation and conduction are valuable steps to the ultimate goal of improved ambulatory surgical pain management.

# APPENDICES

## APPENDIX A

### Compound Action Potential from a Sural Nerve Fascicle

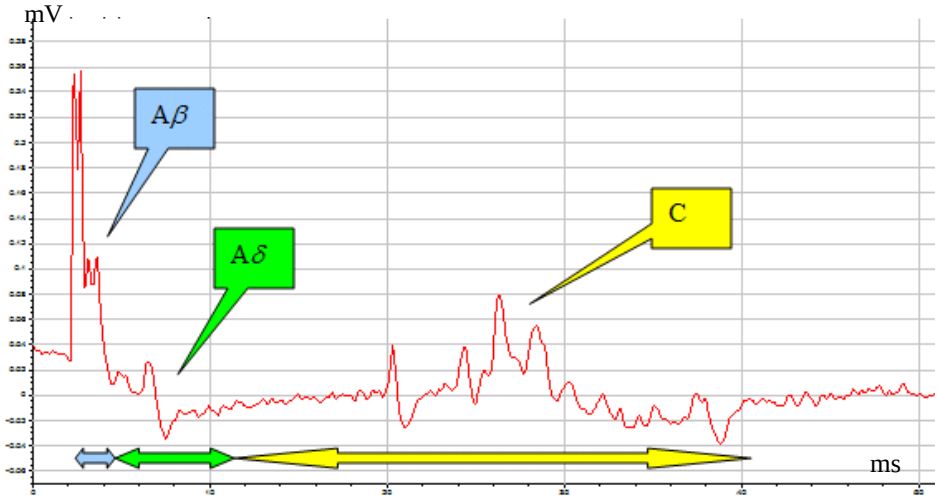


*Figure 1.* Example of a CAP recorded from a 12.5 mm length of a large sural nerve fascicle.

APPENDIX B

Aims and Methods of Previous GABA Studies

Table 1.

*Aims and Methods Used in GABA Studies*

| Aim | Support or Challenge | Method | Study Phase | Variable/Unit of Measure | Level of Analysis |
|---|---|---|---|---|---|
| 1 | Early studies of Bhisitkul (1987); Brown (1978) | Limited electrical: CV | I | Latency (ms) | pre/post test |
| | | Electrical threshold | | Electrical threshold (V) | pre/post test |
| 1 | None | Activity dependent electrical: C-fibers | II | Proportional latency change pre-/post-high frequency stimulus (percentage points | pre/post test change from high frequency stimulation proportional |
| 1 | Animal studies of Carlton (1999); Denda (2002, 2003); Reis (2006, 2007a,b) | Mechanical: VF-constant force Graded | IIIa | Discharge frequency (#/time) | Pre/post test 44% change in frequency |
| | | LMEE-constant pressure | IIIb | VF threshold (kPa) | Pre/post test observed change in threshold |
| | | | IIIc | Discharge frequency (#/time) | Pre/post test 44% change in frequency |
| 1 | Carlton (1999) | Noxious heat: Diode laser | IVa | Discharge frequency (#/time) | Pre/post test 44% change in frequency by fiber |
| | | Diode laser | IVb | Discharge frequency (#/time) | Pre/post test 44% change in frequency by RF area |
| | | Heated SIF to ring reservoir | IVc | Discharge frequency (#/time) | Pre/post test 44% change in frequency by fiber |
| 1 | None | Chemical: Protons to in/outflow reservoir | V | Discharge frequency (#/time) | Pre/post test 44% change in frequency by fiber |
| 1 | None | Innocuous cooling stimulation | VI | Spontaneously ongoing discharge frequency (#/min) | observation of change in discharge frequency |
| 2 | Carlton (1999); Stoyanova (2004), Nakagawa (2003) | Anatomic loci of activity | I, IIIa, IIIb, IVc, V | Quality of effect: suppression or enhancement discharge frequency from GABA | R, S, S-R Groups – observations R=ring, S=superfusate |
| 3 | Paradoxical pro-nociception: Carlton (1999); Ocvirk (2008) | Concentration effects | I, II, IIIabc IVab | Discharge frequency (#/min) | pretest and 2 posttest comparison from change in concentration |

APPENDIX C

Skin-nerve Preparation Schematic Representation and Photograph

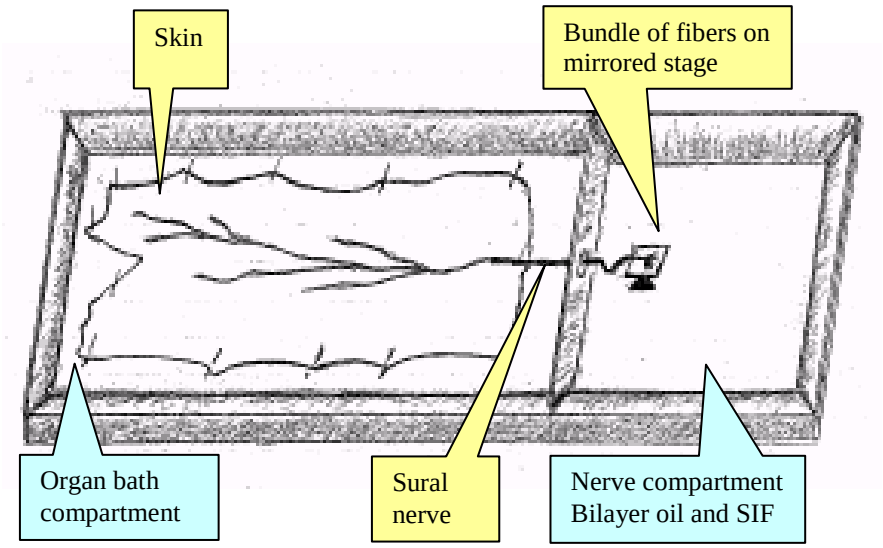


*Figure 2.* Schematic representation of the sural skin-nerve preparation.

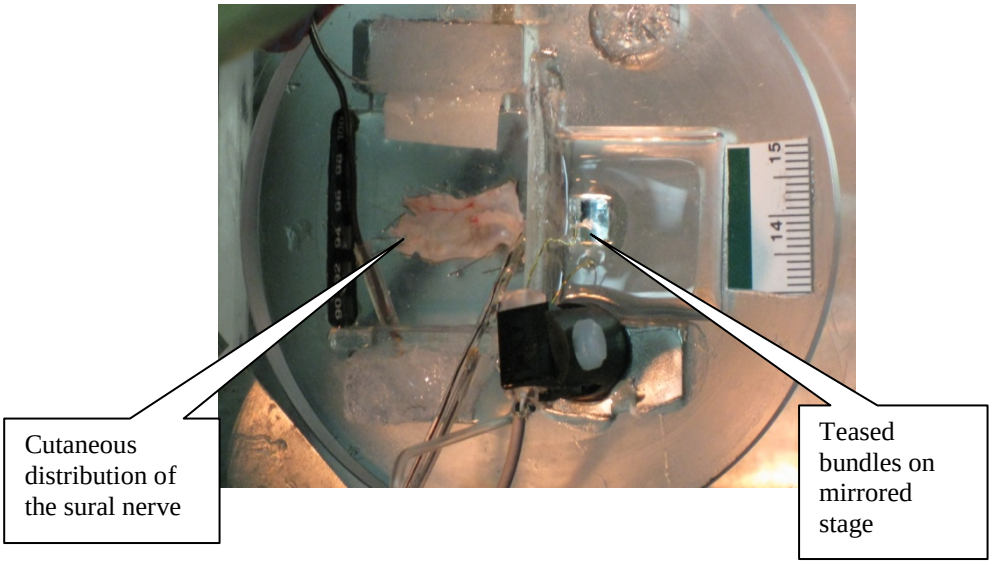


*Figure 3.* Skin-nerve preparation in the dual compartment recording chamber.

APPENDIX D

GABA Analog Formulae and $GABA_{A-C}$ Receptor Figures

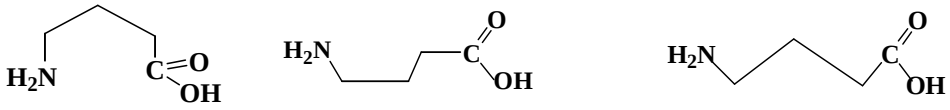

GABA molecules in freely- rotated configurations (1, 2, 3)

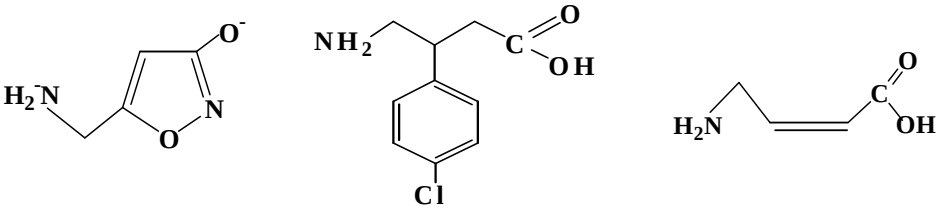

$GABA_{A-C}$ agonists in ring or linear chain restricted configurations
(4. muscimol; 5. baclofen; 6. CACA)

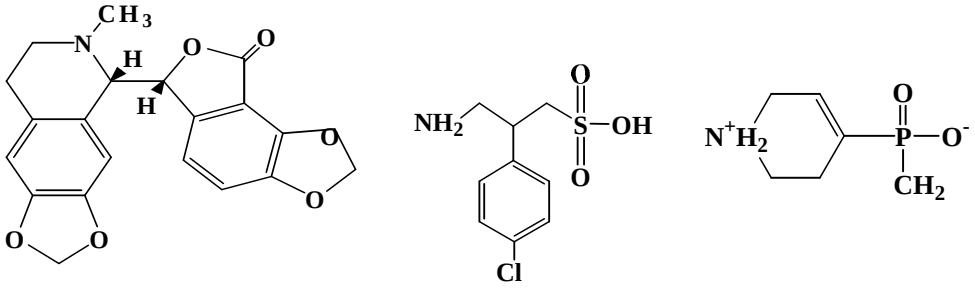

$GABA_{A-C}$ antagonists in ring restricted configurations
(7. bicuculline; 8. saclofen; 9. TPMPA)

*Figure 4.* GABA analog structures [Kerr & Ong (1992), Bowery (1993), Chebib & Johnston (1999)].

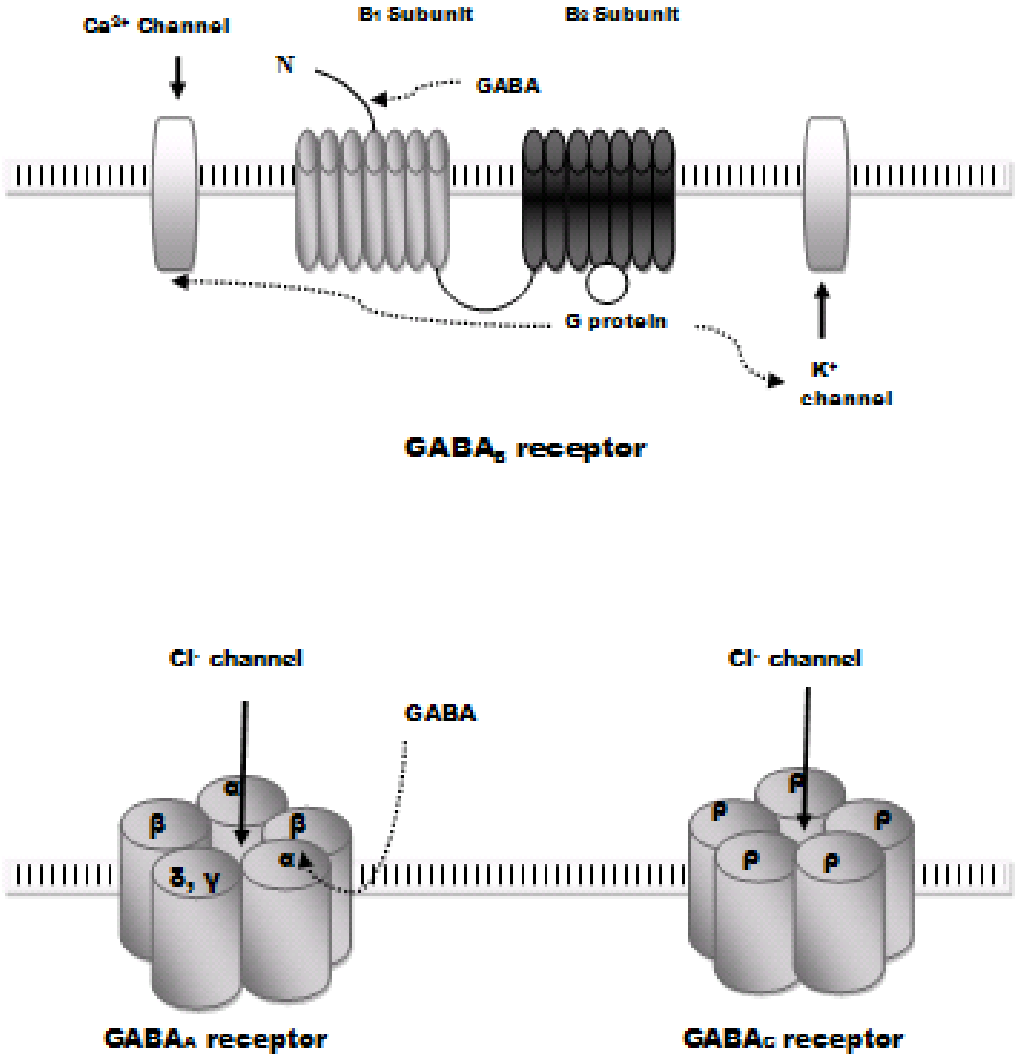


*Figure 5.* $GABA_{A\text{-}C}$ receptor subtype schematic (dotted arrows indicate GABA and G-protein binding sites and solid arrows indicate ion channels).

APPENDIX E

$GABA_{A-C}$ Receptor Properties

Table 2.

*Central $GABA_{A-C}$ Receptor Responsiveness to Pharmacological Agonists, Antagonists, and Allosteric Modulators*

| Receptor Type Pharmacologic Sensitivity[a] | $GABA_A$ | $GABA_B$ | $GABA_C$ |
|---|---|---|---|
| Baclofen | Inactive[b] | Potent agonist[c] | Inactive |
| barbiturates | Positive modulator | Inactive | Inactive |
| benzodiazepines | Positive modulator | Inactive | Inactive |
| Bicuculline | Competitive antagonist[d] | Inactive | Inactive |
| CACA | Weak agonist | Inactive | Partial agonist[e] |
| Calcium | Negative modulator[f] | - | |
| Muscimol | Potent agonist | Inactive | Partial agonist |
| Neurosteroids | Positive & negative modulators | Inactive | Inactive |
| Protons | Positive↓pH<br>Negative ↑pH modulator | - | Negative ↓ pH<br>Positive ↑ pH modulator |
| Phaclofen | inactive | Competitive antagonist | Inactive |
| Picrotoxin | Negative modulator | Inactive | Competitive antagonist |
| Saclofen | Inactive | Competitive antagonist | Inactive |
| TPMPA | Weak antagonist | Weak agonist | Competitive antagonist |

*Notes:*

[a] Compiled from Bormann, 2000; Cherubini & Strata, 1997; Johnston, 1996a, 1996b; Murata, Woodward, Miledi, & Overman, 1996; Wang, Hackam, Guggino, & Cutting, 1995; Wegelius et al., 1996.

[b] Inactive is relative potency with respect to other receptor subtypes and not an absolute measure of activity.

[c] Agonists bind to the GABA receptor site; selectivity is relative to other receptor subtypes and is not absolute.

[d] Competitive antagonists prevent GABA receptor activation through occupancy of GABA receptor site.

[e] Partial agonist is relative to the efficacy of GABA.

[f] Non-competitive positive and negative modulators bind to allosteric binding sites; positive allosteric modulator exhibits similar effect compared to GABA and negative allosteric modulator binds to the same allosteric site but exerts an opposite or inverse effect.

# APPENDIX F

## Solutions and Concentrations for Electrophysiological Recording

Table 3.

*Solutions and Concentrations Used in Electrophysiological Recordings*

| Agent | Desired action | Concentration |
|---|---|---|
| GABA | GABA receptor agonism | 10, 100, 1000 $\mu$M |
| SIF acidified with HCl | TRPV1 receptor agonism | pH ≤ 4.0 |
| Adenosine triphosphate | $P2X_3$ receptor agonism | 100 $\mu$M |
| Capsaicin | TRPV1 receptor agonism | 10 $\mu$M |
| Lidocaine HCl | Sodium channel antagonism | 1 mM |

APPENDIX G

Receptive Field Distributions of Sural and Plantar Nerves

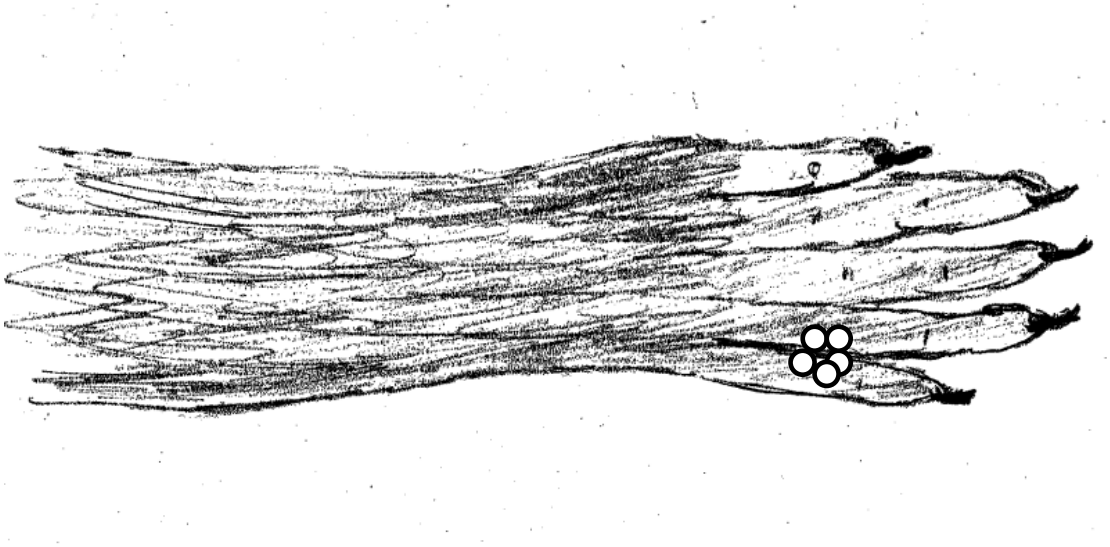

*Figure 6.* Receptive field distribution on hind-paw dorsal surface of sural nerves in GABA and control experiments (upper aspect is medial, lower aspect is lateral, ○ indicates location, but not size).

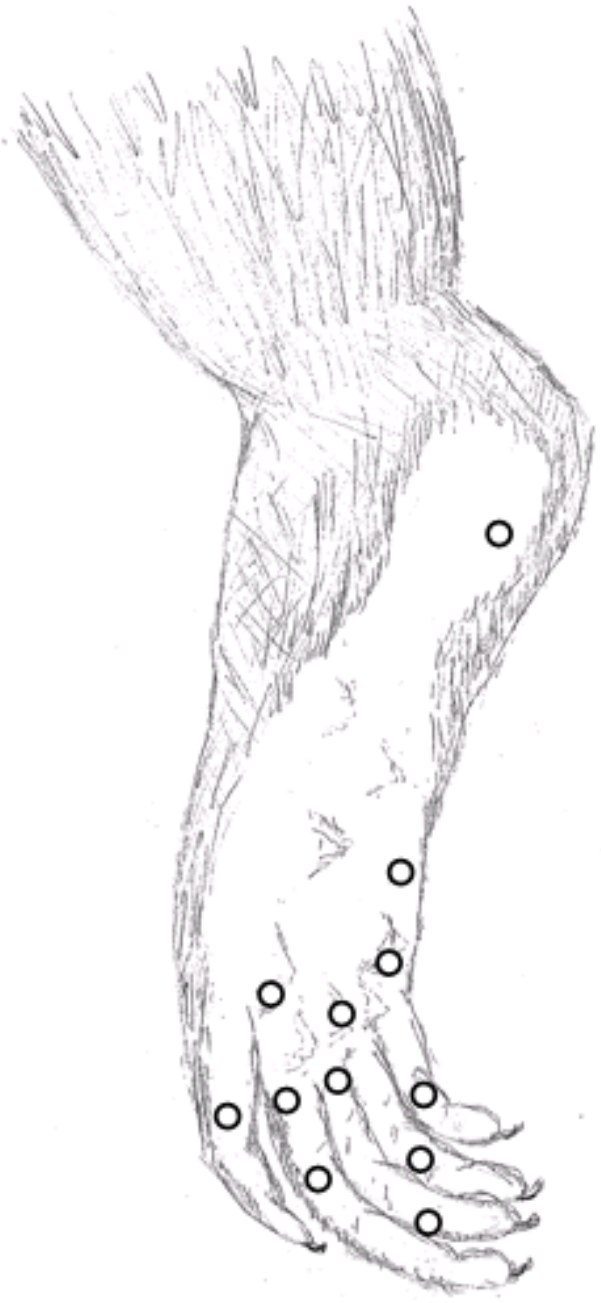

*Figure 7.* Receptive field distribution on hind-paw plantar surface of plantar nerves in GABA and control experiments (medial aspect is right, lateral aspect is left, ○ indicates location not size).

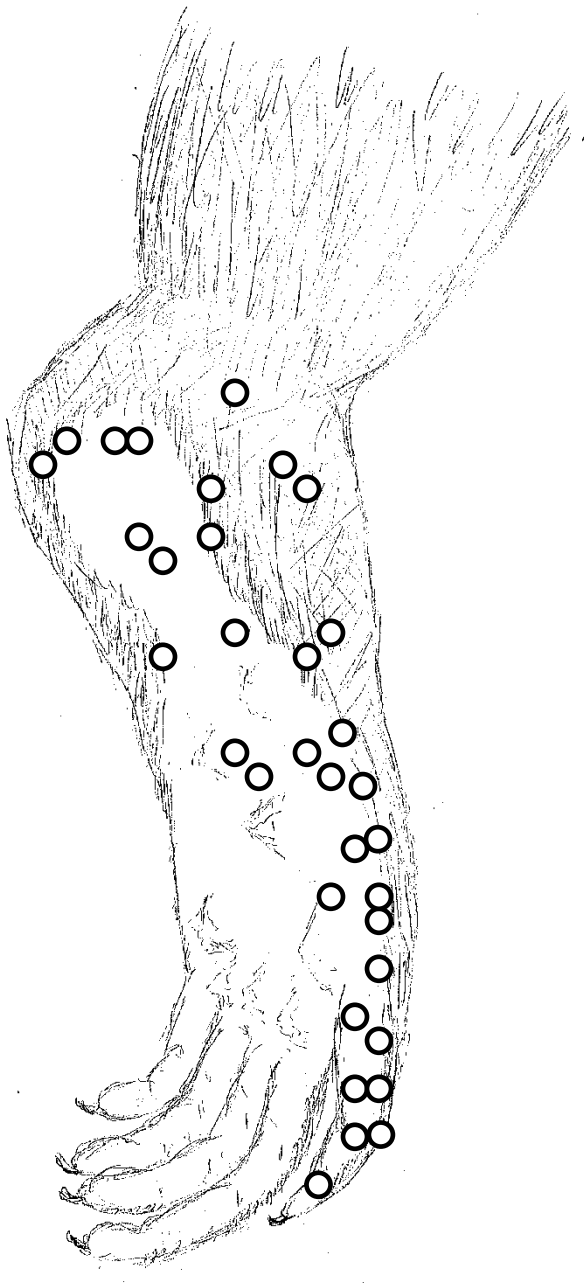

*Figure 8.* Receptive field distribution on hind-paw plantar surface of sural nerves in GABA and control experiments (medial aspect is left, lateral aspect is right, ○ indicates location, but not size).

APPENDIX H

Von Frey Filament Conversion Units

Table 4.

*Conversion Units for Von Frey Filaments*

| Handle marking | Force (g)[a] | Area ($mm^2$)[b] | Pressure ($g/mm^2$)[c] | Force (mN)[d] | Pressure (kPa)[ce] |
|---|---|---|---|---|---|
| 1.65 | 0.0045 | 0.0032 | 1.4063 | 0.078 | 13.79 |
| 2.44 | 0.0275 | 0.0082 | 3.3537 | 0.392 | 32.89 |
| 2.83 | 0.068 | 0.0127 | 5.3543 | 0.686 | 52.51 |
| 3.22 | 0.166 | 0.0196 | 8.4694 | 1.569 | 83.06 |
| 3.61 | 0.407 | 0.0249 | 16.3454 | 3.922 | 160.2 |
| 3.84 | 0.692 | 0.0324 | 21.358 | 5.882 | 209.4 |
| 4.08 | 1.202 | 0.0412 | 29.1748 | 9.804 | 286.1 |
| 4.56 | 3.63 | 0.0995 | 36.4824 | 39.216 | 357.7 |
| 4.74 | 5.495 | 0.114 | 48.2018 | 58.824 | 472.7 |
| 4.93 | 8.511 | 0.1295 | 65.722 | 78.431 | 644.5 |
| 5.07 | 11.749 | 0.1466 | 80.1432 | 98.039 | 785.9 |
| 5.18 | 15.136 | 0.1832 | 82.6201 | 147.059 | 810.2 |
| 5.46 | 28.84 | 0.2454 | 117.5224 | 254.902 | 1152.5 |

*Notes:*

[a] average actual measurements for force as provided by Stoelting

[b] Cross-sectional area calculated from average actual filament diameter (Stoelting Catalog 58011)

[c] Applied pressure is calculated and listed as $g/mm^2$ and kilopascals (pascal: $Pa = N/m^2 = kg/m \cdot s^2$)

[d] individually calibrated by Stoelting in Newtons

[e] Filaments as measured in kPa are ordinal scaled.

APPENDIX I

Reservoir Instruments

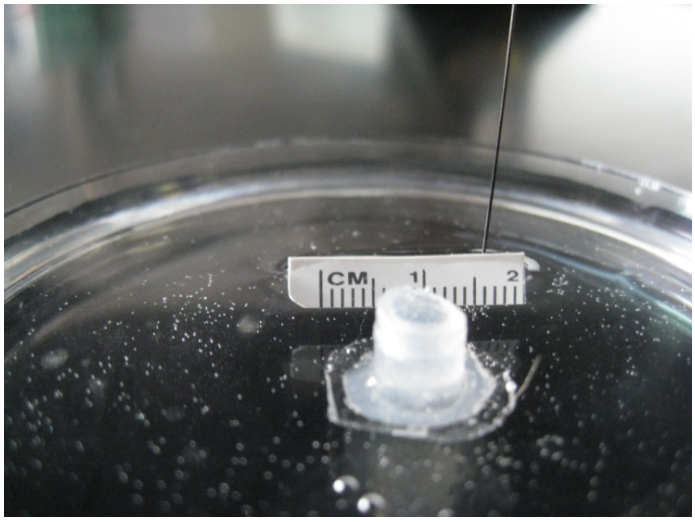


*Figure 9.* Ring reservoir.

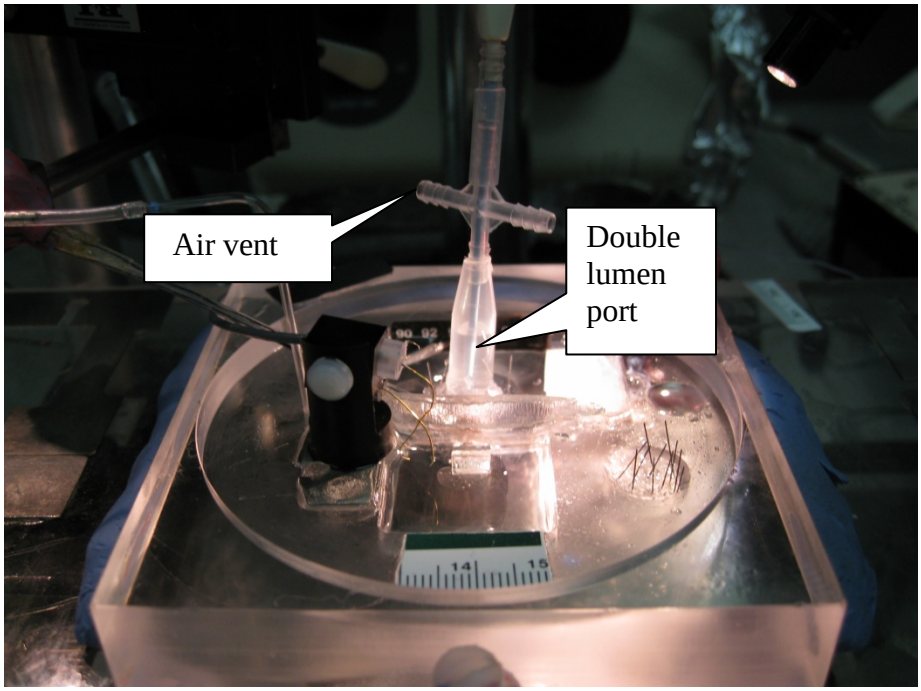


*Figure 10.* Inflow/outflow reservoir for noxious thermal and chemical stimulation.

APPENDIX J

Mechanical Stimulator Design and Representative Recording

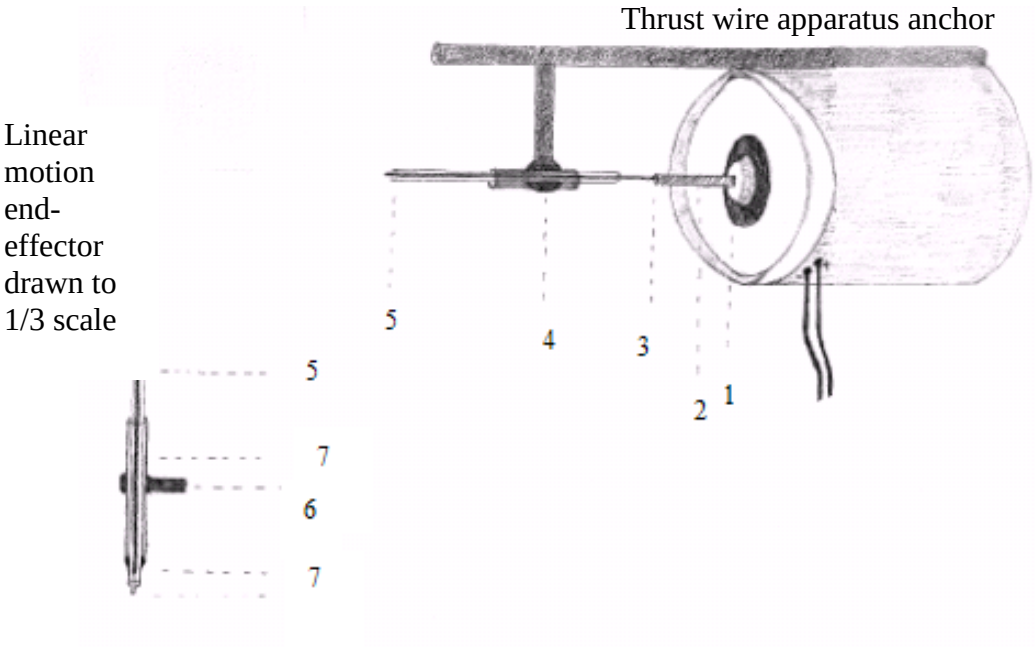


*Notes*:
1. Drive mechanism of actuator
2. Threaded adaptor
3. Flexible stranded stainless steel thrust wire coupled to threaded adaptor
4. Fixed point of semi-rigid plastic tube casing of thrust wire apparatus
5. Continuous semi-rigid plastic casing and flexible stranded stainless steel thrust wire
6. Modified tuberculin syringe secured to xyz micromanipulator and ground wire
7. Stabilization points of plastic tube casing to modified tuberculin syringe
8. Linear motion end-effector (LMEE) device composed of von Frey filament (3cm x 0.3mm$^2$ surface area) attached to thrust wire

*Figure 11.* Permanent magnet-series electrodynamic vibration actuator coupled to flexible end-effector linear motion device for stimulation of mechano-sensitive fibers.

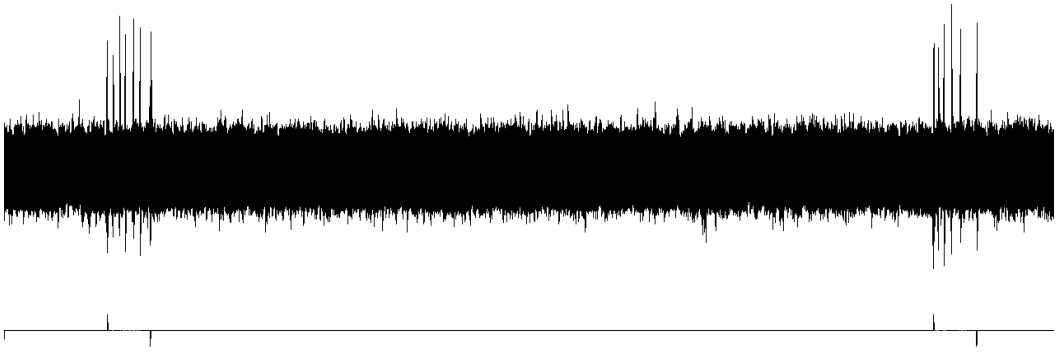

*Figure 12.* Two mechanical pulses (upper trace, interstimulus interval = 1 min) with onsets and offsets of stimulus (bottom trace).

APPENDIX K

Laser Photographs

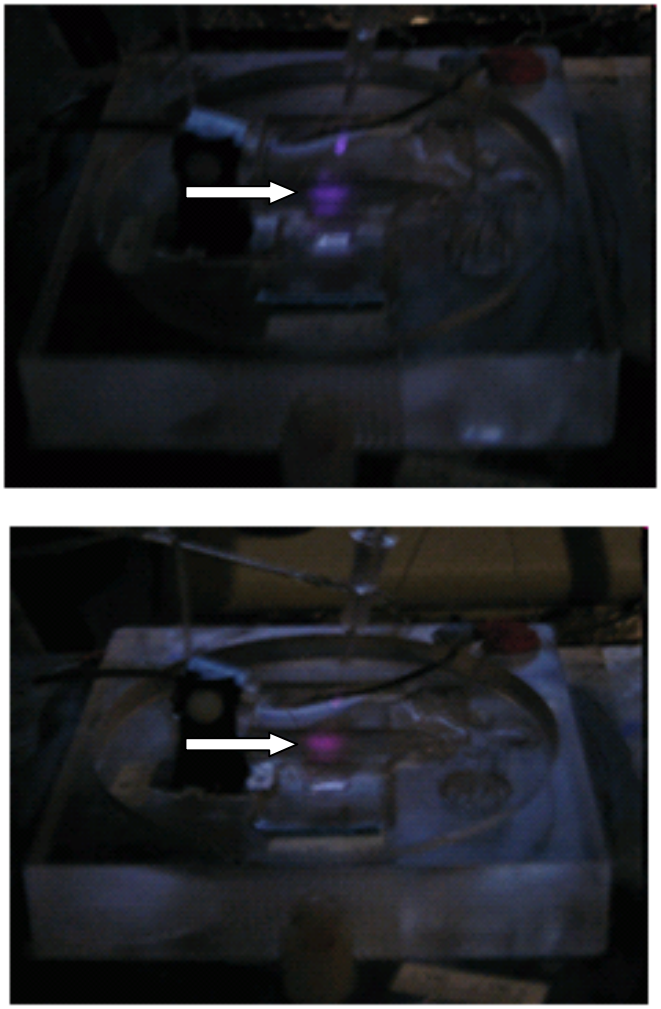

*Figure 13.* Correspondence of infrared beam area (upper image) with visible locator beam area (lower image) indicated with arrows.

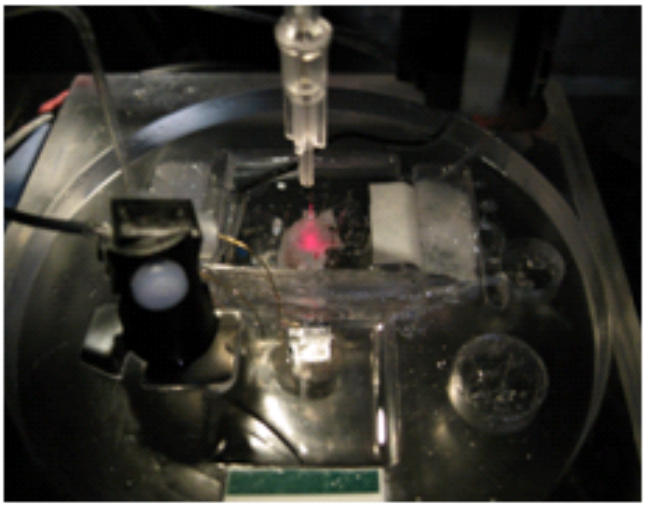

*Figure 14.* Visible beam area (pink) during infrared laser irradiation of mouse cutaneous receptive field in organ bath.

APPENDIX L

Summary of Laser Property Data

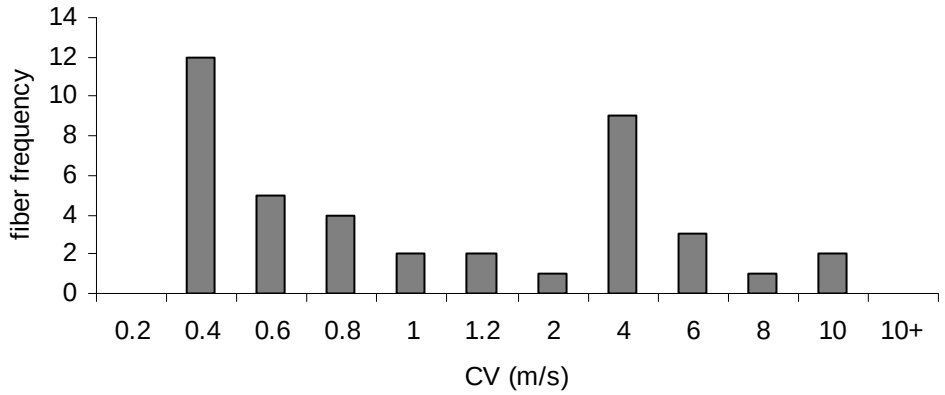


*Figure 15.* Conduction velocity of 41 fibers examined in laser experiments.

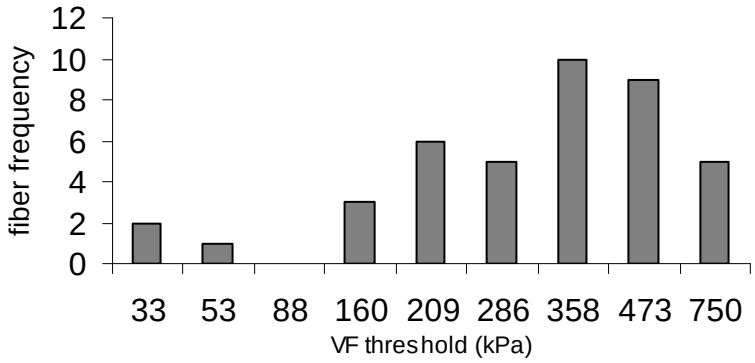


*Figure 16.* Von Frey threshold of 41 fibers examined in laser experiments.

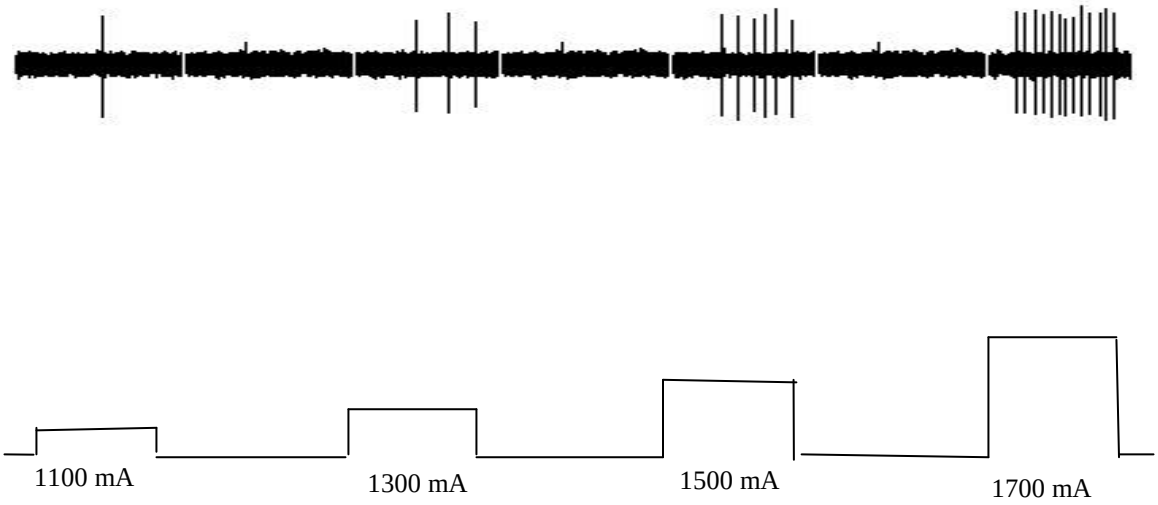


*Figure 17.* Example of responses of a high mechanical threshold C fiber (top trace) to four 7 s pulses of graded laser emissions (bottom trace).

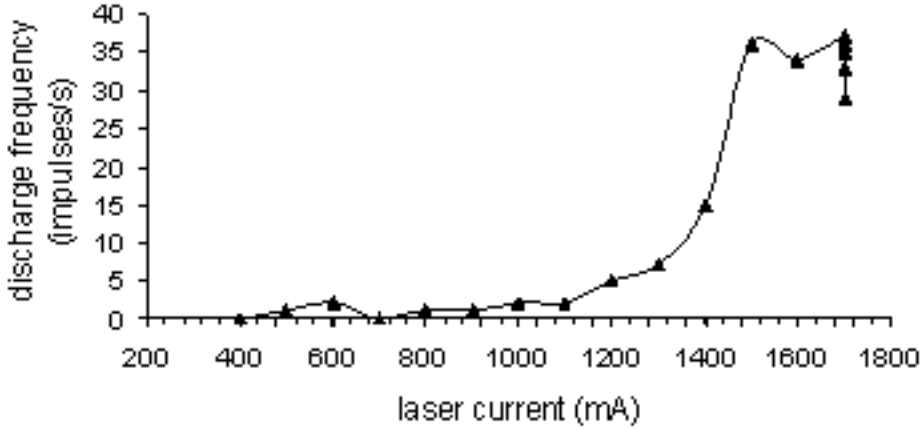


*Figure 18.* Laser stimulus-response relationships of a single high mechanical threshold C fiber to graded increases in laser driver current and repetitive 7 s pulses.

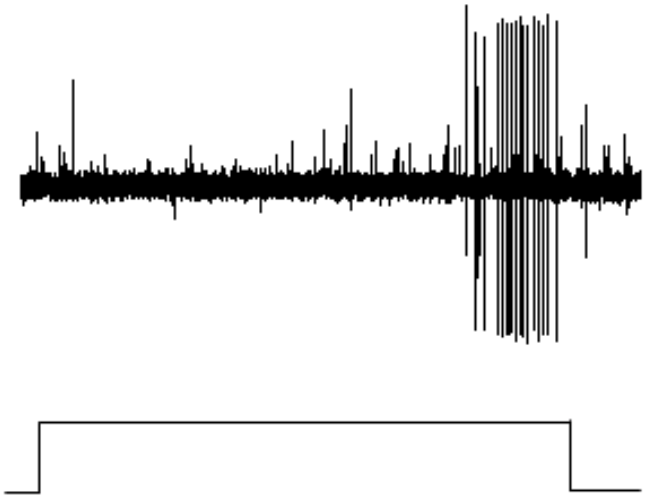

*Figure 19.* Delayed laser-induced discharge pattern (upper trace) of a very high mechanical threshold Aδ fiber to a 7 s laser pulse (lower trace).

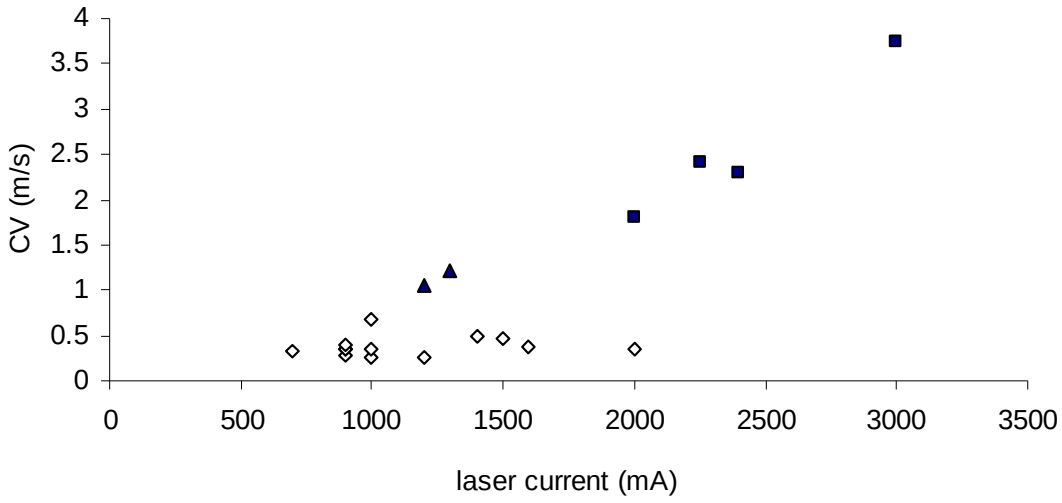


*Figure 20.* Relationship of CV to the laser driver current to stimulate 19 fibers (four Aδ fibers represented by ■, 2 C/Aδ fibers by▲, and 13 C fibers by ◊) to threshold.

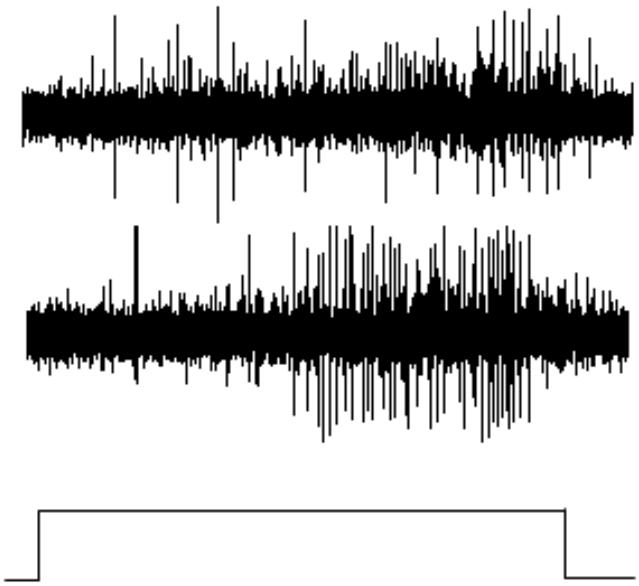

*Figure 21.* Possible laser-induced sensitization from use of laser as search stimulus (upper trace shows initial laser pulse, middle trace shows second identical pulse, and duration of pulse is shown in lowest trace

APPENDIX M

Summary of GABA Data

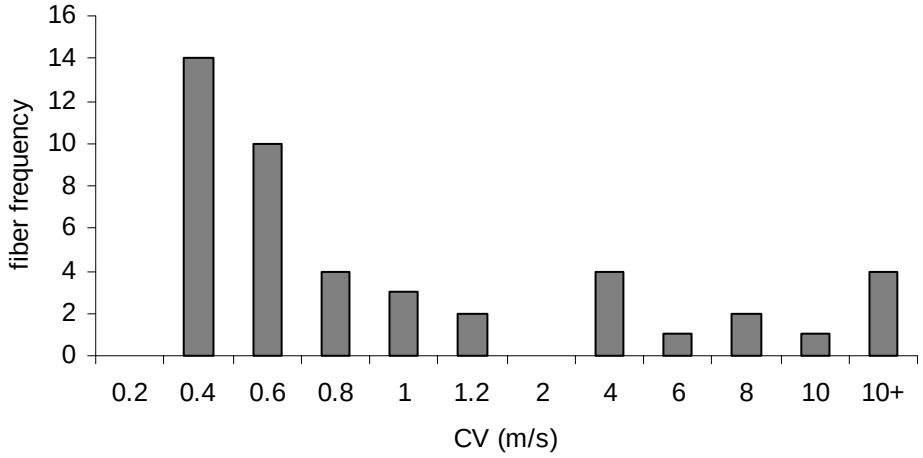


*Figure 22.* Conduction velocity of 45 fibers examined for responsiveness to GABA.

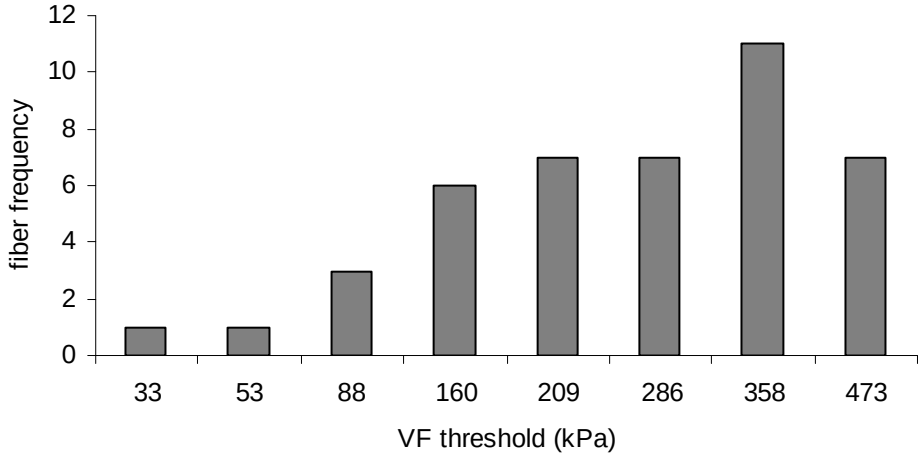


*Figure 23.* Von Frey thresholds of 43 fibers examined for responsiveness to GABA.

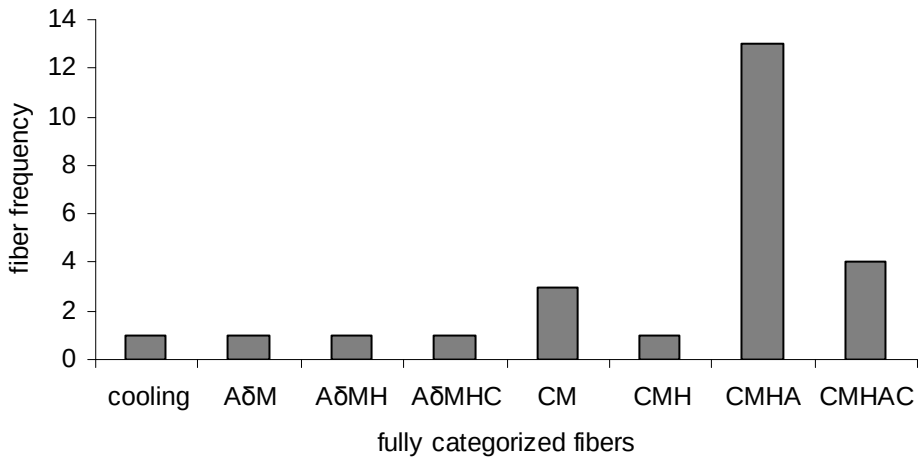


*Figure 24.* Categories of 25 characterized fibers in Studies I-VI.

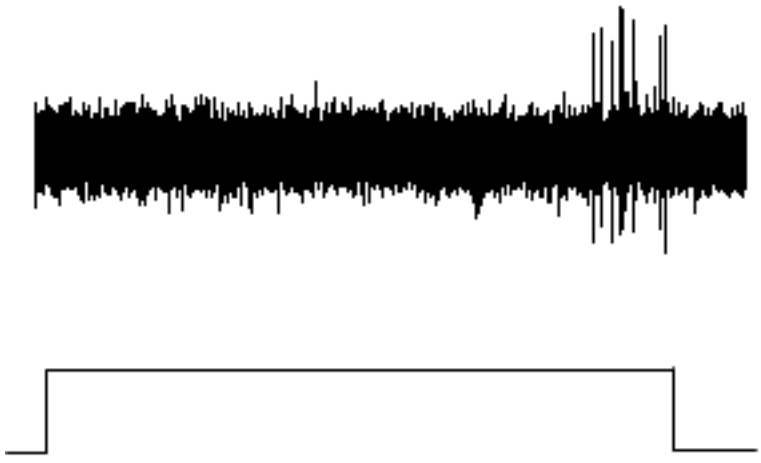

*Figure 25.* Responses from laser stimulation of multiple fibers (upper trace) to a 7 s laser pulse (lower trace).

APPENDIX N

Study II. Representation of Activity Dependent Conduction Delay

The below tracing is an example of activity dependent conduction delay. From top to bottom: the first trace is representative of the pre- GABA treatment condition and before high frequency electrical stimulation of the nerve (black); the second trace is representative of the pre- GABA treatment condition and at the end of 3 min of high frequency stimulation (black); the third trace is representative of 2 min GABA treatment before high frequency stimulation (maroon); and the fourth trace is representative of 5 min of GABA treatment and at the end of 3 min of high frequency stimulation (maroon). Arrows indicate the single fiber action potential under study.

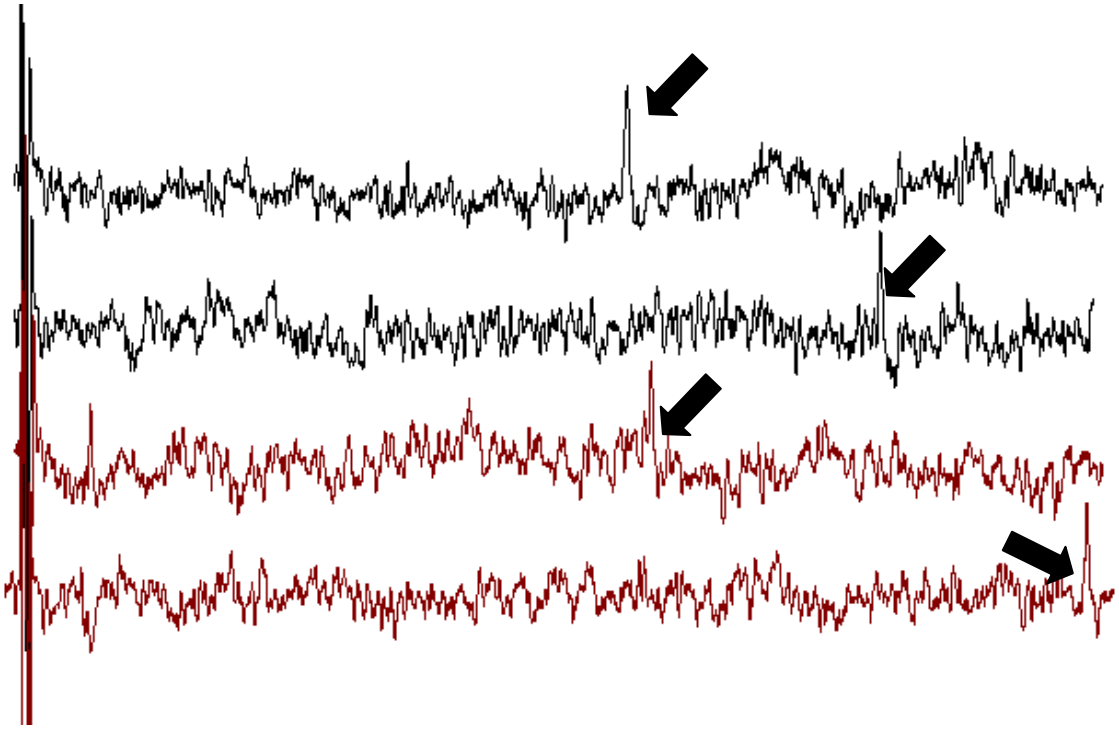

*Figure 26.* Activity dependent conduction delay.

## APPENDIX O

## Study IIIa: Response from Von Frey Stimulation

Table 5.

*Summary of Responses of Von Frey Stimulation in Study IIIa*

| Delivery method | Skin type | Fiber class | CV m/s | Discharge Frequency in Impulses/s | | | |
|---|---|---|---|---|---|---|---|
| | | | | Pre-test | 100 $\mu$M GABA 3 min | 100 $\mu$M GABA 6 min | 1000 $\mu$M GABA 3 min |
| S | g | **A**δM§ | 4 | 12 | 12 | - | 12 |
| S | h | **C/A**δLTh§ | 1.04 | 7 | 7 | - | 7 |
| S | h | **C**MA§ | 0.73 | 8 | 13 | - | 13 |
| S | g | **C**LTh§ | 0.64 | 43 | 42 | 42 | - |
| R | h | **C/A**δM§ | 1.00 | 17 | 40 | - | - |
| R | g | **A**δLTh§ | 5.16 | 20 | 27 | 29 | - |
| R | h | **A**δLTh§ | 6.84 | 40 | 30 | - | 6 |
| R | h | **C**MA§ | 0.69 | 12 | 14 | - | 10 |

*Note:* g = glabrous; h = hairy; **C =** C fiber; **A =** A fiber; LTh= positive response to low pressure mechanical stimuli; M = positive response to high, but not low pressure mechanical stimuli; A = positive response to protons; H = positive response to noxious heat; C= positive response to noxious cold; § = no characterization for noxious thermal stimuli; S = superfusion; R = ring reservoir.

APPENDIX P

Study IIIb: Single Fiber Changes in Von Frey Threshold

Table 6.

*Summary of Single Fiber Changes in Von Frey Threshold in Study IIIb*

| Delivery method | Skin type | Fiber class | CV m/s | Pre-test VF threshold | 3 min 100 $\mu$M GABA threshold | 5 min 100 $\mu$M GABA threshold | 3 min 1000 $\mu$M GABA threshold | [a]Wash 10min [b]100 $\mu$M GABA |
|---|---|---|---|---|---|---|---|---|
| S | g | **A**$\delta$M§ | 4.00 | 358 | 358 | - | 358 | - |
| S | g | **C**MAC§ | 0.25 | 358 | 473 | 358 | - | - |
| S | g | **A**$\delta$LTh§ | 3.21 | 160 | 160 | 209 | 160 | - |
| S | h | **C**MH§ | 0.31 | 209 | 358 | 160 | - | - |
| S | h | **A**$\delta$H§ | 2.95 | 286 | - | 473 | - | - |
| S | h | **C/A**$\delta$LTh§ | 1.04 | 53 | 83 | 83 | - | [a]53 |
| S | h | **C**MA§ | 0.73 | 473 | 358 | | 358 | - |
| S | h | **C**LTH§ | 0.64 | 83 | 83 | 83 | - | - |
| S | g | **A**$\delta$MH | 6.36 | 209 | 209 | 286 | 358 | - |
| S | h | **A**$\beta$SAII | 30.0 | 160 | 160 | 160 | 160 | - |
| R | h | **A**$\delta$M | 8.8 | 209 | 209 | 83 | - | [a]209 |
| R | h | **C/A**$\delta$M§ | 1.00 | 358 | 209 | 83 | - | [a]209 |
| R | h | **A**$\delta$LTh§ | 5.16 | 160 | 160 | 160 | - | [b]286 |
| R | h | **A**$\delta$LTh§ | 6.84 | 160 | 160 | - | 160 | - |
| R | h | **C**MA§ | 0.69 | 358 | 358 | - | 286 | - |
| R | h | **A**$\beta$SAII§ | 31.0 | 83 | 83 | | 83 | - |
| R | g | **A**$\beta$SAII§ | 15 | 83 | 83 | 83 | - | - |

*Note:* g = glabrous; h = hairy; **C =** C fiber; **A =** A fiber; LTh = positive response to low pressure mechanical stimuli; M = positive response to high, but not low pressure mechanical stimuli: A: positive response to protons; H: positive response to noxious heat; C = positive response to noxious cold; § = incomplete characterization for noxious thermal stimuli and/or protons; S = superfusion; R = ring reservoir; SAII = rapid conducting, slow adapting fiber with regular discharge pattern to velocity displacement.

APPENDIX Q

Study IIIc: Single Fiber Responses from Linear Motion End Effector Stimulation

Table 7.

*Summary of Single Fiber Responses from Mechanical Stimulation in Study IIIc*

| Skin type | Fiber class | CV | Discharge Frequency in Impulses/s | | | | | |
|---|---|---|---|---|---|---|---|---|
| | | | Pre-test | 100uM GABA 3min | 100uM GABA 5min | 100 $\mu$M GABA 7.5m | 1000 $\mu$M 3 min | Wash 10-15 min |
| h | **C**LTh§ | 0.81 | 6.4 | 4.4 | 6.8 | - | - | 5.4 |
| h | **A**βSAI +C | 12 | 8.3 | 8.0 | - | - | - | 8.0 |
| g | **C**MHAC | 0.47 | 2.2 | 2.2 | - | - | - | - |
| g | **C**MHAC | 0.34 | 8.2 | 4.6 | - | - | - | 4.8 |
| h | **C**M | 0.45 | 4.3 | 6.72 | - | - | - | - |
| h | **C**MHA | 0.30 | 2.7 | 2.8 | - | - | - | - |
| h | **C**MHA | 0.29 | 4 | 4.8 | - | - | - | - |
| h | **C**MHA | 0.29 | 3.7 | 3.2 | 2.0 | 3.4 | 2.6 | |
| h | **C**MHAC | 0.37 | 1.4 | 1.6 | - | - | - | 2.0 |
| h | **A**δMHC | 2.4 | 9.5 | 9.6 | 7.5 | - | - | 9.6 |
| h | **C**M | 0.90 | 2.6 | 2.8 | 2.8 | 3.2 | - | - |
| h | **C**MHAC | 0.30 | 4.8 | 4.8 | 6 | 5 | - | 5.4 |
| h | **C**MHA | 0.27 | 1.8 | 1.6 | 1.8 | 1.6 | - | 1.4 |

*Note:* g = glabrous; h = hairy; **C** = C fiber; **A** = A fiber; LTh = positive response to low pressure mechanical stimuli; M = positive response to high pressure mechanical stimuli, but not low mechanical threshold stimuli; A = positive response to protons; H= positive response to noxious heat; C = positive response to noxious cold; § = incomplete characterization for noxious thermal stimuli and/or protons; SAI = rapid conducting, slow adapting fiber with irregular discharge pattern to velocity displacement.

APPENDIX R

Study IVa: Single Fiber Responses from Laser Stimulation

Table 8.

*Summary of Single Fiber Responses from Laser Stimulation in Study IVa*

| Skin type | Fiber class | CV | Laser driver current mA | Discharge Frequency in Impulses/7s | | | | |
|---|---|---|---|---|---|---|---|---|
| | | | | Pre-test | 100 $\mu$M GABA 2 min | 100 $\mu$M GABA 4min | 100 $\mu$M GABA 6 min | Wash 25min |
| g | **C/A**δH | 1.21 | 1300 | 11 | 12 | 6 | - | 11 |
| g | **C**MHAC | 0.30 | 900 | 13 | 13 | 10 | 8 | 8 |
| g | **C**§ | 0.37 | 900 | 34 | 12 | 11 | 15 | - |
| h | **C**MHA | 0.36 | 1000 | 15 | 11 | 13 | 15 | 7 |
| g | **C**MHA | 0.49 | 1500 | 12 | 12 | 5 | 6 | 10 |
| h | **C**MH | 0.35 | 1200 | 32 | 34 | 13 | 15 | - |

*Note:* g = glabrous; h = hairy; **C** = C fiber; **A =** A fiber; M = positive response to high pressure mechanical stimuli; A = positive response to protons; H = positive response to noxious heat; C = positive response to noxious cold; § = incomplete characterization to noxious thermal stimuli and/or protons.

APPENDIX S

Discharge Frequency from Laser Stimulation of Multiple Heat Sensitive Fibers

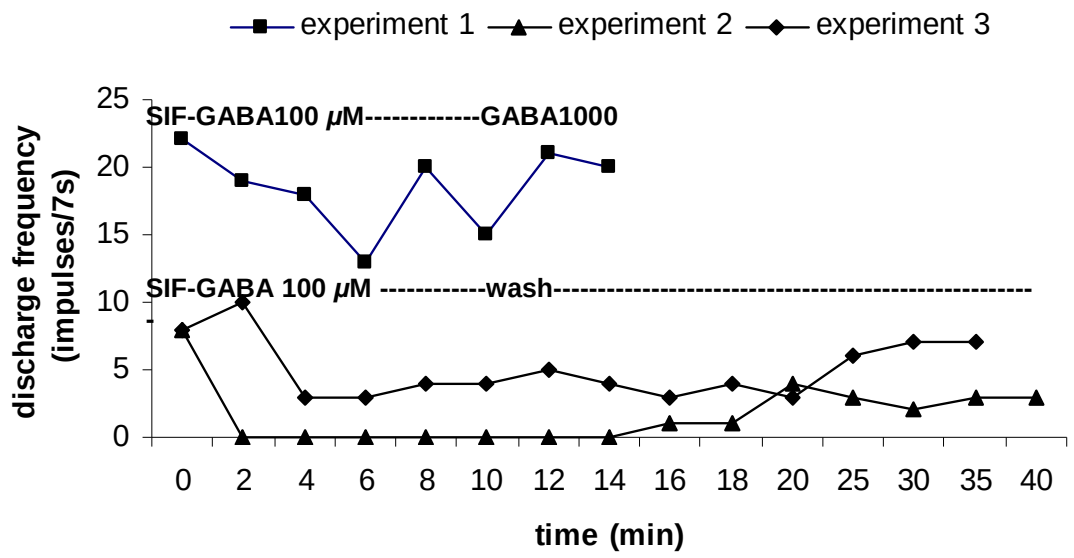


*Figure 27.* Discharge frequencies generated from laser stimulation of 3 receptive fields by multiple heat sensitive fibers.

APPENDIX T

GABA Responsiveness of High and Low Fibers by Study Phase

Table 9.

*Summary of High and Low Threshold Fibers for GABA Responsiveness by Study Phase*

| Study Phase | High Mechanical Threshold Responder | High Mechanical Threshold Total Fibers | Low Mechanical Threshold Responder | Low Mechanical Threshold Total Fibers | Excluded |
|---|---|---|---|---|---|
| II | 3 | 6 | 0 | 0 | 0 |
| IIIa,b | 3 | 6 | 0 | 4 | 7 |
| IIIc | 2 | 11 | 0 | 2 | 0 |
| IVa | 4 | 6 | 0 | 0 | 0 |
| IVc | 0 | 1 | 0 | 0 | 0 |
| V | 1 | 1 | 0 | 0 | 0 |
| VI | 0 | 0 | 0 | 1 | 0 |

APPENDIX U

Dual Compartment Recording Chamber Design Plans

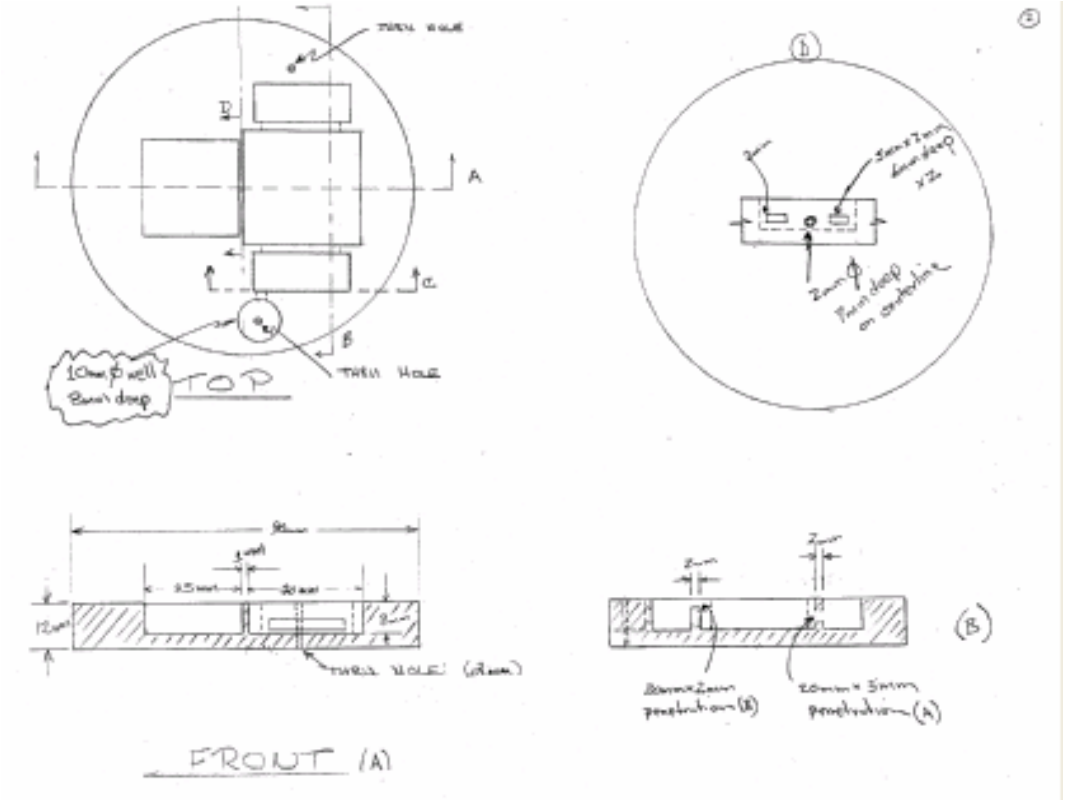


*Figure 28.* Recording chamber design plans (top and front views).

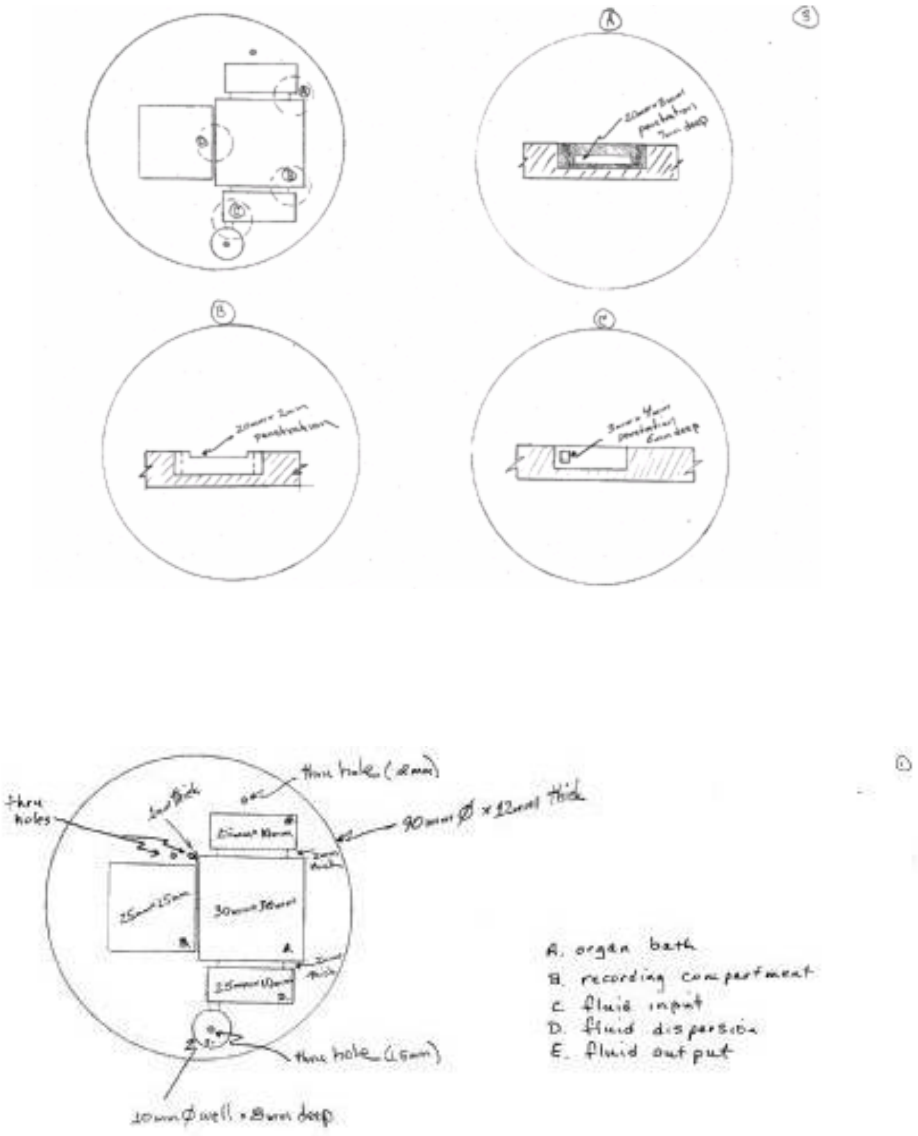


*Figure 29.* Recording chamber internal feature plans.

# REFERENCES


Agrawal, S. G., & Evans, R. H. (1986). The primary afferent depolarizing action of kainate in the rat. *British Journal of Pharmacology, 87*, 345-355.

Akopian, A., Sivilotti, L., & Wood, J. N. (1996). A tetrodotoxin resistant voltage-gated sodium channel expressed by sensory neurons. *Nature, 379*, 257-262.

Andrew, D., & Greenspan, J. D. (1999). Mechanical and heat sensitization of cutaneous nociceptors after peripheral inflammation in the rat. *Journal of Neurophysiology, 82*(5), 2649-2656.

Aptel, H., Hilaire, C., Pieraut, S., Boukhaddaoui, H., Mallie, S., Valmier, J., et al. (2007). The $Cav_{3.2}/\alpha_{1H}$ T-type $Ca^{2+}$ current is a molecular determinant of excitatory effects of GABA in adult sensory neurons. *Molecular and Cellular Neuroscience, 36*, 293-303.

Ault, B., & Hildebrand, L. M. (1994). $GABA_A$ receptor-mediated excitation of nociceptive afferents in the rat isolated spinal cord-tail preparation. *Neuropharmacology, 33*(1), 109-114.

Bai, D., Pennefather, P., MacDonald, J., & Orser, B. (1999). The general anesthetic propofol slows deactivation and desensitization of $GABA_A$ receptors. *Journal of Neuroscience, 19*(24), 10635-10646.

Battaglia, G., & Rustioni, A. (1988). Coexistence of glutamate and substance P in DRG neurons of the rat and monkey. *Journal of Comparative Neurology, 277*, 308-312.

Belmonte, C. (1996). Signal transduction in nociceptors: general principles. In C. Belmonte & F. Cervero (Eds.), *Neurobiology of Nociceptors* (pp. 243-257). Oxford, UK: Oxford University Press.

Ben-Ari, Y. (2002). Excitatory actions of GABA during development: the nature of the nurture. *Nature Reviews Neuroscience, 3*, 728-739.

Ben-Shlomo, I., & Hsueh, A. (2005). Three's company: two or more unrelated receptors pair with the same ligand. *Molecular Endocrinology, 19*(5), 1097-1109.

Bernardini, N., Reeh, P. W., & Sauer, S. K. (2001). Muscarinic M2 receptors inhibit heat-induced CGRP release from isolated rat skin. *NeuroReport, 12*(11), 2457-2460.

Bernardini, N., Roza, C., Sauer, S., Gomeza, J., Wess, J., & Reeh, P. W. (2002). Muscarinic M2 receptors on peripheral nerve endings: a molecular target of antinociception. *Journal of Neuroscience, 22*, RC229 221-225.

Bernardini, N., Sauer, S., Haberberger, R., Fischer, M. J. M., & Reeh, P. W. (2001). Excitatory nicotinic and desensitizing muscarinic (M2) effects on C-nociceptors in isolated rat skin. *Journal of Neuroscience, 21*(9), 3295-3302.

Bessou, P., & Perl, E. R. (1969). Response of cutaneous sensory units with unmyelinated fibers to noxious stimuli. *Journal of Neurophysiology, 32*, 1025-1043.

Bhisitkul, R. B., Villa, J. E., & Kocsis, J. D. (1987). Axonal GABA receptors are selectively present on normal and regenerated sensory fibers in rat peripheral nerve. *Exp. Brain Res., 66*, 659-663.

Birder, L. A., & Perl, E. R. (1994). Cutaneous sensory receptors. *Journal of Clinical Neurophysiology, 11*(6), 534-552.

Blunk, J., Seifert, F., Schmelz, M., Reeh, P. W., & Koppert, W. (2003). Injection pain of rocuronium and vecuronium is evoked by direct activation of nociceptive nerve endings. *European Journal of Anaesthesiology, 20*, 245-253.

Bormann, J. (2000). The 'ABC' of GABA receptors. *Trends Pharmacol Sci, 21*, 16-19.

Bouche, N., & Fromm, H. (2004). GABA in plants: just a metabolite? *Trends in Plant Science, 9*(3), 110-115.

Bowery, N. G. (1993). $GABA_B$ receptor pharmacology. *Annu. Rev. Pharmacol. Toxicol., 33*, 109-147.

Bowery, N. G., & Smart, T. G. (2006). GABA and glycine as neurotransmitters: a brief history. *British Journal of Pharmacology, 147*, S109-S119.

Bretag, A. H. (1969). Synthetic interstitial fluid for isolated mammalian tissue. *Life Sci, 8*(Part I), 319-329.

Brown, D. A., & Marsh, S. (1978). Axonal GABA-receptors in mammalian peripheral nerve trunks. *Brain Research, 156*, 187-191.

Burgess, P. R., & Perl, E. R. (1967). Myelinated afferent fibres responding specifically to noxious stimulation of the skin. *Journal of Physiology, 190*, 541-562.

Burgess, P. R., & Perl, E. R. (1973). Cutaneous mechanoreceptors and nociceptors. In A. Iggo (Ed.), *Handbook of Sensory Physiology* (Vol. II, pp. 29-78). Berlin: Springer.

Cain, D. M., Khasabov, S. G., & Simone, D. A. (2001). Response properties of mechanoreceptors and nociceptors in mouse glabrous skin: an *in vivo* study. *Journal of Neurophysiology, 85*, 1561-1574.

Campbell, J. N., & Meyer, R. A. (1983). Sensitization of unmyelinated nociceptive afferents in monkey varies with skin type. *Journal of Neurophysiology, 49*(1), 98-110.

Canellakis, Z., Milstone, L., LL, M., Young PR, & Bondy, P. (1983). GABA from putrescine is bound in macromolecular form in keratinocytes. *Life Sci., 33*(7), 599-603.

Carlton, S. M. (2005). Glutamate receptors and their role in acute and inflammatory pain. In S. Gill & O. Pulido (Eds.), *Glutamate Receptors in Peripheral Tissue* (pp. 9687-). New York: Kluwer Academic/Plenum Publisher.

Carlton, S. M., Du, J., Davidson, E., Zhou, S., & Coggeshall, R. E. (2001). Somatostatin receptors on peripheral primary afferent terminals: inhibition of sensitized nociceptors. *Pain, 90*, 233-244.

Carlton, S. M., Du, J., Zhou, S., & Coggeshall, R. E. (2001). Tonic control of peripheral cutaneous nociceptors by somatostatin receptors. *The Journal of Neuroscience, 21*(11), 4042-4049.

Carlton, S. M., Zhou, S., & Coggeshall, R. E. (1999). Peripheral $GABA_A$ receptors: Evidence for peripheral primary afferent depolarization. *Neuroscience, 93*(2), 713-722.

Charles, K., Evans, M., Robbins, M., Calver, A., Leslie, R., & Pangalos, M. (2001). Comparative immunohistochemical localisation of $GABA_{B1a}$, $GABA_{B1b}$, and $GABA_{B2}$ subunits in rat brain, spinal cord and dorsal root ganglion. *Neuroscience, 106*, 447-467.

Chebib, M., & Johnston, G. A. R. (1999). The 'ABC' of GABA receptors: a brief review. *Clinical and Experimental Pharmacology and Physiology, 26*, 937-940.

Chen, X., Tanner, K., & Levine, J. D. (1999). Mechanical sensitization of cutaneous C-fiber nociceptors by prostaglandin E2 in the rat. *Neuroscience Letters, 267*, 105-108.

Cherubini, E., & Strata, F. (1997). $GABA_C$ receptors: a novel receptor family with unusual pharmacology. *News Physiol. Sci., 12*, 136-141.

Davis, H., & Forbes, A. (1936). Chronaxie. *Physiol. Rev., 16*, 407-441.

De Col, R., Messlinger, K., & Carr, R. (2008). Conduction velocity is regulated by sodium channel inactivation in unmyelinated axons innervating the rat cranial meninges. *J Physiol, 586*(4), 1089-1103.

de Groat, W. C., Lalley, P. M., & Saum, W. R. (1972). Depolarization of dorsal root ganglia in the cat by GABA and related amino acids: antagonism by picrotoxin and bicucullin. *Brain Research, 44*(1), 273-277.

de Jong, R. (1994). *Local Anesthetics*. Saint Louis, MO: Mosby.

Delpire, E. (2000). Cation-chloride co-transporters in neuronal communication. *News Physiol. Sci., 15*, 309-312.

Denda, M., Fuziwara, S., & Inoue, K. (2003). Influx of calcium and chloride ions into epidermal keratinocytes regulates exocytosis of epidermal lamellar bodies and skin permeability barrier homeostasis. *J. Invest. Dermatol, 121*(362-367).

Denda, M., Inoue, K., Inomata, S., & Denda, S. (2002). $GABA_A$ receptor agonists accelerate cutaneous barrier recovery and prevent epidermal hyperplasia induced by barrier disruption. *J. Invest. Dermatol, 119*, 1041-1047.

Desarmenien, M., Feltz, P., & Headley, P. (1980). Does glial uptake affect GABA responses? An intracellular study on rat dorsal root ganglion neurones in vitro. *Journal of Physiology, 307*, 163-182.

Desarmenien, M., Feltz, P., Occhipinti, G., Santangelo, F., & Schlichter, R. (1984). Coexistence of $GABA_A$ and $GABA_B$ receptors on Aδ and C primary afferents. *Br. J. Pharmac., 81*, 327-333.

Desarmenien, M., Santangelo, F., Loeffler, J.-P., & Feltz, P. (1984). Comparative study of GABA-mediated depolarizations of lumbar Aδ and C primary afferent neurones of the rat. *Exp Brain Res, 54*, 521-528.

Djouhri, L., Fang, X., Okuse, K., Wood, J. N., Berry, C. M., & Lawson, S. M. (2003). The TTX-resistant sodium channel Na 1.8 (SNS/PN3): expression and correlation with membrane properties in rat nociceptive primary afferent neurons. *J Physiol, 550*(3), 739-752.

Dobretsov, M., Hastings, S., & Stimers, J. (1999). Non-uniform expression of α subunit isoforms of the $Na^+/K^+$ pump in rat dorsal root ganglion neurons. *Brain Research, 821*, 212-217.

Duthey, B., Diehl, S., Hubner, A., Pfeffer, J., & Boehncke, W. (2008). Attenuation of allergic contact dermatitis by the $GABA_B$ receptor agonist baclofen. *Experimental Dermatology, 17*(3), 242.

Enna, S. (2007). The GABA receptors. In S. Enna (Ed.), *The GABA Receptors* (3rd ed., pp. 1-22). Totowa, New Jersey: Humana Press, Inc.

Enz, R., & Cuttin, G. (1998). Molecular composition of $GABA_C$ receptors. *Vision Research, 38*, 1431-1441.

Erdo, S. (1985). Peripheral GABAergic mechanisms. *Trends in Pharmacological Sciences, 6*, 205-208.

Farrant, M. (2007). Differential activation of $GABA_A$-receptor subtypes. In S. Enna & H. Mohler (Eds.), *The GABA Receptors* (pp. 87-110). Totowa, NJ: Humana Press, Inc.

Farrant, M., & Nusser, Z. (2005). Variations on an inhibitory theme: phasic and tonic activation of $GABA_A$ receptors. *Nature Reviews, 6*, 215-229.

Gallagher, J. P., Higashi, H., & Nishi, S. (1978). Characterization and ionic basis of GABA-induced depolarizations recorded in vitro from cat primary afferent neurones. *J. Physiol., 275*, 263-282.

Gammon, C., Lyons, S., & Morell, P. (1990). Modulation by neuropeptides of bradykinin-stimulated second messenger release in dorsal root ganglion neurons. *Brain Research, 518*, 159-165.

Gee, M., Lynn, B., & Cotsell, B. (1996). Activity-dependent slowing of conduction velocity provides a method for identifying different functional classes of C-fibre in the rat saphenous nerve. *Neuroscience, 73*(3), 667-675.

Greffrath, W., Nemenov, M., Schwarz, S., Baumgartner, U., Vogel, H., Arendt-Nielsen, L., et al. (2002). Inward currents in primary nociceptive neurons of the rat and pain sensations in humans elicited by infrared diode laser pulses. *Pain, 99*(1-2), 145-155.

Guenther, S., Reeh, P. W., & Kress, M. (1999). Rises in [Ca2+]i mediate capsaicin- and proton-induced heat sensitization of rat primary nociceptive neurons. *European Journal of Neuroscience, 11*(9), 3143-3150.

Hablitz, J. (1992). Voltage-dependence of $GABA_A$-receptor desensitization in cultured chick cerebral neurons. *Synapse, 12*, 169-171.

Hamann, M., Rossi, D., & Attwell, D. (2002). Tonic and spillover inhibition of granule cells control information flow through cerebellar cortex. *Neuron, 33*, 525-633.

Han, D., Kim, H.-Y., Lee, H.-J., Shim, I., & Hahm, D.-H. (2007). Wound healing activity of gamma-aminobutyric acid (GABA) in rats. *J. Microbiol. Biotechnol., 17*(10), 1661-1669.

Hoffman, A., Jensen, M. P., Abresch, R., & Carter, G. (2005). Chronic pain in persons with neuromuscular disease. *Phys Med Rehabil Clin N Am, 16*(4), 1099-1112.

Horch, K. W., Tuckett, R. P., & Burgess, P. R. (1977). Key to the classification of cutaneous mechanoreceptors. *Journal of Investigative Dermatology, 69*, 75-82.

Ito, K., Tanaka, K., Nishibe, Y., Hasegawa, J., & Ueno, H. (2007). GABA-synthesizing enzyme, GAD67, from dermal fibroblasts: evidence for a new skin function. *Biochemica et Biophysica Acta, 1770*, 291-296.

Johnston, G. A. R. (1996a). $GABA_A$ receptor pharmacology. *Pharmacol. Ther., 69*(3), 173-198.

Johnston, G. A. R. (1996b). $GABA_C$ receptors: relatively simple transmitter-gated ion channels? *TIPS, 17*, 319-323.

Kerr, D., & Ong, J. (1992). GABA agonists and antagonists. *Medicinal Research Reviews, 12*(6), 593-636.

Khirug, S., Yamada, J., Afzalov, R., Volpio, J., Khiroug, L., & Kaila, K. (2008). GABAergic depolarization of the axon initial segment in cortical principal neurons is caused by the Na-K-2Cl cotransporter NKCC1. *Journal of Neuroscience, 28*(18), 4635-4639.

Koltzenburg, M., Stucky, C. L., & Lewin, G. R. (1997). Receptive properties of mouse sensory neurons innervating hairy skin. *J.Neurophysiology, 78*, 1841-1850.

Korpi, E., Grunder, G., & Luddens, H. (2002). Drug interactions at $GABA_A$ receptors. *Progress in Neurobiology, 67*, 113-159.

Krogsgaard-Larsen, P., Scheel-Kruger, J., & Koford, H. (1979). *GABA-neurotransmitters, pharmacochemical, biochemical and pharmacological aspects*. Denmark: Scandinavian University Books.

Kruger, L., Perl, E. R., & Sedivec, M. J. (1981). Fine structure of myelinated mechanical nociceptor endings in cat hairy skin. *The Journal of Comparative Neurology, 198*, 137-154.

Kwan, K., Allchorne, A., Vollrath, M., Christensen, A., Zhang, D.-S., Woolf, C. J., et al. (2006). TRPA1 contributes to cold, mechanical and chemical nociception but is not essential for hair-cell transduction. *Neuron, 50*, 277-289.

Lawson, J. J., McIlwrath, S. L., Woodbury, C. J., Davis, B. M., & Koerber, H. R. (2008). TRPV1 unlike TRPV2 is restricted to a subset of mechanically insensitive cutaneous nociceptors responding to heat. *Journal of Pain, 9*(4), 298-308.

Lawson, S. M., Crepps, B. A., & Perl, E. R. (1997). Relationship of substance P to afferent characteristics of dorsal root ganglion neurones in guinea-pig. *J Physiol, 505*(1), 177-191.

Lawson, S. N. (2005). The peripheral sensory nervous system: dorsal root ganglion neurons. In P. J. Dyck & P. K. Thomas (Eds.), *Peripheral Neuropathy* (4th ed., Vol. 1, pp. 163-202). Philadelphia: Saunders.

Leem, J. W., Willis, W. D., & Chung, J. M. (1993). Cutaneous sensory receptors in the rat foot. *Journal of Neurophysiology, 69*(5), 1684-1699.

Lewin, G. R., & Moshourab, R. (2004). Mechanosensation and pain. *Journal of Neurobiology, 61*(1), 30-44.

Light, A. R., & Perl, E. R. (1993). Peripheral sensory systems. In P. J. Dyck, P. K. Thomas, J. W. Griffin, P. A. Low & J. F. Poduslo (Eds.), *Peripheral Neuropathy* (pp. 149-165). Philadelphia, PA: Saunders.

Lohmann, T., Hawa, M., Leslie, R., Lane, R., Picard, J., & Londei, M. (2000). Immune reactivity to glutamic acid decarboxylase 65 in stiff-man syndrome. *The Lancet, 356*, 31-35.

Lynn, B., & Carpenter, S. (1982). Primary afferent units from the hairy skin of the rat hind limb. *Brain Research, 238*, 29-43.

MacIver, M., & Tanelian, D. (1993). Functional specialization of Aδ and C fiber free nerve endings innervating rabbit corneal epithelium. *Journal of Neuroscience, 13*(10), 4511-4524.

Magnaghi, V. (2007). GABA and neuroactive steroid interactions in glia: new roles for old players? *Current Neuropharmacology, 5*, 47-64.

Magnaghi, V., Ballabio, M., Camozzi, F., Colleoni, M., Consoli, A., Gassmann, M., et al. (2008). Altered peripheral myelination in mice lacking $GABA_B$ receptors. *Molecular and Cellular Neuroscience, 37*, 599-609.

Magnaghi, V., Ballabio, M., Cavarretta, I., Froestl, W., Lambert, J., Zucchi, I., et al. (2004). $GABA_B$ receptors in Schwann cells influence proliferation and myelin expression. *European Journal of Neuroscience, 19*(10), 2641-2649.

Maurer, K., Bostock, H., & Koltzenburg, M. (2007). A rat in vitro model for the measurement of multiple excitability properties of cutaneous axons. *Clinical Neurophysiology, 118*(11), 2404-2412.

Meinek, H.-M., Ricker, K., Hulser, P.-J., Schmid, E., Peiffer, J., & Solimena, M. (1994). Stiff man syndrome: clinical and laboratory findings in eight patients. *Journal of Neurology, 241*, 157-166.

Mendell, L. M., Albers, K. M., & Davis, B. M. (1999). Neurotrophins, nociceptors, and pain. *Microscopy Research and Technique, 45*(4-5), 252-261.

Meyer, R., Davis, K., Cohen, R., Treede, R. D., & Campbell, C. M. (1991). Mechanically insensitive afferents (MIAs) in cutaneous nerves of monkey. *Brain Research, 561*, 252-261.

Mogil, J. S., & Chanda, M. (2005). The case for the inclusion of female subjects in the basic science studies of pain. *Pain, 117*, 1-5.

Mogil, J. S., Miermeister, F., Seifert, F., Strasburg, K., Zimmermann, K., Reinold, H., et al. (2005). Variable sensitivity to noxious heat is mediated by differential expression of the CGRP gene. *PNAS, 102*(36), 12938-12943.

Monsivais, P., & Rubel, E. (2001). Accommodation enhances depolarizing inhibition in central neurons. *The Journal of Neuroscience, 21*(19), 7823-7830.

Morris, M., Di Dostanzo, A., Fox, S., & Werman, R. (1983). Depolarizing action of GABA on myelinated fibers of peripheral nerves. *Brain Research, 278*, 117-126.

Murata, Y., Woodward, R., Miledi, R., & Overman, L. (1996). The first selective antagonist for a $GABA_C$ receptor. *Bioorganic & Medicinal Chemistry Letters, 6*(17), 2073-2076.

Nakagawa, H., Hiura, A., & Kubo, Y. (2003). Preliminary studies of GABA-immunoreactive neurons in the rat trigeminal ganglion. *Okajimas Folia Anat. Jpn, 80*(1), 15-22.

Nemenov, M. (2008). Portable laser and process for producing controlled pain. U.S.: Washington, DC: US Patent and Trademark Office.

Nishi, S., Minota, S., & Karczmar, A. G. (1974). Primary afferent neurones: the ionic mechanism of GABA-mediated depolarization. *Neuropharmacology, 13*, 215-219.

Nusser, Z., Roberts, J., Baude, A., Richards, J., & Somogyi, P. (1995). Relative densities of synaptic and extrasynaptic $GABA_A$ receptors on cerebellar granule cells as determined by a quantitative immunogold method. *Journal of Neuroscience, 15*, 2948-2960.

Ocvirk, R., Murphy, B., Franklin, K., & Abbott, F. (2008). Antinociceptive profile of ring A-reduced progesterone metabolites in the formalin test. *Pain, In Press*.

Page, A. J., & Blackshaw, L. A. (1999). $GABA_B$ Receptors Inhibit Mechanosensitivity of Primary Afferent Endings. *Journal of Neuroscience, 19*(19), 8597.

Pathirathna, S., Brimelow, B., Jogodi, M., Krishnan, K., Jiang, X., Zorumski, C., et al. (2005). New evidence that both T-type calcium channels and $GABA_A$ channnels are reponsible for the potent peripheral analgesic effects of 5α-reduced neuroactive steroids. *Pain, 114*, 429-443.

Perves, D., Augustine, G. J., Fitzpatrick, D., Hall, W. C., LaMantia, A.-S., & Williams, S. M. (2004). Neurotransmitters and their receptors. In D. Perves, G. J. Augustine, D. Fitzpatrick, W. C. Hall, A.-S. LaMantia & S. M. Williams (Eds.), *Neuroscience* (pp. 143-147). Sunderland, MA: Sinauer.

Petruska, J., Napaporn, J., Johnson, R., Gu, J., & Cooper, B. (2000). Subclassified acutely dissociated cells of the rat DRG: histochemistry and patterns of capsaicin-, proton-, and ATP-activated currents. *Journal of Physiology, 84*(5), 2365-2379.

Plaghki, L., & Mouraux, A. (2003). How do we selectively activate skin nociceptors with a high power infrared laser? Physiology and biophysics of laser stimulation. *Neurophysiologie Clinique, 33*, 269-277.

Potenzieri, C., Brink, T., Pacharinsak, C., & Simone, D. (2008). Cannabinoid modulation of cutaneous Aδ during inflammation. *J Neurophysiol, in press*, in press.

Price, M., McIlwrath, S. L., Xie, J., Cheng, C., Qiao, J., Tarr, D., et al. (2001). The DRASIC cation channel contributes to the detection of cutaneous touch and acid stimuli in mice. *Neuron, 32*, 1071-1083.

Pugliese, A., Solimena, M., Awdeh, Z., Alper, C., Bugawan, T., Erlich, H., et al. (1993). Association of HLA-DQB1*0201 with stiff-man syndrome. *Clinical Endocrinology & Metabolism, 77*, 1550-1553.

Ragsdale, D., McPhee, J., Scheuer, T., & Catterall, W. (1994). Molecular determinants of state-dependent block of $Na^+$ channels by local anesthetics. *Science, 265*, 1724-1728.

Raja, S. N., Campbell, J. N., & Meyer, R. A. (1984). Evidence for different mechanisms of primary and secondary hyperalgesia following heat injury to the glabrous skin. *Brain, 107*(4), 1179-1188.

Raymond, S., Thalhammer, J., Popitz-Bergez, F., & Strichartz, G. (1990). Changes in axonal impulse conduction correlate with sensory modality in primary afferent fibers in the rat. *Brain Research, 526*, 318-321.

Razum, N. (2001). Laser physics for surgical applications. In G. Keller, V. Lacombe, P. Lee & J. Watson (Eds.), *Lasers in Aesthetic Surgery* (pp. 3-13). New York: Thieme.

Reeh, P. W. (1986). Sensory receptors in mammalian skin in an *in vitro* preparation. *Neuroscience Letters, 66*, 141-146.

Reeh, P. W., Bayer, J., Kocher, L., & Handwerker, H. O. (1987). Sensitization of nociceptive cutaneous nerve fibers from the rat's tail by noxious mechanical stimulation. *Exp Brain Res, 65*, 505-512.

Reis, G., & Duarte, I. (2006). Baclofen, an agonist at peripheral $GABA_B$ receptor, induces antinociception *via* activation of TEA-sensitive potassium channels. *British Journal of Pharmacology, 149*, 733-739.

Reis, G., & Duarte, I. (2007). Involvement of chloride channel coupled $GABA_C$ receptors in the peripheral antinociceptive effect induced by $GABA_C$ receptor agonist cis-4-aminocrotonic acid. *Life Sci, 80,* 1268-1273.

Reis, G., Pacheco, D., Francischi, J., Castro, M., Perez, A., & Duarte, I. (2007). Involvement of $GABA_A$ receptor-associated chloride channels in the peripheral antinociceptive effect induced by $GABA_A$ receptor agonist muscimol. *European Journal of Pharmacology, 564,* 112-115.

Represa, A., & Ben-Ari, Y. (2005). Trophic actions of GABA on neuronal development. *Trends in Neurosciences, 28*(6), 278-283.

Richmond, J., & Jorgensen, E. (1999). One GABA and two acetylcholine receptors function at the C. *elegans* neuromuscular junction. *Nature Neuroscience, 2*(791-797), 791-797.

Roy, G., Philippe, E., Gaulin, F., & Guay, G. (1991). Peripheral projection of the chick primary sensory neurons expressing GABA immunoreactivity. *Neuroscience, 45*, 177-185.

Shea, V., & Perl, E. R. (1985). Sensory receptors with unmyelinated (C) fibers innervating the skin of the rabbit's ear. *Journal of Neurophysiology, 54*(3), 491-501.

Skerry, T., & Genever, P. (2001). Glutamate signalling in non-neuronal tissues. *Trends in Pharmacological Sciences, 22*(4).

Slugg, R., Meyer, R., & Campbell, J. N. (2000). Response of cutaneous A- and C-fiber nociceptors in the monkey to controlled-force stimuli. *J Neurophysiol, 83,* 2179-2191.

Soghomonian, J.-J., & Martin, D. (1998). Two isoforms of glutamate decarboxylase, why? *Trends in Pharmacological Sciences, 19*(12), 500-505.

Spray, D. (1986). Cutaneous temperature receptors. *Annual Review Physiology, 48,* 625-638.

Stampfli, R. (1954). A new method for measuring membrane potentials with external electrodes. *Experientia, 10*(12), 508-509.

Steen, K., & Reeh, P. W. (1993). Actions of cholinergic agonists and antagonists on sensory endings in rat skin, in vitro. *Journal of neurophysiology, 70*(1), 397-405.

Steen, K., Steen, A., & Reeh, P. W. (1995). A dominant role of acid pH in inflammatory excitation and sensitization of nociceptors in rat skin, *in vitro*. *Journal of Neuroscience, 15*(5), 3982-3989.

Stoyanova, I. (2004). GABA immunostaining in trigeminal, nodose, and spinal ganglia of the cat. *Acta Histochemica, 106*(4), 309-314.

Stucky, C. L., Koltzenburg, M., Schneider, M., Engle, M., Albers, K. M., & Davis, B. M. (1999). Overexpression of nerve growth factor in skin selectively affects the survival and functional properties of nociceptors. *Journal of Neuroscience, 19*(19), 8509-8516.

Tamayama, T., Kanbara, K., Maemura, K., Kuno, M., & Watanabe, M. (2001). Localization of GABA, $GAD_{65}$, and $GAD_{67}$ in rat epiphyseal growth chondrocytes. *Acta Histochemica Cytochemica, 34*(3), 201-206.

Tetzlaff, J. (2000). *Clinical Pharmacology of Local Anesthetics*. Woburm, MA: Butterworth-Heineman.

Thalhammer, J., Raymond, S., Popitz-Bergez, F., & Strichartz, G. (1994). Modality-dependent modulation of conduction by impulse activity in functionally characterized single cutaneous afferents in the rat. *Somatosensory and Motor Research, 11*(3), 243-357.

Torebjork, H. E., Schady, W., & Ochoa, J. (1984). Sensory correlates of somatic afferent fiber activation. *Human Neurobiology, 3*, 15-20.

Treede, R. D., Meyer, R., Raja, S. N., & Campbell, J. N. (1995). Evidence for two different heat transduction mechanisms in nociceptive primary afferents innervating monkey skin. *Journal of Physiology, 483*(3), 747-758.

Tzabazis, A., Klyukinov, M., Manering, N., Nemenov, M., Shafer, S., & Yeomans, D. (2005). Differential activation of trigeminal C or Aδ nociceptors by infrared diode laser in rats: behavioral evidence. *Brain Research, 1037*(1-2), 148-156.

Valeyev, A., Hackman, J. C., Wood, P. M., & Davidoff, R. A. (1996). Pharmacologically novel GABA receptor in human dorsal root ganglion neurons. *Journal of Neurophysiology, 76*(5), 3555-3558.

Veldhuijzen, D., Nemenov, M., Keaser, M., Zhou, J., Gullapalli, R., & Greenspan, J. (2009). Differential brain activation associated with laser-evoked burning and pricking pain: An event-related fMRI study. *Pain, 141*, 104-113.

Wagers, P., & Smith, C. (1960). Responses in dental nerves of dogs to tooth stimulation and the effects of systemically administered procaine, lidocaine and morphine. *Journal of Pharmacology and Experimental Therapeutics, 130*(1), 89-105.

Walsh, J. (1997). Tissue cutting: traditional lasers, solid-state devices, and diode laser. In K. Arndt, J. Dover & S. Olbricht (Eds.), *Lasers in Cutaneous and Aesthetic Surgery* (pp. 188-205). Philadelphia: Lippincott-Raven.

Wang, T., Hackam, A., Guggino, W., & Cutting, G. (1995). A single amino acid in gamma-aminobutyric acid rho 1 receptors affects competitve and noncompetitve components of picrotoxin inhibition. *PNAS, 92*(25), 11751-11755.

Wegelius, K., Reeben, M., Rivera, C., Kaila, K., Saarma, M., & Pasternack, M. (1996). The Rho 1 GABA receptor cloned from rat retina is down-modulated by protons. *NeuroReport, 7*, 2005-2009.

Wenk, H. N., Brederson, J.-D., & Honda, C. N. (2006). Morphine directly inhibits nociceptors in inflamed skin. *J Neurophysiol, 95*, 2083-2097.

White, P. (2002). The role of non-opioid analgesic techniques in the management of pain after ambulatory surgery. *Anesthesia and Analgesia, 94*, 577-585.

Zhang, D., Pan, Z.-H., Awobuluyi, M., & Lipton, S. (2001). Structure and function of $GABA_C$ receptors: a comparison of native versus recombinant receptors. *Trends in Pharmacological Sciences, 22*(3), 121-131.

Zylka, M., Rice, F. L., & Anderson, D. (2005). Topographically distinct epidermal nociceptive circuits revealed by axonal tracers targeted to Mrgprd. *Neuron, 45*, 17-25.